



**UNIVERSITÀ DI PARMA**

**Corso di DOTTORATO DI RICERCA in**  
*Scienze del Farmaco, delle Biomolecole e dei*  
*Prodotti per la Salute*

**Ph.D. Course in**  
*Drugs, Biomolecules and Health Products*  
**XXXII Cycle**

**FORMULATION STUDY OF CYSTEAMINE**  
**MICROPARTICULATE SYSTEMS**

Coordinator:

Chiar.mo Prof. MARCO MOR

Supervisor:

Chiar.ma Prof. ALESSANDRA ROSSI

Ph.D. Candidate: GRETA ADORNI

*A Davide,  
la luce che illumina i miei giorni.*

# INDEX

Chapter I .....	0
1. INTRODUCTION .....	1
1.1 Physiopathology of nephropathic cystinosis .....	1
1.2 Cysteamine .....	2
1.2.1 Cysteamine bitartrate structure .....	3
1.3 Therapeutic benefits .....	4
1.4 Neurodegenerative diseases.....	4
1.5 Treatment with cysteamine.....	5
1.5.1 Side effects of cysteamine.....	6
1.5.2 Compliance .....	6
1.6 Sustained drug release systems.....	7
1.6.1 Reservoir drug delivery systems.....	7
1.6.1.1 Procysbi® enteric-coated cysteamine formulation .....	8
1.6.2 Matrix drug delivery system.....	8
1.7 Cysteamine matrix-based drug delivery system: the novel formulation approach.....	9
1.7.1 Cysteamine extemporaneous powder for oral administration.....	9
1.7.2 Taste masking .....	10
1.7.3 Lipid excipients for the control of the drug release .....	11
1.8 Spray congealing technology .....	11
2. AIM.....	14
3. MATERIALS.....	16
3.2 METHODS .....	17
3.2.1 Manufacturing of cysteamine bitartrate lipid microparticles by spray- congealing.....	17
3.2.1.1 Laboratory scale production .....	17
3.2.1.2 Industrial scale-up production of lipid microparticles of cysteamine bitartrate	17
3.2.2 HPLC quantification of cysteamine bitartrate .....	18
3.2.2.1 Laboratory scale production of lipid microparticles of cysteamine bitartrate .....	18
3.2.2.2 Scale-up of spray congealing prototypes .....	19

3.2.2.3	HPLC determination of impurities in cysteamine bitartrate lipid microparticles .....	19
3.2.3	Drug content determination .....	20
3.2.4	Solid Lipid Microparticles (SLMs) characterization .....	21
3.2.4.1	Particle size distribution .....	21
3.2.4.2	Scanning Electron Microscopy (SEM) .....	21
3.2.4.3	Differential Scanning Calorimetry (DSC).....	21
3.2.4.4	Hot Stage Microscopy (HSM).....	22
3.2.4.5	Powder X-ray Diffraction (PXRD) .....	22
3.2.5	<i>In vitro</i> dissolution studies.....	22
3.2.5.1	Laboratory scale production of lipid microparticles of cysteamine bitartrate	22
3.2.5.2	Scale-up production of lipid microparticles of cysteamine bitartrate.	22
3.2.6	Dry coating of cysteamine lipid microparticles with spray-dried excipients.....	23
3.2.6.1	Mannitol/lecithin spray-dried microparticles .....	23
3.2.6.2	Sucralfate/lecithin spray dried microparticles .....	23
3.2.7	Odour Masking Efficiency .....	24
3.2.8	Stability tests of Xedev prototypes after 2 weeks at 30°C/65%RH.....	24
4.	RESULTS AND DISCUSSION .....	25
4.1	Preformulation study of cysteamine bitartrate pediatric extemporaneous dosage form for taste masking and prolonged release.....	25
4.1.1	Laboratory scale manufacturing of Solid Lipid Microparticles of cysteamine bitartrate .....	25
4.1.1.1	Spray-congealing manufacturing .....	25
4.1.2	Solid Lipid Microparticles characterization .....	27
4.1.2.1	Scanning Electron Microscopy (SEM) .....	27
4.1.2.2	Thermal behaviour .....	30
4.1.3	Odour masking efficiency.....	34
4.1.4	<i>In vitro</i> dissolution studies.....	35
4.1.5	Dry coating of cysteamine lipid microparticles with spray-dried excipients.....	38
4.2	No-GMP scale-up production of Solid Lipid Microparticles of cysteamine bitartrate.....	40

4.2.1	Spray congealing manufacturing .....	40
4.2.2	Particle size distribution .....	41
4.2.3	Scanning Electron Microscopy (SEM) .....	42
4.2.4	<i>In vitro</i> dissolution studies.....	43
4.2.5	Particle size distribution .....	45
4.2.6	Scanning Electron Microscopy (SEM) .....	46
4.2.7	Solid Lipid Microparticles characterization .....	47
4.2.7.1	Differential Scanning Calorimetry (DSC).....	47
4.2.7.2	Hot Stage Microscopy (HSM).....	48
4.2.7.3	Microparticles X-ray Powder Diffraction (PXRD) .....	51
4.2.8	<i>In vitro</i> dissolution studies.....	53
4.2.9	Odour masking efficiency.....	54
4.2.10	Amount of product to be administered.....	54
4.2.11	Particle size distribution .....	56
4.2.12	Analysis of the cysteamine bitartrate spray congealing batches at t = 0 .....	56
4.2.12.1	Drug content determination and impurities assay.....	56
4.2.12.2	Scanning Electron Microscopy (SEM) .....	57
4.2.13	Solid Lipid Microparticles characterization .....	58
4.2.13.1	Differential Scanning Calorimetry .....	58
4.2.13.2	Microparticles X-ray Powder Diffraction (PXRD) .....	59
4.2.14	<i>In vitro</i> dissolution studies.....	60
4.2.15	Analysis of the cysteamine bitartrate spray congealing batches after 2 weeks at 30°C and 65% RH.....	60
4.2.15.1	Drug content determination and impurities assay.....	60
4.2.16	<i>In vitro</i> dissolution studies.....	61
4.	CONCLUSIONS .....	62
	REFERENCES .....	64
	Chapter II.....	68
1.	INTRODUCTION .....	69
1.1	General aspect of pulmonary administration .....	69
1.2	Mechanism of aerosol deposition .....	69
1.3	Factors affecting the therapeutic effect .....	71
1.3.1	Airway geometry.....	71

1.3.2	The physics and chemistry of an aerosol .....	71
1.3.3	Airflow rate .....	72
1.3.4	Particle clearance.....	72
1.3.5	Diseases .....	73
1.4	Inhalation drug products.....	73
1.4.1	Dry powder inhalers.....	73
1.5	Production of inhalation products .....	74
1.6	<i>In vitro</i> models of pulmonary drug absorption .....	76
1.7	Cystic Fibrosis .....	77
1.7.1	Pathogenesis of Cystic Fibrosis.....	77
1.7.2	Bacterial infections by <i>Pseudomonas Aeruginosa</i> .....	79
1.7.3	Antibiotic treatments .....	79
1.7.4	Mucolytic agents in the treatment of cystic fibrosis.....	80
1.8	Cysteamine (Lynovex®) in the treatment of cystic fibrosis .....	81
1.8.1	Inhalable cysteamine formulations for the treatment of lung diseases.	82
1.8.2	Cysteamine base.....	82
1.9	Hyaluronic acid .....	82
1.10	L-Leucine .....	84
1.11	Trehalose.....	84
1.12	Polyvinylpyrrolidone .....	85
1.13	Ascorbic acid.....	85
1.14	Cyclodextrins .....	86
2.	AIM.....	87
3.1	MATERIALS.....	89
3.2	METHODS .....	90
3.2.1	Development process for the obtainment of cysteamine hyaluronate microparticles.....	90
3.2.1.1	Preparation of hyaluronic acid solution by ion exchange method .....	90
3.2.1.2	Acid-base titration for the determination of hyaluronic acid/cysteamine base ratio for the preparation of spray-dried microparticles.....	91
3.2.1.3.	Manufacturing of cysteamine hyaluronate microparticles by spray-drying .....	92
3.2.1.4	Two fluid and three fluid nozzles to produce cysteamine hyaluronate microparticles.....	92

3.2.2	Formulation study of cysteamine bitartrate spray-dried microparticles	93
3.2.3	HPLC quantification of cysteamine	93
3.2.4	Drug content determination of cysteamine	94
3.2.5	Characterization of the cysteamine hyaluronate microparticles	94
3.2.5.1	Determination of the particle size distribution	94
3.2.5.2	Scanning Electron Microscopy (SEM)	95
3.2.5.3	Thermogravimetric Analysis (TGA)	95
3.2.5.4	FT-IR spectroscopy analysis	95
3.2.5.5	<sup>13</sup> C NMR analysis	95
3.2.6	<i>In vitro</i> aerodynamic characterization	95
3.2.6.1	Fast Screening Impactor (FSI)	95
3.2.6.2	Next Generation Impactor (NGI)	96
3.2.7	Stability studies	97
3.2.8	<i>In vitro</i> cell culture studies on the cysteamine hyaluronate microparticles	97
3.2.8.1	Calu-3 cell line	97
3.2.8.2	NuLi-1 and CuFi-1 cell lines	98
3.2.8.3	MTS Assay	98
3.2.9	Airways mucous mimetic models	99
4.	RESULTS AND DISCUSSION	100
4.1	Preformulation study of spray-dried cysteamine microparticles	100
4.1.1	Cysteamine hyaluronate spray-dried microparticles	100
4.1.2	Drug content determination	103
4.1.3	Characterization of the cysteamine hyaluronate microparticles	103
4.1.3.1	Thermogravimetric analysis (TGA)	103
4.1.3.2	Scanning Electron Microscopy (SEM)	104
4.1.3.3	Determination of the particle size distribution	106
4.1.4	<i>In vitro</i> aerodynamic characterization	108
4.1.5	FT-IR spectroscopy analysis	108
4.1.6	<sup>13</sup> C NMR analysis	111
4.1.7	Stability studies	112
4.2	Formulation development of cysteamine hyaluronate microparticles	113
4.2.1	Particle size distribution	113
4.2.2	<i>In vitro</i> aerodynamic characterization	115

4.2.3	MTS cytotoxicity assays.....	116
4.2.3.1	MTS assay on Calu-3 cell line.....	116
4.2.3.2	MTS assay on CuFi-1 cell line .....	118
4.2.3.3	MTS assay on NuLi-1 cell line.....	120
4.2.4	Airways mucous mimetic models .....	121
4.3	Preformulation study of cysteamine bitartrate spray-dried microparticles.....	124
4.3.1	Drug content determination .....	125
4.3.2	Thermogravimetric analysis (TGA).....	125
4.3.3	Scanning Electron Microscopy (SEM) .....	126
4.3.4	<i>In vitro</i> aerodynamic characterization .....	127
3.	CONCLUSIONS .....	128
	REFERENCES .....	130

## PREFACE

The present research project addressed the employment of the drug cysteamine towards two different target diseases. The first one is the nephropathic cystinosis, a rare genetic disease that affects primarily paediatric patients, whereas the second one is cystic fibrosis. Two distinct formulation approaches were developed and financially supported by Recordati Industria Chimica e Farmaceutica S.p.A. The herein proposed projects led to the submission of two patent applications.

To efficiently treat nephropathic cystinosis and to manage the related symptoms thus improving patients' quality of life, an extemporaneous oral dosage powder, to be dispersed in water or similar fluid, was proposed for the treatment of cystinotic patients. The oral formulation was developed by incorporating the drug in a matrix made of lipid excipients, by means of spray congealing technology. Lipids were selected since the main goal of the project was either to guarantee an efficient taste masking of the drug, having cysteamine an unpleasant taste and smell, either to perform a control on the release to avoid the presence of a huge amount of cysteamine in the stomach that could lead to GI side effects.

In addition to nephropathic cystinosis, in recent times cysteamine obtained the orphan drug designation for the treatment of cystic fibrosis patients' infections. Cysteamine was shown to exercise a mucolytic effect towards the biofilm produced by *P. Aeruginosa* that colonises the lungs, thus enhancing the efficacy of the antibiotic treatment that is, so far, the mainstay of the disease. Novel inhalation cysteamine hyaluronate salts were obtained by spray drying technology employing hyaluronic acid and other deaggregating excipients, compatible with the inhalation route of administration. The novel formulation could be administered by means of a dry powder inhaler in order to easily reach the lungs where they are supposed to provide a therapeutic effect. Part of this project, in particular the experiments related to the *in vitro* cytotoxicity assays on cell cultures and the assessment of the rheological properties, was carried out at the Woolcock Institute of Medical Research (Sydney, Australia) as part of the period abroad during the third-year Ph.D. course.

By employing the same drug molecule, the two different research projects led to the development of two novel formulations; the first proposed for the oral treatment of nephropathic cystinosis in paediatric patients and the second for the management of cystic fibrosis patients' lung infections.

# Chapter I

## 1. INTRODUCTION

### 1.1 Physiopathology of nephropathic cystinosis

Cystinosis is an orphan and autosomal recessive disease characterized by a lysosomal storage disorder. Even though its pathogenesis has not been clearly described, researches in the late 1990s have identified the mutations on the CTNS gene, a 23-kb gene containing 12 exons that encode for a 367-amino acid called cystinosin,<sup>1</sup> as a possible cause of the onset of the disease.<sup>2</sup> In healthy people, cystinosin is responsible for the transport of the disulfide amino acid cystine out of lysosomes into the cytoplasm of cells, where it is then reduced into cysteine.<sup>3</sup> Impairment on the CTNS gene led to an intra-lysosomal accumulation of cystine, a dimer of the amino acid cysteine, resulting in the precipitation of characteristic crystals accumulating within various tissues and many organs including the spleen, liver, lymph nodes, kidney, bones, brain and eyes.<sup>4</sup>

Based on the various symptoms and the age of presentation, three clinical types of cystinosis can be described: infantile nephropathic, juvenile nephropathic and ocular non-nephropathic cystinosis.<sup>5</sup> Nephropathic cystinosis is the most common and infantile form. It begins in infancy at 6-8 months of age causing electrolyte imbalance, poor growth and proximal renal tubular damage (known as renal Fanconi syndrome) characterized by polyuria, polydipsia and failure to thrive within the first year of life.<sup>6</sup> In the absence of specific treatment, the disease progresses to end stage renal failure before the age of 10, thus requiring kidney transplantation.<sup>7</sup> Other signs and symptoms that may occur in untreated people, especially after adolescence, include muscle deterioration, difficulty to swallow, diabetes, thyroid and nervous system problems, and an inability to father children (infertility) in affected men. In addition, the accumulation of cysteine crystals in the cornea and conjunctiva are ophthalmic manifestation of cystinosis. Initially, the formation of crystals of cysteine is asymptomatic even if many patients develop photophobia within the first decade of life associated to blepharospasm.<sup>8</sup> Juvenile nephropathic cystinosis is very similar to the infantile form even though its progression is slower and the symptoms appear generally in the late childhood or during adolescence. Finally, the ocular non-nephropathic cystinosis is diagnosed in adulthood and only corneal crystal deposition is implicated without any other systemic involvement.<sup>5</sup> It has been demonstrated that the estimated incidence of the disease is 1 in 100,000-200,000 live births.<sup>4</sup>

## 1.2 Cysteamine

Cysteamine, introduced as a possible treatment for cystinosis in 1976 and approved by the U.S. Food and Drug Administration in 1994, is, to date, the only drug available for the treatment of cystinotic patients.<sup>6</sup> Cysteamine (also known as  $\beta$ -mercaptoethylamine, 2-aminoethanethiol, 2-mercaptoethylamine and mercaptamine) is an amino thiol whose chemical structure is  $\text{HSCH}_2\text{CH}_2\text{NH}_2$ .<sup>7</sup> Over the years, different molecular forms of cysteamine were used, including cysteamine hydrochloride ( $\text{C}_2\text{H}_7\text{NS}\cdot\text{HCl}$ , 1 mg = 0.7 mg of cysteamine base) and cysteamine bitartrate ( $\text{C}_2\text{H}_7\text{NS}\cdot\text{C}_4\text{H}_6\text{O}_6$ , 1 mg = 0.3 mg of cysteamine base).<sup>7</sup> Endogenously, cysteamine has been described as part of the coenzyme A degradation pathway (Figure 1) even though its plasma concentration remains very low.

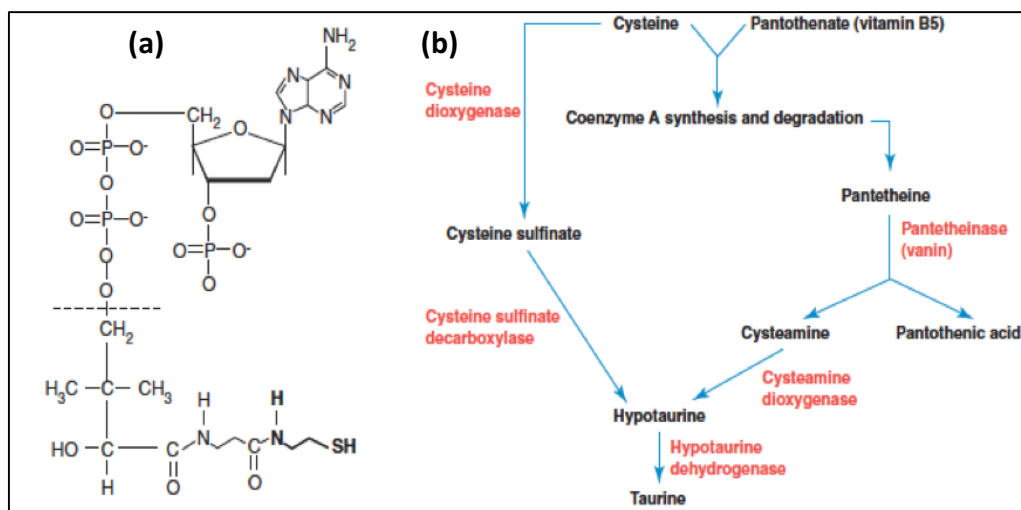


Figure 1. Molecular structure of Coenzyme A (a) and *in vivo* metabolism of cysteamine (b). Cysteamine originates from pantetheine, a degradation product of the Coenzyme A pathway, and is then converted into hypotaurine, which is finally oxidized into taurine.<sup>4</sup>

The mechanism by which cysteamine depletes lysosomes from cystine is illustrated in Figure 2. In detail, cysteamine enters the lysosome through an unidentified transporter and cleaves the disulphide bond in cystine leading to an equimolar formation of a cysteine molecule and a cysteine-cysteamine disulfide dimer that can leave the lysosomes through the lysine cationic transport system, that is maintained functional in cystinotic lysosomes, thus decreasing the accumulation of cystine.<sup>9</sup>

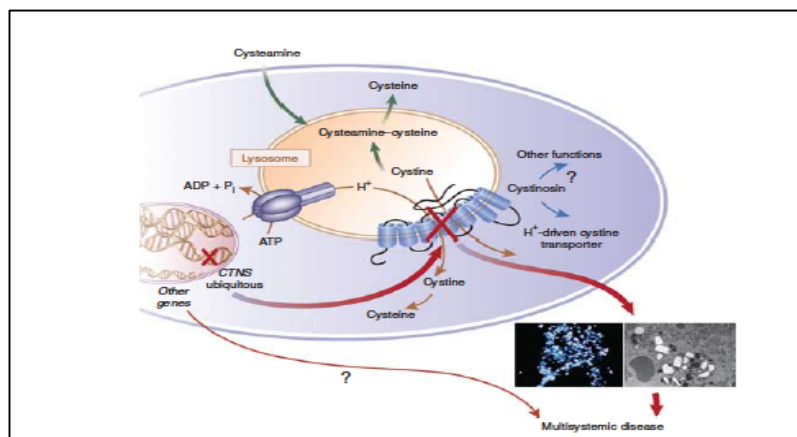


Figure 2. Mechanism of action of cysteamine.<sup>6</sup>

Cysteamine, whose chemical structure is reported in Figure 3, contains a thiol group extremely susceptible to oxidation forming the corresponding disulphide cystamine, the main degradation product. Moreover, cysteamine is highly hygroscopic.

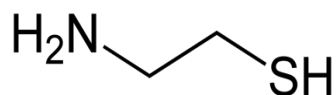


Figure 3. Chemical structure of cysteamine.

### 1.2.1 Cysteamine bitartrate

Cysteamine bitartrate is the salted form of cysteamine base. It appears as a white powder soluble in water and methanol, whereas it is insoluble in other organic solvents. The chemical structure of cysteamine bitartrate is reported in Figure 4. It is a hygroscopic powder, but more stable than cysteamine base. In presence of oxygen and through contact with metals, cysteamine bitartrate easily oxidizes into its degradation products.

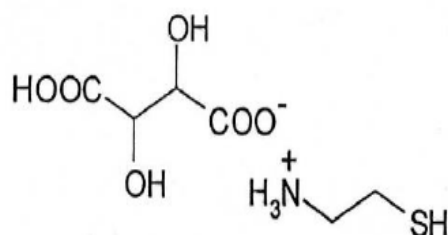


Figure 4. Chemical structure of cysteamine bitartrate.

The molecular weight of cysteamine bitartrate is 227.24 g/mol. The chemical and physical characteristics of cysteamine bitartrate are reported in Table I.

Table I. Chemical and physical properties of cysteamine bitartrate.

Water Solubility	20 mg/ml
Melting temperature (°C)	118-121°C
pKa amine	10.34
pKa thiol	8.32

Due to the hygroscopicity and the risk of oxidation of the drug into the degradation products, cysteamine bitartrate must be handled with plastic spatulas and preferably stored at 2 - 8 °C.

### 1.3 Therapeutic benefits

Early diagnosis, cysteamine administration and strict adherence to the treatment are mandatory for the impact on long-term prognosis. When compliance is consistent, cysteamine can decrease cellular cystine concentration up to 95%. In fact, it has been confirmed that cysteamine is capable of extending the life of patients, delaying at the same time kidney disease progression and the necessity of renal replacement therapy. In addition, cysteamine decreases the severity of extra renal complications.<sup>10,11</sup> Apart from cystine depleting effect, cysteamine has been proved to increase intracellular glutathione levels in cystinotic cells, re-establishing in this way the altered redox state of the cells.<sup>7</sup>

### 1.4 Neurodegenerative diseases

Beside its application in nephropathic cystinosis, studies have demonstrated that cysteamine proved to have antioxidant activity and neuroprotective properties in the treatment of neurodegenerative diseases.<sup>12</sup> In fact, cysteamine has been shown to exercise a protective action towards the liver against acetaminophen poisoning thanks to its capability to enhance the antioxidant glutathione (GSH) system. Additionally, cysteamine is active in the management of Huntington disease where it stimulates the striatal neuroprotection decreasing huntingtin (htt) inclusions. Furthermore, animal studies have evidenced the positive neuroprotective effect of cysteamine in the

treatment of Parkinson disease.<sup>13</sup> Cysteamine administration decreased dopaminergic neuronal cell death into the *substantia nigra* and improved dopamine status.<sup>7</sup>

### 1.5 Treatment with cysteamine

Cysteamine treatment is available in form of oral, ophthalmic solution and lubricant gel formulations.<sup>5</sup> The most widely employed formulations of the drug refer to cysteamine bitartrate (Cystagon<sup>®</sup>, Mylan Pharma, VA, USA).<sup>14</sup> Cystagon<sup>®</sup> has been approved in USA since 1994 and in Europe since 1997. Cystagon<sup>®</sup> is commercially available as 50 and 150 mg capsules (equal to 17 and 51 mg of cysteamine base) for the immediate release of the drug in the stomach.<sup>15</sup> As previously stated, cysteamine is part of the Coenzyme A pathway. In humans, basal plasma cysteamine is generally below the limit of detection (< 0.1  $\mu\text{M}$ ).<sup>16</sup> After administration of the drug, a peak in plasma cysteamine concentration is achieved after one hour. Then, a decrease in cysteamine plasma levels, associated to an increase in WBC cystine levels to original values, is observed after six hours.<sup>7</sup> For this reason, to keep low intracellular cystine levels, patients are required to take oral cysteamine four times a day, which means having to awake from sleep.<sup>17</sup> Since the oral administration of cysteamine is not capable to treat the ocular manifestations of the disease, topical preparations were developed to decrease corneal cystine crystals. In the late 1980s, Cystaran<sup>™</sup> (Sigma-Tau Pharmaceuticals, Gaithersburg, MD, USA), containing cysteamine hydrochloride as active agent, was found to be effective in dissolving cystine crystals. However, there were two main issues to face. First, the administration must be very frequent, in particular every hour while awake or at least six times a day.<sup>4</sup> Secondly, specific storage conditions must be followed. In fact, at room temperature, cysteamine oxidizes in the degradation disulfide form cystamine. For this reason, Cystaran<sup>™</sup> must be stored in the fridge, kept away from oxygen and used within one week of opening to prevent cysteamine degradation.<sup>8</sup> In 2017, a new gel formulation of cysteamine hydrochloride, Cystadrops<sup>®</sup> (Orphan Europe, Paris, France), was approved by EMA and succeeded to reduce the frequency of application, that so far was challenging for most of the patients. Being formulated with carboxymethylcellulose as viscous agent, that extends the residence time of the drug in the eye, the recommended dose of Cystadrops<sup>®</sup> is one drop in each eye four times per day.<sup>5</sup> Cystadrops<sup>®</sup> requires to be kept in the refrigerator at 2-8°C before the opening but, once opened, it is proved to be stable at room temperature for seven days, whether refrigerated at night.<sup>4</sup>

The administered dose of cysteamine strictly depends on the age of cystinotic patients. The daily dose of cysteamine in Cystagon<sup>®</sup>, for children below 12 years of age or weighing less than 50 kg, is 50 mg/kg/day (1.30 g/m<sup>2</sup>/day). On the contrary, for children over 12 years of age or weighing more than 50 kg, the daily dose is 2 g/day, with a maximum dose of 90 mg/kg/day (1.95 g/ m<sup>2</sup>/day). Cystagon<sup>®</sup> has to be administered every six hours in four equal portions and the amount prescribed refers to cysteamine free base.<sup>18</sup> The goal is to administer to patients a sufficient cysteamine dose able to keep the WBC cystine levels below the value of 0.1 μM, as previously described. However, the daily schedule is quite heavy for patients; in addition, the taste and smell of the drug are nauseating. Therefore, there is the evident need for formulations and delivery technologies that guarantee an increase on the plasma levels, and thus intracellular concentrations of cysteamine as well as decreasing the number of daily doses.

#### 1.5.1 Side effects of cysteamine

To date, the most frequent adverse effect of cysteamine involves gastrointestinal (GI) complaints that can lead to nausea and vomiting after drug administration. When orally administered to children with cystinosis, cysteamine has been reported to generate a 3-fold increase in the gastric acid production and a 50% rise of serum gastrin levels.<sup>16,19</sup> For this reason, the simultaneous use of proton pump inhibitors is highly recommended.<sup>7</sup> What is more, cysteamine and its derivatives are unpalatable as they are characterized by an offensive taste and smell. Cysteamine and its metabolites are typically excreted in sweat and breath leading to the rise of halitosis and body odour.<sup>20</sup>

#### 1.5.2 Compliance

To prevent and control renal and non-renal complications of cystinosis, a lifetime cysteamine treatment should be adopted. Because of the heavy regimen and the associated symptoms, patient non-adherence to the treatment remains a major problem, especially among adolescent and young adults. For this reason, compliance in cystinotic patients is very challenging.<sup>21</sup> In fact, to keep low intracellular blood cystine levels, the administration of oral cysteamine (Cystagon<sup>®</sup>) should occur every 6 hours, as previously stated in Section 1.1.3, meaning that patients are required to awake from sleep. In addition, the ocular eye drops should be administered once an hour. All these

factors have a significant impact on the life of cystinotic patients and relatives.<sup>6</sup> Therefore, the reduction of the frequency of cysteamine dose by formulating a controlled release preparation and the improvement of the taste and smell of the drug would increase the adherence to the therapy.

### 1.6 Sustained drug release systems

Oral controlled drug delivery systems have had a great impact over the last years in the field of the pharmaceutical technology. In fact, when compared to conventional oral dosage forms, they exhibit several advantages. First of all, controlled release formulations allow a reduction of the dose frequency since the drug is released over a long period of time. At the same time, there is a reduction on the adverse side effects mainly caused by high plasma concentrations of the drug.<sup>22</sup> In addition, the decrease of the frequency of dosing led to a better patient compliance and adherence to the therapy. Modified release systems are often described as *polymeric systems* since the control of the release is generally performed by a polymeric substance which incorporates or contains the drug.<sup>23</sup> The mechanism by which the drug is released by polymeric systems strictly depends either on the characteristics of the drug either on the chemical physical properties of the polymer itself that undergoes possible physical, chemical and physiological stimulations. Among the different mechanisms that regulate the drug release process, there are the diffusion controlled, dissolution controlled, erosion controlled and the osmotic pump systems. Sustained drug release systems are mainly classified into reservoir-based and monolithic matrix drug delivery systems.<sup>24</sup>

#### 1.6.1 Reservoir drug delivery systems

In a *reservoir drug delivery system*, the active pharmaceutical ingredient (API) is situated in a *core* surrounded by a polymeric membrane that control the release of the drug. Generally, the polymeric substance dissolves before the active agent is released from the formulation, thus delaying the dissolution of the *core* itself. A schematic representation of a reservoir-based drug delivery system is reported in Figure 5.

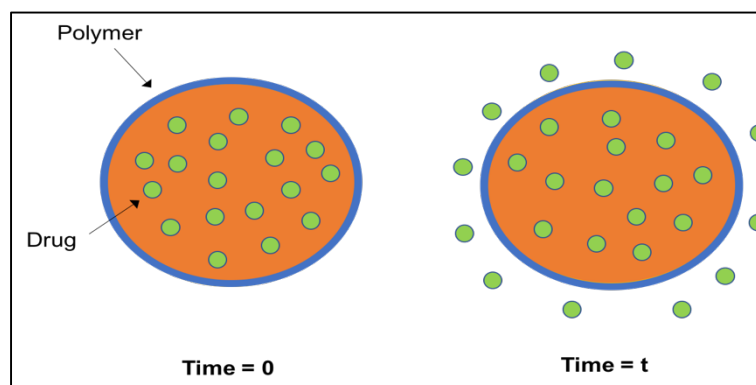


Figure 5. Schematic drawing of a reservoir drug delivery system.

#### 1.6.1.1 Procysbi<sup>®</sup> enteric-coated cysteamine formulation

In 2007, it was found that the administration of cysteamine in the small intestine tract resulted in the increase of plasma levels of cysteamine with an area under the curve higher, when compared with gastric administration of the drug (Cystagon<sup>®</sup>).<sup>7</sup> In detail, the white blood cell (WBC) cystine levels remained suppressed for up to 15 hours.<sup>25</sup> This led to the development of an enteric-coated cysteamine bitartrate formulation (Procysbi<sup>®</sup>, Raptor Pharmaceutical Inc., California, USA) which is administered every 12 hours, thus enhancing the adherence to the therapy.

International patent application WO 2007/002325 is related to an “enterically coated” tablet with a membrane that remains intact thorough the stomach and finally dissolves releasing the drug in the small intestine tract.<sup>26</sup> A suitable enteric coated formulation is a reservoir based system composed of a pH-sensitive polymer that dissolves in intestinal juices at a pH greater than 4.5, within the small intestine. A phase III clinical report demonstrated that Procysbi<sup>®</sup> was as effective as Cystagon<sup>®</sup> in maintaining low WBC cystine levels.<sup>14</sup> The commercially available capsules, containing 50 and 150 mg of cysteamine bitartrate, normally dissolving in the stomach, were coated with Eudragit L30D 55 polymer to obtain a delayed-release formulation which dissolve at pH values of between 5.5 to 6.<sup>26</sup> Hence, the twice-daily doses required by Procysbi<sup>®</sup> resulted to be effective in the improvement of the compliance and of patients’ quality of life.

#### 1.6.2 Matrix drug delivery system

Unlike the previously described reservoir drug based systems, *matrix drug delivery systems* include drug to be encapsulated or dispersed in a matrix. In detail, the drug is

dispersed in a polymer matrix to form a homogenous system. A schematic representation of a matrix based drug system is illustrated in Figure 6. A system with such characteristics can be used to form hydrophobic and/or hydrophilic matrices to allow a control and a prediction of drug release.<sup>27</sup>

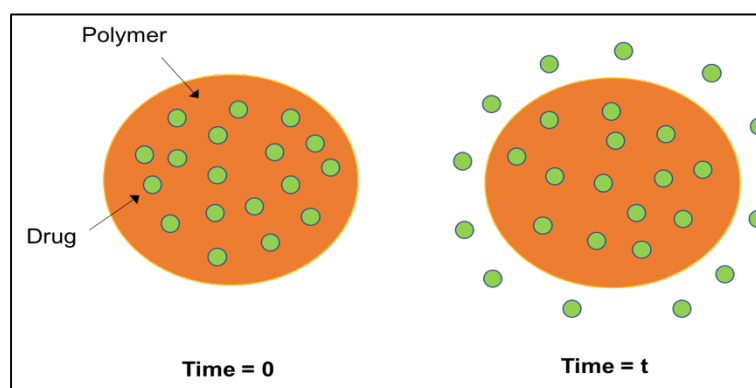


Figure 6. Schematic drawing of a matrix drug delivery system.

### 1.7 Cysteamine matrix-based drug delivery system: the novel formulation approach

As previously reported in Section 1.6.1.1, Procysbi<sup>®</sup> demonstrated to be useful for the long-term treatment of cysteamine in order to decrease the gastrointestinal side effects and provide an effective treatment for cystinosis. However, since the amount of cysteamine necessary for exercising the therapeutic effect differs from subject to subject, depending on age, weight and intensity of the condition, a more flexible pharmaceutical dosage form would be preferred. In fact, gastro-resistant tablets containing a fixed dose of the drug can not be divided in two pieces without damaging the gastro-resistance of the formulation. What is more, since cystinosis mainly affects pediatric patients, the administration of a tablet or a capsule would be very challenging.

#### 1.7.1 Cysteamine extemporaneous powder for oral administration

The solution could be an extemporaneous multi-unit dosage form, to be dispensed in sachets or in a dosing container that does not dissolve, releasing the drug, in the short period required by its dispersion in the liquid and swallowing. The proposed formulation offers several advantages. It is characterized by a notable flexibility since the dose is easy to tailor, allowing a dose titration according to patients needs following the physician prescription. In addition, cysteamine microparticles easily disperse in water

or other liquids, providing the obtainment of a smooth suspension to ingest. Finally, as a function of the polymers involved, the taste and the smell of the drug at the administration time could remain entrapped.

### 1.7.2 Taste masking

Nowadays, the majority of the pharmaceuticals are preferably administered through the oral route of administration since it is demonstrated to provide an easy and low-cost administration that ensures dosing accuracy.<sup>28</sup> However, a common issue to face is that several oral pharmaceuticals have unpleasant taste.<sup>29</sup> During the development of an oral pharmaceutical dosage form, taste plays a key role in governing patient acceptability and compliance, especially for paediatric and geriatric population.<sup>30</sup> In fact, it is proved that poor palatability and bitter taste are among the main reasons for patients non-compliance. Masking the bitter taste of drugs is a major challenge in the design and development of an oral pharmaceutical dosage form and it is of fundamental importance to improve the adherence to the therapy and therefore the therapeutic efficacy of the formulation.<sup>31</sup> It is important to highlight that only the soluble portion of the drug can produce the sensation of taste. Therefore, coating the active ingredient with a selected polymer film can prevent the release of the drug in saliva within the oral cavity thus masking the unpalatable taste.<sup>32</sup>

Taste masking is successfully obtained when, in the time points from 0 up to 5 minutes, the bitter drug is not detected or its detection is below the taste perception.<sup>30</sup> Various techniques have been identified to mask the bitter taste of drugs and enhancing at the same time the bioavailability of the dosage forms.<sup>33</sup> The most widely employed techniques for large scale production of pharmaceuticals dosage forms include: use of flavours and sweeteners, coating application, microencapsulation and inclusion complex formation. The addition of flavours is the simplest way to mask the bitter taste; however, sweet excipients alone are not entirely effective at masking the taste of bitter drugs.<sup>34</sup> On the contrary, by means of microencapsulation, the coating of the drug particles generate a physical barrier between the active agent and the taste buds, useful for masking the bad taste.<sup>35</sup> The most popular technologies for the manufacturing of microparticles include coacervation, solvent evaporation, fluid bed coating, spray drying and spray congealing.

### 1.7.3 Lipid excipients for the control of the drug release

The use of lipid-based dosage forms for sustained release has drawn considerable interest from pharmaceutical scientists.<sup>36</sup> Furthermore, lipid excipients are widely used as carriers to obtain a controlled release of the drug due to the ease of use, the versatility and their potential to create intellectual property through innovation in drug delivery especially in the field of modifying drug release systems.<sup>37,38</sup> Lipids are generally insoluble in water and are designated by means of their fatty acid composition, melting point and Hydrophilic-Lipophilic Balance (HLB). The FDA has disclosed a list of substances defined as GRAS (Generally Recognize as Safe) since not all the excipients are inert agents. In addition to this, there is also an official document named as Inactive Ingredient Guide (IIG) that collect a list of the maximum amount permitted for each excipient for a specific route of administration.<sup>37</sup> The most commonly lipids used include fats, oils, waxes, and complex lipids involved in various biological processes such as sterols, phospholipids, glycolipids, lipoproteins and sphingolipids.<sup>39</sup> In detail, lipid excipients can be generally classified, according to their composition, in: triglycerides, mixed glycerides and polar oils, co-solvents, surfactants and additives.<sup>37</sup> Triglyceride vegetable oils are employed very frequently as carriers for drug delivery. For example, D-tocopheryl polyethylene glycol succinate, derived from tocopherols, is commonly used as absorption enhancer for poorly water-soluble drugs.<sup>39</sup> Mixtures of glycerides and polar oils, like sorbitan trioleate (Span 85) and oleic oil, are useful to improve the solubilizing and the dispersing capacity of the formulation. In addition, co-solvents such as propylene glycol and polyethylene glycols (PEG) are normally utilized. Water-insoluble surfactants, having HLB values of between 8 and 12, including polyoxyethylene sorbitan trioleate (Tween 85), are in employment. What is more, water-soluble surfactants, including cetostearyl alcohol ethoxylate (Cetomacrogol), are of common use. Finally, even different lipid anti-oxidants, such as alpha-tocopherol, beta-carotene and propyl gallate, are often employed.<sup>37,39</sup> Solid lipid microparticles (MPs) can be manufactured using various technologies such as melt dispersion technique, solvent evaporation, hot and cold homogenization, spray drying and spray congealing.

### 1.8 Spray congealing technology

In recent years, several publications have focused the attention on the feasibility of the spray congealing technique for the manufacturing of solid lipid microparticles (SLMs)

to obtain sustained release formulations and to mask the unpleasant taste of bitter drugs.<sup>40,41</sup> Spray congealing, also named as spray chilling or spray cooling, has been widely employed since it offers many advantages. First of all, it is a rapid, single-operation and cost-effective technology that does not require the usage of any organic or aqueous solvents being in this way an environmental friendly manufacturing process because it avoids the need to remove residual solvents.<sup>42</sup> In addition, it is a less consuming technique in terms of time and energy.<sup>43</sup> Furthermore, it is easy to industrialize and for this reason it is highly recommended for industrial scale-up.<sup>44,45</sup> Since the process does not require the evaporation of solvents, the microparticles obtained are usually dense and non-porous, characterized by a smooth surface.<sup>46</sup> Apart from the previously reported advantages, spray congealing technology presents some drawbacks. For example, highly viscous liquids are generally difficult to process and the maximum drug loading attainable is set at 30-40% w/w. In addition, the process led to the obtainment of microparticle powders with a broad size distribution (50-600 microns) with a predominance of small and large microparticles depending on the viscosity of the liquid molten mass.<sup>40</sup> Because of the increasing attention toward biotechnological active agents, such as antibodies, vaccines and hormones, the major challenge in the development of protein based drug delivery system is the need to maintain protein integrity, stability and bioactivity during the manufacturing process.<sup>47</sup> Since spray congealing does not employ any solvents, it was proved to be particularly suitable to produce protein loaded drug delivery systems.<sup>48,49</sup>

The spray congealing process can be easily summarized into four main steps (Figure 7):

- atomization of a solution, emulsion or suspension of the drug in the carrier molten mass (generally lipids or polymers) which melts at a relatively low temperature, between 45-75 °C;
- contact between the droplets and the cold congealing gas (air or nitrogen) entering the drying chamber, normally in co-current configuration, maintained at a temperature below the carrier melting point;
- rapid cooling and solidification of the droplets into particles;
- separation of the particles from the congealing gas.

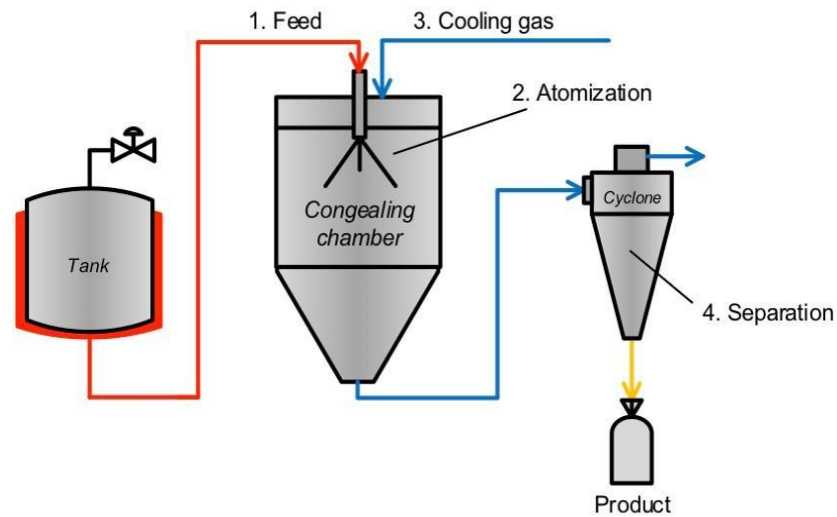


Figure 7. Spray Congealing setup.

As reported in many scientific papers, the success of the spray congealing technique strictly depends on various parameters, such as the atomization efficiency of the lipid molten mixture.<sup>40</sup> The proper selection of the ratio between the drug and the lipid carrier together with the control on the process parameters, such as temperature, nozzle wheel speed and feed flow rate has a strong impact on the final drug product. Among the several advantages, by selecting the lipophilic/hydrophilic excipient, it is possible to control either the release of the drug or to enhance the dissolution rate of poorly soluble drugs

## 2. AIM

The aim of the research project, that led to the submission of the European Patent Application EP 3308773A1, was the assessment of the feasibility of the spray congealing technique in the design and development of an oral dosage form composed of lipid matrix microparticles of cysteamine, optionally layered with a powder.<sup>50</sup>

Since the goal of the novel formulation approach herein presented was the improvement of the quality of life of patients, more palatable and controlled release formulations of cysteamine were manufactured. The preparation of a controlled release formulation was performed in order to prevent the drug from starting the release immediately during the administration in an appropriate liquid. The rationale is that, if the drug is not immediately available, even the organoleptic characteristics remain masked. This aspect is essential since nephropathic cystinosis mainly affect paediatric patients for which masking the unpleasant odour of the API is of crucial importance.

Therefore, cysteamine was formulated as a microparticle powder, by means of a controlled pharmaceutical dosage form, to control the release of high amount of cysteamine in the stomach, responsible of the adverse side effects as well as the unpleasant taste and smell of the drug. Cysteamine can be used as free base or as a derivative, such as a salt, a biological precursor or a metabolite.

In this part of the research project cysteamine bitartrate was used. The novel formulation idea described is based on the construction of a pharmaceutical dosage form structurally different from the *reservoir* coated systems. In detail, the formulation approach investigated is based on a *matrix* drug delivery system in which cysteamine is homogeneously dispersed in a polymer matrix. Each microparticle formed a micro-matrix, from which the drug was released by diffusion through the particle porosity. The final proposed drug product of cysteamine could be an extemporaneous oral powder dosage form filled in a sachet and dispersed by the patient in water or similar fluid before the administration.

To control the taste and even for drug release purpose, cysteamine was formulated with lipid excipients. As previously stated, the control on the drug availability can improve the adherence to the therapy. Moreover, the delivery of cysteamine at slow release rate could reduce the risk of gastric ulceration since the gastric mucosa would be not loaded with high amount of dissolved drug, at the same time, that determines nausea and the stomach distress.

A manufacturing process easy to industrialize and open to patent possibilities has been identified in the spray congealing technology on which several contract manufacturing companies created their business. Thus, lipid microparticles of cysteamine bitartrate were manufactured by means of the spray congealing technique. Usually, lipids having a low HLB value, hence lipophilic characteristics, are preferred for obtaining controlled release systems.<sup>51,52</sup>

Cysteamine lipid microparticles were characterized in terms of drug content and *in vitro* dissolution studies. Furthermore, an investigation on the solid state was performed. In addition, a taste masking efficiency test was assessed since one of the main goal was to mask the smell of the API.

In the preliminary explorative part of the project, a spray congealing equipment of a laboratory scale facility was employed to investigate the feasibility of the spray congealing technique in the manufacturing of lipid microparticles of cysteamine bitartrate. After the initial formulation design on a laboratory scale facility, the scale-up of no-GMP batches was carried out at Xedev bvba production site (Zelzate, Belgium). Since the lipid cysteamine bitartrate formulations are hydrophobic, the dispersion of the final product in water or in another fluid could be impaired. To overcome this issue, lipid microparticles were layered with spray-dried excipient microparticles, made of mannitol/lecithin or sucralfate/lecithin to form a hydrophilic layer on the surface of the microparticles, thus improving the wettability of the final drug product. Moreover, the excipient microparticles could mask the unpleasant taste of the drug. What is more, the presence of sucralfate microparticles could protect the gastric mucosa, since sucralfate is generally prescribed for the treatment of GI ulcers, thus combining to the increase in the surface wettability properties a protective action towards the gastric adverse effects of cysteamine.

### 3. MATERIALS AND METHODS

#### 3.1 MATERIALS

- Cysteamine bitartrate (batch n. 13100571, Recordati, Campoverde (MI), Italy);
- Carnauba wax (batch n. 56541, A.C.E.F., Fiorenzuola d'Arda (PC), Italy);
- Glyceril tristearate (stearin, batch n. D1408009, A.C.E.F., Fiorenzuola d'Arda (PC), Italy);
- Precirol ATO 5 (glycerol distearate type I, EP, batch n. 168141, Gattefossé, Saint-Priest, France);
- Compritol HD 5 ATO (behenoyl polyoxyl-8-glycerides NF, batch n. 159399, Gattefossé, Saint-Priest, France);
- Phosphoric acid 85% (batch n. 18H214004, A.C.E.F., Fiorenzuola d'Arda (PC), Italy);
- Sodium dodecyl sulphate (batch n. 31K0101, Sigma-Aldrich, St. Louis, USA);
- Sodium phosphate monobasic monohydrate ( $\text{Na}_2\text{HPO}_4 \cdot \text{H}_2\text{O}$ , batch n. 10186427, Merck, Darmstadt, Germany);
- Potassium dihydrogen phosphate ( $\text{KH}_2\text{PO}_4$ , batch n. Mø119104, A.C.E.F., Fiorenzuola d'Arda (PC), Italy);
- Sodium chloride (batch n. Nø133603, A.C.E.F., Fiorenzuola d'Arda (PC), Italy);
- Ethylenediaminetetraacetic acid (batch n. 61930, Riedel-de-Haën, Germany);
- Mannitol Ph.Eur. (batch n. 724028, Roquette, France);
- Sucralfate gel (batch n. 15-523-30, Lisapharma S.p.A., Erba (CO), Italy);
- Lecithin LIPOIDS45 (batch n. 574510-3130009, Lipoid AG, Charm, Switzerland).

All materials and reagents used were of analytical grade according to Ph.Eur. and USP.

## 3.2 METHODS

### 3.2.1 Manufacturing of cysteamine bitartrate lipid microparticles by spray congealing

#### 3.2.1.1 Laboratory scale production

The first object of the research project was the manufacturing of a microparticle powder consisting of lipid microparticles of cysteamine bitartrate by means of spray congealing technique. In this preliminary phase, a laboratory spray congealing equipment of the university of Bologna (Italy) was employed. Several lipid excipients, having different melting point and/or HLB (hydrophilic-lipophilic balance) values, were used. The melting point range of the selected lipid excipients is reported in Table II.

Table II. Melting point of the lipid excipients selected.

<b>Lipid excipients</b>	<b>Melting point (°C)</b>
Carnauba wax	82-86
Stearin	54-72*
Precirol ATO 5	53-57
Compritol HD 5 ATO	62-65

\* the broad melting range of stearin depends on the fact that stearin can crystallize on three polymorphic forms

The lipid microparticles of cysteamine bitartrate were prepared according to the following procedure. Primarily, the lipid carrier was heated at about 10 °C above its melting point until complete melting. Subsequently, keeping the heating temperature constant, cysteamine bitartrate was added under stirring to the lipid molten mass and left at that temperature for 5 minutes. A dispersion of the active principle in the lipid molten mass was observed. The suspension was sprayed through the spray congealing nozzle and, then, the lipid microparticles were collected and stored at room temperature. Batches of about 10 g each were manufactured.

#### 3.2.1.2 Industrial scale-up production of lipid microparticles of cysteamine bitartrate

After the initial formulation design on laboratory scale spray congealing equipment, the scale-up of no-GMP batches was carried out at Xedev bvba (Zelzate, Belgium) through the manufacturing of batches of 100 g of drug lipid microparticles. The equipment used was a Pro-CepT instrument. The method used for the obtainment of the spray congealing batches was the same previously described in Section 3.2.1.1. The schematic representation of the instrument employed is reported in Figure 8.

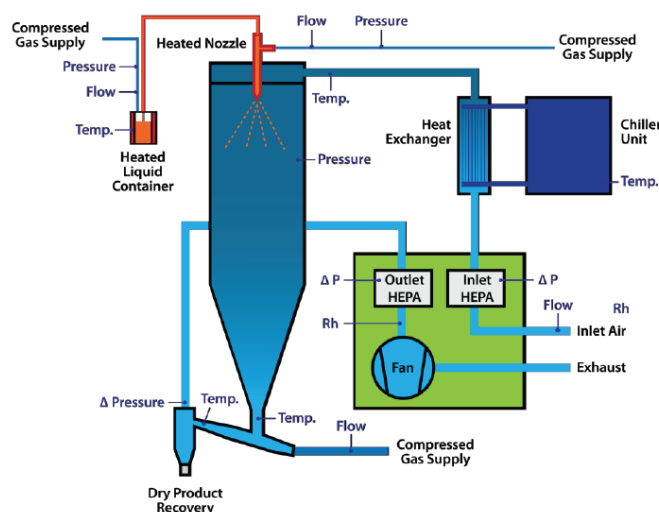


Figure 8. Representation of the Pro-CepT Spray Congealer.

### 3.2.2 HPLC quantification of cysteamine bitartrate

The analytical determination of cysteamine bitartrate in the lipid microparticles was carried out by means of HPLC (High Performance Liquid Chromatography). Two different analytical methods, regarding the two different phases of the project, the laboratory facility and the scale-up, were employed, respectively. The first one reported makes use of an isocratic method whereas the second one, used for the industrial scale-up production, is a gradient method that allows to investigate the amount of cysteamine impurities contained in the lipid microparticles.

#### 3.2.2.1 Laboratory scale production of lipid microparticles of cysteamine bitartrate

A Shimadzu chromatograph (LC-10AT, Shimadzu Europe GmbH, Duisburg, Germany) equipped with an isocratic LC-10AS pump and a SPD-10A UV-VIS spectrometer set at a fixed wavelength of 210 nm was employed. For the stationary phase, a Jupiter C18 column (4.6 x 150 mm, 5  $\mu\text{m}$ , 300  $\text{\AA}$ ; Phenomenex, USA) set at 50°C was used. The composition of the mobile phase was as follows: 620 ml of Millipore Grade water, 330 ml of acetonitrile, 50 ml of methanol, 1.4 ml of  $\text{H}_3\text{PO}_4$  85% (v/v) and 11.52 g of sodium dodecyl sulphate. The HPLC analysis was conducted at a flow rate of 1.6 ml/min, with an injection volume of 20  $\mu\text{l}$  (Waters 717 plus Autosampler, Waters Corporation, Milford, USA). The run time was 6 minutes, since the retention time of the peak corresponding to cysteamine was at about 4 minutes. The method was validated for linearity in the range 0.05-1 mg/ml ( $R^2$ : 0.99995), precision (RSD < 2%), LOD (0.3  $\mu\text{g/ml}$ ) and LOQ (1.2  $\mu\text{g/ml}$ ).

### 3.2.2.2 Scale-up of spray congealing prototypes

The analytical quantification of cysteamine in the lipid microparticles was performed by means of high performance liquid chromatography (HPLC) using a Thermo BDS C18 5  $\mu\text{m}$  250x4.6 mm column (CPS Analitica S.r.l., Milan, Italy) as stationary phase. In detail, the HPLC was equipped with a Shimadzu LC-10AT chromatograph (LC-10AT, Shimadzu Europe GmbH, Duisburg, Germany), provided with LC-10AS pumps and SPD-10A UV-VIS spectrometer. Mobile phase was composed of solvent A (11.52 g of sodium dodecyl sulphate dissolved in 380 ml of Milli-Q grade water, 300 ml of acetonitrile, 320 ml of methanol and 1.4 ml of  $\text{H}_3\text{PO}_4$  85% v/v) and solvent B (acetonitrile), mixed with gradient method according to Table III.

Table III. Gradient program used for the quantification of cysteamine bitartrate.

TIME (min)	Solvent A (% v/v)	ACN (% v/v)
0	100	0
6	100	0
8	60	40
11	60	40
15	100	0
25	100	0

The HPLC analysis was conducted at room temperature at a fixed wavelength of 210 nm, at a flow rate of 1.4 ml/min, with an injection volume of 100  $\mu\text{l}$  (Waters 717 plus Autosampler, Waters Corporation, Milford, USA). The run time was set at 25 minutes. The method was validated for linearity and limit of quantification (LOQ).

### 3.2.2.3 HPLC determination of impurities in cysteamine bitartrate lipid microparticles

The analytical method for the assay purity of cysteamine bitartrate was carried out in order to quantify the amount of impurities of cysteamine bitartrate present in the lipid microparticles. In particular, the quantification of cystamine, the major degradation product of cysteamine, and other unknown impurity products were deeply investigated. The analytical standards used for the determination of the impurities were as follows:

- Cysteamine bitartrate (REC 22/448, batch n. 551/75);
- 2,2-dimethylthiazolidine (batch n. 551/81);
- Cystamine 2HCl (batch n. BCBL6131V);
- Dicystamine acetone (batch n. 130054\_6).

Quantification of cysteamine bitartrate and its impurities was performed by HPLC on an Agilent apparatus (Series 1100). Gradient elution was carried out with Solvent A (composition for 1 liter: dissolve 11.52 g sodium dodecyl sulphate in 380 ml of HPLC grade water; then, add 300 ml of acetonitrile, 320 ml of methanol and 1.4 ml di H<sub>3</sub>PO<sub>4</sub> 85% v/v) and acetonitrile, according to the gradient program shown in Table IV.

Table IV. Gradient program used for the quantification of cysteamine bitartrate impurities.

TIME (min)	Solvent A (% v/v)	ACN (% v/v)
0	100	0
7	100	0
27	40	60
32	40	60
35	100	0
45	100	0

The method was validated for linearity in the range 12-210 µg/ml ( $R^2$ : 0.9999), precision (RSD < 2%) and LOQ (0.38) µg/ml. For the preparation of the standard solution, 10 mg of cysteamine bitartrate were accurately weighed in a 50 ml volumetric flask. Phosphate buffer pH 7.4 (Ph. Eur.) containing 0.1% (w/v) EDTA was added up to 50 ml for powder dissolution (Solution A). Then, a 1 mg/ml mother solution of cystamine 2HCl was prepared using phosphate buffer pH 7.4 (Ph. Eur.) containing 0.1% (w/v) EDTA (Solution B). Finally, 9.8 ml of Solution A and 0.2 ml of Solution B were mixed to obtain the standard solution (Solution C), 100 µl of which were injected into the HPLC apparatus. Samples were prepared according to the procedure described in Section 3.2.1.1 and then analyzed through HPLC.

### 3.2.3 Drug content determination

The determination of the drug content in the lipid microparticles was performed using the procedure here described. An accurately weighed amount of lipid microparticles, containing theoretically 25 mg of drug, was dispersed in a 100 ml volumetric flask containing 80 ml of phosphate buffer pH 7.4 (Ph. Eur.) and 0.1% (w/v) of EDTA. The dispersion was heated up, under magnetic stirring, to 100 °C and maintained at that temperature for 15 minutes to allow the complete melting of the lipid carrier. The flask was left to cool to room temperature under magnetic stirring and then brought to volume with the phosphate buffer pH 7.4, containing 0.1% (w/v) of EDTA. The dispersion was filtered through a 0.45 µm cellulose membrane and analysed by HPLC, following the method described in Section 3.2.2.1.

Standard solution was prepared by weighing 7.5 mg of cysteamine bitartrate and dissolving it in a 50 ml volumetric flask containing 50 ml of preheated phosphate buffer pH 7.4 and 0.1% (w/v) of EDTA.

### 3.2.4 Solid Lipid Microparticles (SLMs) characterization

#### 3.2.4.1 Particle size distribution

Particle size distribution was carried out at Xedev by dry powder laser diffraction (Sympatec, Etten-Leur, Netherlands). Powders were dispersed with compressed air at 1.5 bar through a Rodos dry disperser before sizing with a HELOS laser diffraction sensor. For each formulation, two measurements were combined with the combination software to obtain a stable PSD. The particle size distribution was further investigated by means of analytical sieving method according to Ph.Eur. 9<sup>th</sup> edition. The basic analytical method involves stacking of the steel sieves on top of one another in ascending degrees of coarseness. The powders were then placed on the top sieve. All stacked sieves were subjected to a standardized period of agitation, and then the weight of the powder retained on each sieve was accurately determined. The results are expressed as the weight percentage of powder in each sieve size range. The test sieving analysis is complete when the weight on any of the test sieves does not change by more than 5% or 0.1 g.<sup>53</sup>

#### 3.2.4.2 Scanning Electron Microscopy (SEM)

Morphological analysis was carried out by scanning electron microscopy (SEM) to investigate the morphology of the lipid powders and the surface characteristics of the spray-dried excipient microparticles. The microscope (SUPRA 40, Carl Zeiss NTS GmbH, Oberkochen, Germany) was operated under high vacuum conditions with 1.5 kV accelerating voltage, at different magnifications. Each powder was gently deposited on a double-sided adhesive black carbon tape pre-mounted on aluminum stubs and imaged without the need of a metallization process.

#### 3.2.4.3 Differential Scanning Calorimetry (DSC)

The thermal behaviour of lipid microparticles of cysteamine bitartrate was investigated by differential scanning calorimetry (DSC). Thermal events, associated to cysteamine bitartrate raw material and lipid microparticles, were analysed by means of a Mettler DSC 821<sup>e</sup> STAR<sup>e</sup> system (Mettler Toledo, Switzerland) micro calorimeter. Samples of about 4–5 mg in pierced aluminum crucibles and under a dynamic nitrogen atmosphere (100 ml·min<sup>-1</sup>) were

subjected to specific thermal program (25 – 140°C, 10 °C/min). Instrument calibration was performed with standard indium and zinc samples (purity > 99.99%) of known temperatures and enthalpies of melting.

#### 3.2.4.4 Hot Stage Microscopy (HSM)

The thermal behaviour of cysteamine lipid microparticles was further investigated by means of the hot stage microscopy (HSM). A hot stage apparatus (HSF 91, Linkam Scientific Instruments, Tadworth, UK) equipped with a polarising microscope (Labophot II Nikon, Tokyo, Japan) and a colour video camera (XC-003P Sony, Tokyo, Japan), supported by Image-Pro<sup>®</sup> Plus 4.0 software (Media Cybernetics, MD) allowed the recording of images during temperature scans. Samples were placed between two glass cover slides for the visual analysis through the video camera and subjected to heating scan from 25°C to 130°C at 10 °C/min.

#### 3.2.4.5 Powder X-ray Diffraction (PXRD)

Powder X-ray diffractometric (PXRD) patterns were recorded on a PW1050 diffractometer (Philips Analytical, Almelo, Netherlands), equipped with a curved graphite crystal, using Cu K $\alpha$  radiation. The scanning rate employed was 0.5° per minute over a 2 $\theta$  range of 2-50°.

### 3.2.5 *In vitro* dissolution studies

#### 3.2.5.1 Laboratory scale production of lipid microparticles of cysteamine bitartrate

*In vitro* dissolution tests were performed by means of the USP Apparatus II (Erweka DT6R, Dusseldorf, Germany) equipped with paddle rotating at 100 rpm, in 500 ml of simulated gastric fluid without enzymes at pH 1.2 set at a temperature of 37 ± 0.5 °C. The simulated gastric environment was selected to evaluate the drug release in the stomach. Standard solution was prepared by weighing 7.5 mg of cysteamine bitartrate and dissolving it in a 50 ml volumetric flask with simulated gastric fluid without enzyme at pH 1.2. Samples were collected after 5, 10, 15, 30, 45 and 60 minutes, filtered through a 0.45  $\mu$ m cellulose membrane and analysed by means of HPLC, following the procedure described in Section 3.2.2.1.

#### 3.2.5.2 Scale-up production of lipid microparticles of cysteamine bitartrate

In the scale-up of spray-congealing microparticles of cysteamine bitartrate, a dissolution method different from the one previously described in Section 3.2.5.1. was employed. The

dissolution method followed was developed by Recordati Industria Chimica e Farmaceutica S.p.A. In details, *in vitro* dissolution tests were performed by means of the USP Apparatus II (Erweka DT6R, Dusseldorf, Germany) equipped with paddle rotating at 75 rpm, in 900 ml of HCl 0.1N at pH 1.0 at a temperature of  $37 \pm 0.5$  °C. Standard solution was prepared by accurately weighing 15 mg of reference standard of cysteamine bitartrate; the powder was transferred in a 100 ml calibrated flask, dissolved and diluted to volume with Ultrapure water. After 5, 10, 15, 30, 45 and 60 minutes, samples were collected, filtered through a 0.45  $\mu\text{m}$  cellulose membrane and analysed by HPLC following the method described in Section 3.2.2.2.

### 3.2.6 Dry coating of cysteamine lipid microparticles with spray-dried excipients

To increase the wettability of the lipid microparticles and to improve the taste masking effect, the lipid microparticles were mixed with spray-dried mannitol/lecithin microparticles or with spray-dried sucralfate/lecithin microparticles in the ratio 9:1 (w/w %) lipid microparticles/excipient microparticles. In details, lipid microparticles were tumbled inside a bakelite cylindrical jar rotating on the major axis at 30 rpm for 45 minutes. The tumbling process was performed by introducing two stainless steel spheres, having a diameter of 1 cm, into the jar.<sup>54</sup>

#### 3.2.6.1 Mannitol/lecithin spray-dried microparticles

Spray-dried excipients of mannitol/lecithin microparticles were prepared with the following procedure. 18 g of mannitol were dissolved in 450 ml of Millipore water. 2 g of lecithin was dispersed in 50 ml of ethanol at 40°C. The two solutions were mixed together and spray dried by means of a Büchi Mini Spray Dryer B-191 (Büchi Labortechnik AG, Switzerland) according to the parameters here reported: inlet temperature 130°C, outlet temperature 64°C, feed rate 4 ml/min, nozzle diameter 0.7 mm, drying air flow 600 L/h.

#### 3.2.6.2 Sucralfate/lecithin spray-dried microparticles

Sucralfate/lecithin excipients microparticles were prepared by spray drying, starting from a dispersion of sucralfate gel with lecithin. In detail, 10 g of sucralfate gel, as sucralfate humid gel, were dispersed in 240 ml of Millipore water and homogenized by means of Ultraturrax (IKA® - Werke GmbH & Co, Germany). 0.5-1.5 g of lecithin was dissolved in 10 ml of ethanol at 40°C and mixed with sucralfate gel dispersion. Sucralfate gel and lecithin ratios used were between 95:5 and 85:15 (w/w %) keeping the solid concentration in the dispersion to spray

at 4% (w/v). The dispersion was spray dried using a Büchi Mini Spray Dryer B-191 (Büchi Labortechnik AG, Switzerland) set with the following parameters: inlet temperature 120-130°C, outlet temperature 51-62°C, feed rate 5-6 ml/min, nozzle diameter 0.7 mm, drying air flow 600 L/h.

### 3.2.7 Odour Masking Efficiency

As one of the goal of the research project was to mask the bad taste of cysteamine bitartrate, operators have smelled, separately, the lipid formulations. In particular, three operators were involved in the test during the laboratory scale-up whereas, regarding the industrial scale-up, the number of operators was increased to six. A scale from 0-5 was assigned to the cysteamine bitartrate lipid microparticles, following the scheme reported in Table V.

Table V. Scale used for the determination of the taste masking efficiency.

Scale	Smell of the lipid microparticles
0	Odourless
1	Low intensity
2	Medium intensity
3	Strong intensity
4	Very strong odour

### 3.2.8 Stability tests of Xedev prototypes after 2 weeks at 30°C/65% RH

The spray-congealing samples manufactured during the industrial scale-up of no-GMP batches were investigated for the stability assessment. Samples were stored two weeks at 30°C and 65% RH and then analysed. The results were compared to those collected at time 0.

## 4. RESULTS AND DISCUSSION

### 4.1 Preformulation study of cysteamine bitartrate pediatric extemporaneous dosage form for taste masking and prolonged release

#### 4.1.1 Laboratory scale manufacturing of Solid Lipid Microparticles of cysteamine bitartrate

##### 4.1.1.1 Spray congealing manufacturing

Spray congealing process was used for the manufacturing of cysteamine bitartrate lipid microparticles to obtain both taste masking effect and controlled release of the drug. Cysteamine bitartrate was formulated with lipid excipients. The presence of glyceril tristearate (stearin) in the formulation lowers the solidification temperature of the carnauba/stearin wax binary mixture. Carnauba wax is a complex mixture of acid and hydroxyl acid esters used to obtain controlled release formulations. Carnauba wax mainly contains esters of fatty acids (80-85%), fatty alcohols (10-15%), acids (3-6%) and hydrocarbons (1-3%); it is soluble in chloroform and toluene and practically insoluble in water. It appears as light brown-yellow powder and has no smell; it is commonly considered as non-irritating and non-toxic excipient. Furthermore, Precirol ATO 5 (glycerol distearate type I Ph. Eur., HLB = 2) and Compritol HD 5 ATO (behenoyl polyoxyl-8 glycerides, HLB = 5) were employed. They are common lipid excipients used as coating agents for controlled and prolonged release. The melting point of the Precirol ATO 5 is between 53 and 57 °C; it is a fine and white powder. Precirol ATO 5 is biodegradable and is also used to mask the flavor. Compritol HD 5 ATO is glyceride with an intermediate melting point containing PEG-8 esters. Cysteamine lipid microparticles were prepared using the composition in which the cysteamine bitartrate content was between 25 and 40% (w/w) and the lipid excipients from 60 to 75% (w/w). Different types of lipid microparticles containing cysteamine bitartrate, using the spray congealing technique, were prepared. The composition of each formulation, the yield of the process and the process parameters used are reported in Table VI.

Table VI. Composition of the lipid microparticles of cysteamine bitartrate produced by spray congealing, process parameters and experimental drug content. Results are expressed as mean value  $\pm$  standard deviation (n=3).

Formulations	Composition	Theoretical drug/excipient ratio (w/w %)	Nozzle Temperature (°C)	Atomization pressure (bar)	Yield (%)
#1	Cysteamine bitartrate/ Carnauba wax	25:75	91	2	56
#2	Cysteamine bitartrate/ Carnauba wax/Stearin	30:35:35	92	2	60
#3	Cysteamine bitartrate/ Carnauba wax/Stearin	40:30:30	92	2	46
#4	Cysteamine bitartrate/ Precirol ATO 5	25:75	50	2.5	52
#5	Cysteamine bitartrate/ Precirol ATO 5	25:75	70	2.5	77
#6	Cysteamine bitartrate/ Precirol ATO 5	30:70	71	2.5	36
#7	Cysteamine bitartrate/ Compritol HD 5 ATO	25:75	70	2.5	56
#8	Cysteamine bitartrate/ Compritol HD 5 ATO	30:70	72	2.5	49

The drug content determination was carried out according to the procedure described in Section 3.2.3. The results are reported in Table VII.

Table VII. Content (%) of cysteamine bitartrate in the lipid microparticles.

Results are expressed as mean value  $\pm$  standard deviation (n=3).

Formulations	Drug content (%)
#1	23.2 $\pm$ 0.3
#2	35.1 $\pm$ 3.3
#3	37.8 $\pm$ 0.4
#4	22.9 $\pm$ 2.2
#5	26.6 $\pm$ 1.3
#6	31.7 $\pm$ 2.9
#7	23.2 $\pm$ 1.5
#8	27.1 $\pm$ 0.9

A variability in the drug content, compared to the theoretical value, was observed. This was probably due to the difficulty to obtain an homogeneous dispersion of cysteamine bitartrate in the molten lipid excipient during the spray congealing process. In fact, increasing the amount of cysteamine bitartrate dispersed in the molten lipid excipient, the drug particles tended to sediment during the spray congealing process.

#### 4.1.2 Solid Lipid Microparticles characterization

##### 4.1.2.1 Scanning Electron Microscopy (SEM)

The morphological characterization of the lipid microparticles was performed with scanning electron microscopy (SEM). The lipid microparticles, consisting of carnauba wax or carnauba wax/stearin, were almost spherical, but with an irregular surface (Figure 9). Also in the case of lipid microparticles obtained with Precirol ATO 5, the shape was spherical but the irregularity of the surface was more evident (Figure 10).

Finally, the lipid microparticles made of Compritol HD 5 ATO showed round shape with more homogeneous surface (Figure 11).

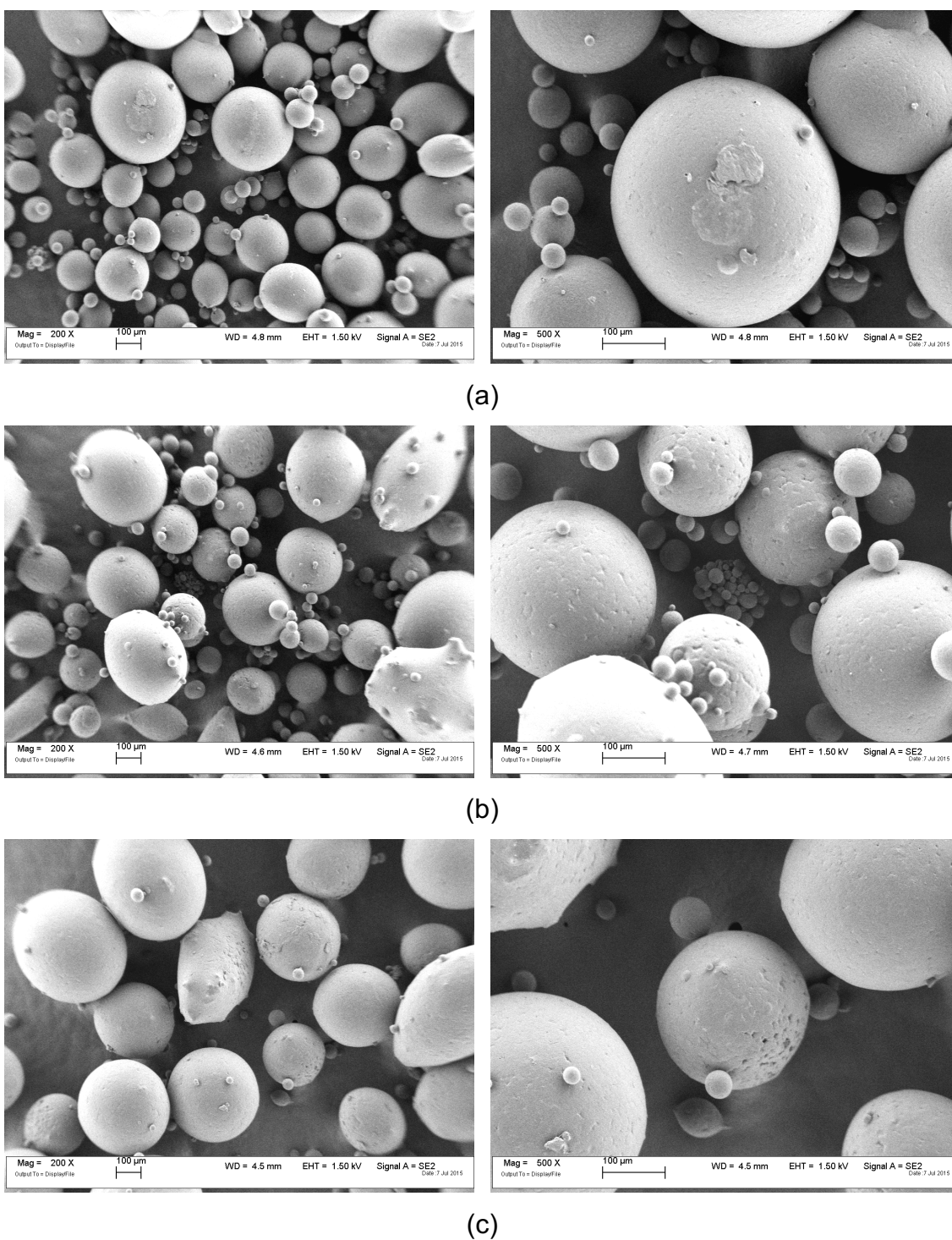
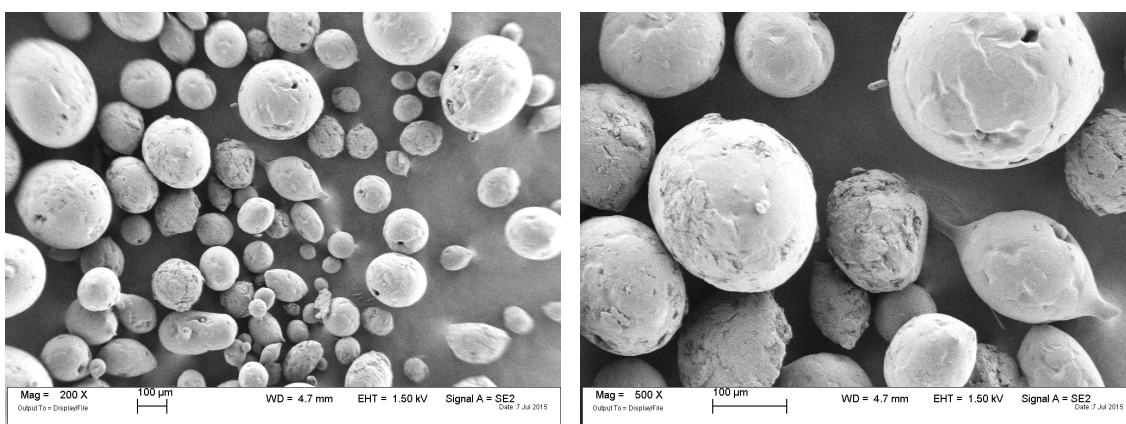
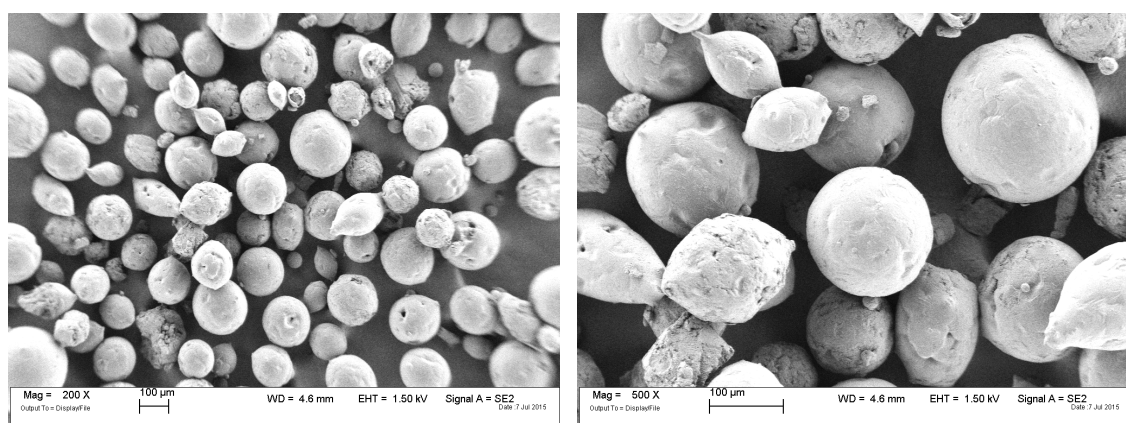


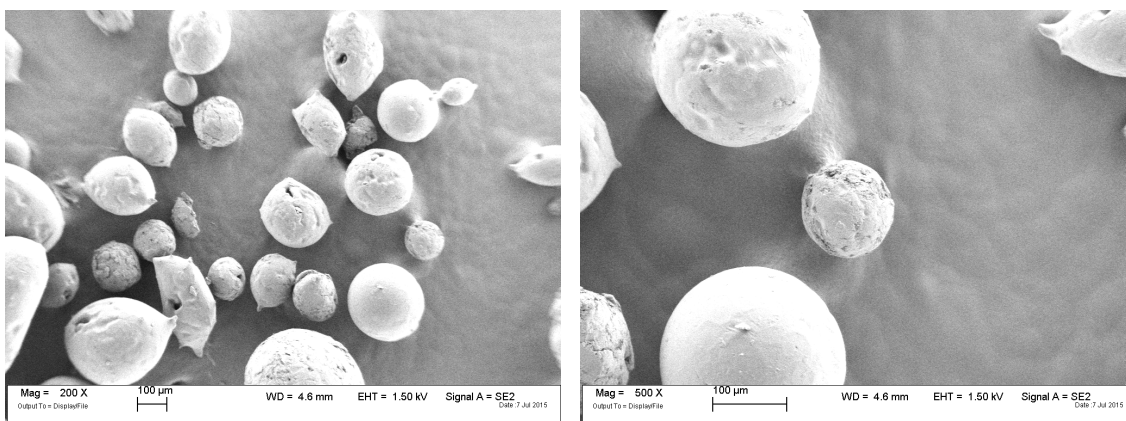
Figure 9. SEM Images of cysteamine bitartrate lipid microparticles at two different magnifications (left side 200X and right side 500X): (a) Formulation #1\_ Cysteamine bitartrate/Carnauba wax 25:75%, (b) Formulation #2\_ Cysteamine bitartrate/Carnauba wax/Stearin 30:35:35% and (c) Formulation #3\_ Cysteamine bitartrate/Carnauba wax/Stearin 40:30:30%.



(a)



(b)



(c)

Figure 10. SEM Images of cysteamine bitartrate lipid microparticles at two different magnifications (left side 200X and right side 500X): (a) Formulation #4\_Cysteamine bitartrate/Precirol ATO 5 25:75% (nozzle temp. 50°C), (b) Formulation #5\_ Cysteamine bitartrate/Precirol ATO 5 25:75% (nozzle temp. 70°C) and (c) Cysteamine bitartrate/Precirol ATO 5 30:70%.

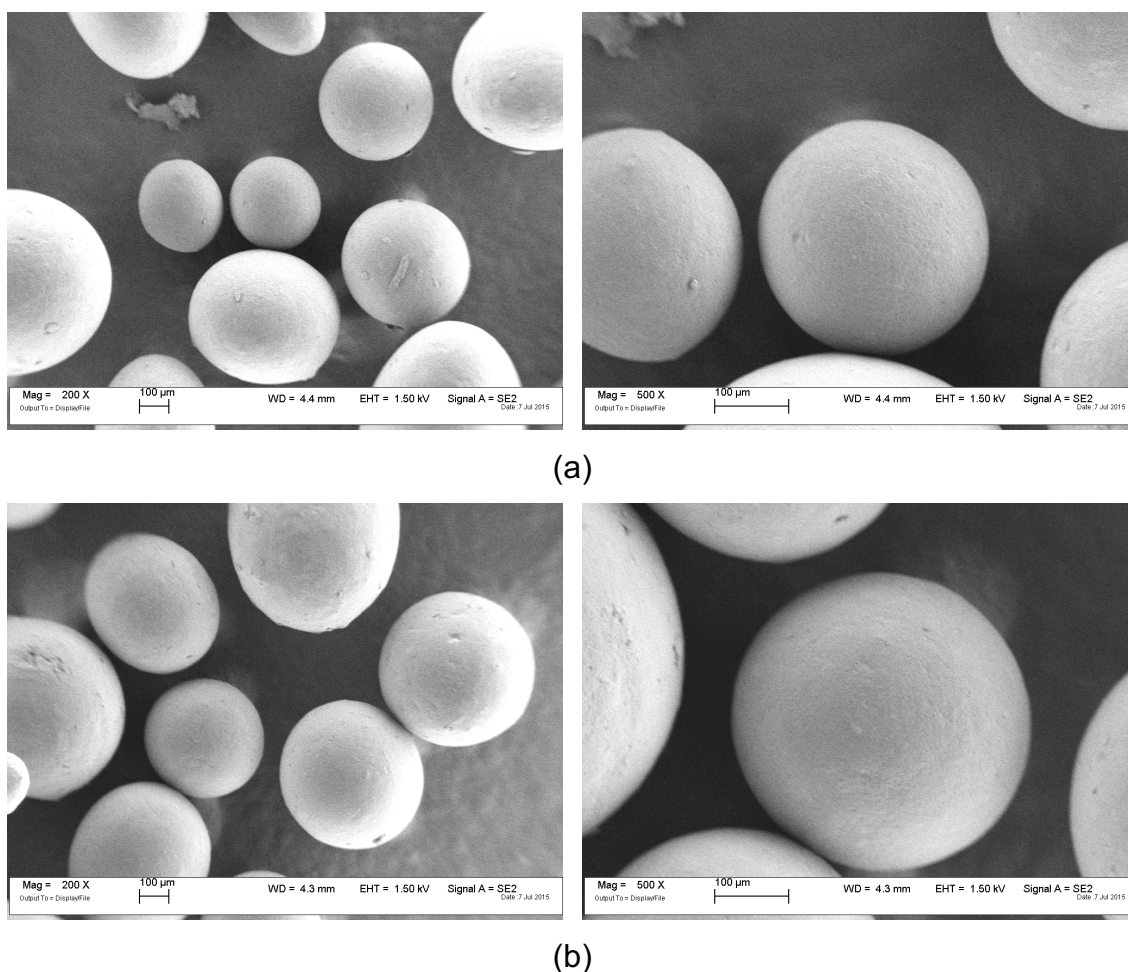


Figure 11. SEM Images of cysteamine bitartrate lipid microparticles at two different magnifications (left side 200X and right side 500X): (a) Formulation #7\_Cysteamine bitartrate/Compritol HD 5 ATO 25:75% and (b) Formulation #8\_Cysteamine bitartrate/Compritol HD 5 ATO 30:70%.

#### 4.1.2.2 Thermal behaviour

The thermal behaviour of the cysteamine lipid microparticles was investigated by differential scanning calorimetry and hot stage microscopy.

The thermogram of cysteamine bitartrate raw material was characterized by a broad endothermic band in the 50-80°C temperature range, associated with an endothermic peak at about 78°C (1<sup>st</sup> event), followed by a narrow peak at 120°C (2<sup>nd</sup> event) (Figure 12). This behaviour was explained by the presence of two polymorphs of cysteamine bitartrate. The polymorphism of another cysteamine salt, i.e. cysteamine hydrochloride, has been described in literature.<sup>55</sup> Then, the first event could be attributed to a solid-solid transition from the polymorphic form I, stable at room temperature, in the polymorph III, having melting point of 120°C.

Concerning the thermal behaviour of the lipid microparticles obtained by spray congealing,

Formulation #1, containing carnauba wax as lipid carrier, showed two superimposed endothermic peaks at around 74 and 84°C, due to the melting of cysteamine bitartrate polymorph I and carnauba wax, respectively (see Figure 12). The endothermic event corresponding to the fusion of cysteamine bitartrate polymorph III was at limits of detection around 120°C. The thermogram of Formulation #2 (containing carnauba wax/stearin as lipid carrier) differed for the presence of an endothermic peak at 55°C, due to the melting of stearin, and a broad endothermic peak at about 78°C, attributed to the overlapping of both cysteamine bitartrate polymorph I and carnauba wax melting. The second endothermic event of cysteamine bitartrate was detectable around 120°C, even if an event of small entity. The thermogram of lipid microparticles #2 differed for the presence of an endothermic peak at 55°C, due to the melting of stearin, and a broad endothermic peak at about 78°C, attributed to the fusion of both cysteamine bitartrate (1<sup>st</sup> event) and carnauba wax. Finally, in the case of lipid microparticles #3, the 2<sup>nd</sup> endothermic event of cysteamine bitartrate was more evident, due to the presence of a higher amount of drug in the lipid microparticles.

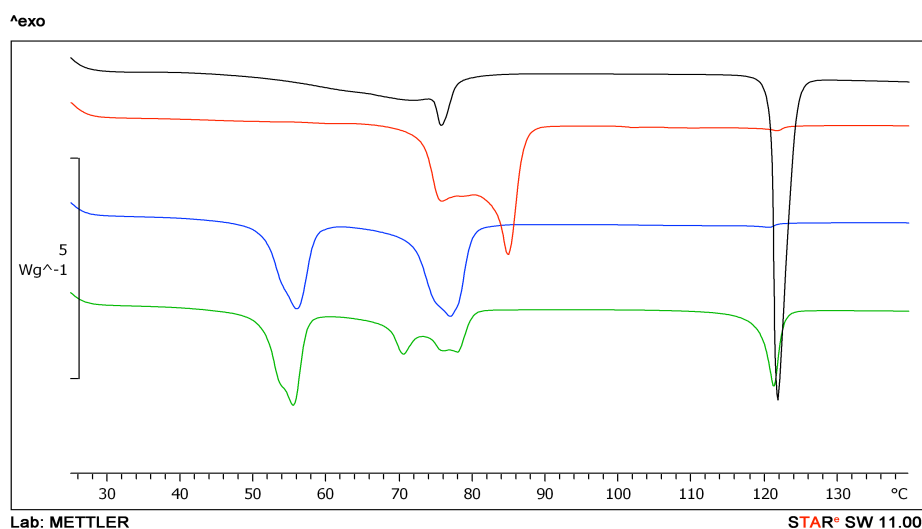


Figure 12. DSC thermograms of cysteamine bitartrate raw material (black curve), Formulation #1 (Cysteamine bitartrate/Carnauba wax 25:75%, red curve), Formulation #2 (Cysteamine bitartrate/Carnauba wax/Stearin 30:35:35%, blue curve) and Formulation #3 (Cysteamine bitartrate/Carnauba wax/Stearin 40:30:30%, green curve).

The thermal behaviour of Formulations #4 - #6, containing Precirol 5 ATO, was characterized by the presence of peak around 60°C, attributed to the lipid carrier, and the two endothermic events attributed to the drug (Figure 13).

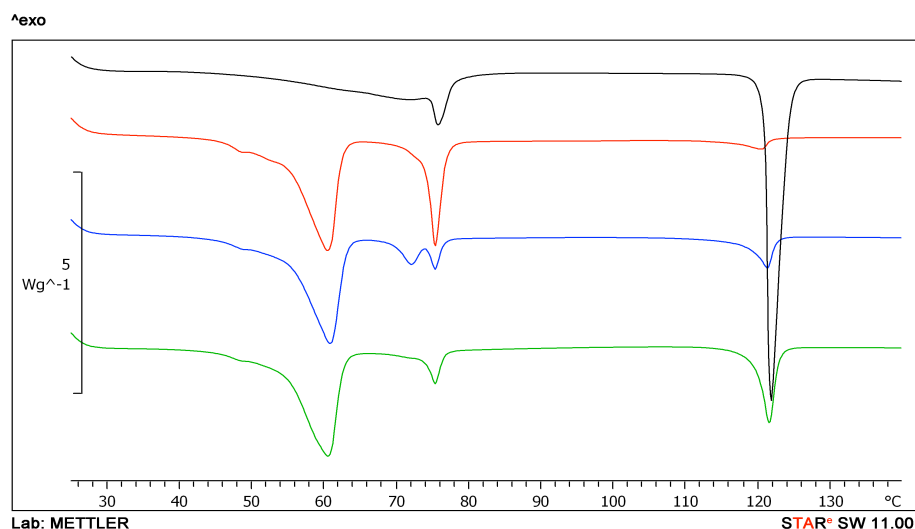


Figure 13. DSC thermograms of cysteamine bitartrate raw material (black curve), Formulation #4 (Cysteamine bitartrate/Precirol ATO 5 25:75%, nozzle temp. 50°C, red curve), Formulation #5 (Cysteamine bitartrate/Precirol ATO 5 25:75%, nozzle temp. 70°C, blue curve) and Formulation #6 (Cysteamine Bitartrate/Precirol ATO 5 30:70%, nozzle temp. 70°C, green curve).

Even in the case of Formulations #7 and #8, both containing Compritol HD 5 ATO, the melting of both lipid carrier, in 55-65°C range, and drug (about 78 and 120°C) was detectable (Figure 14).

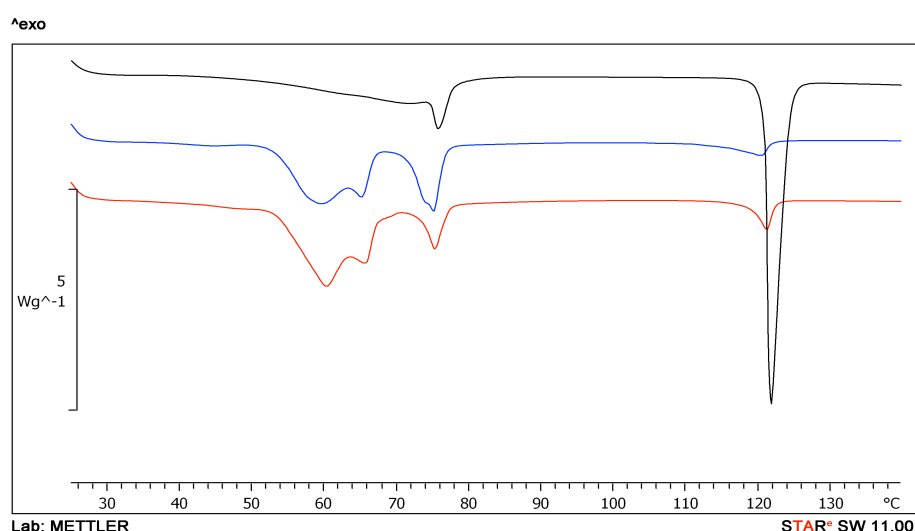


Figure 14. DSC thermograms of cysteamine bitartrate raw material (black curve), Formulation #7 (Cysteamine bitartrate/Compritol HD 5 ATO 25:75%, blue curve) and Formulation #8 (Cysteamine Bitartrate/Compritol HD 5 ATO 30:70%, red curve).

The thermal behaviour of cysteamine lipid microparticles was also confirmed by HSM. As example, the HSM images of lipid microparticles Formulation #3 are reported in Figure 15. The changes in the images at 58, 74 and 83 °C were due to the melting of stearin, cysteamine bitartrate (1<sup>st</sup> event) and carnauba wax, respectively. The crystals still present (Figure 15(d)) are attributed to cysteamine bitartrate which completely melts at 120°C.

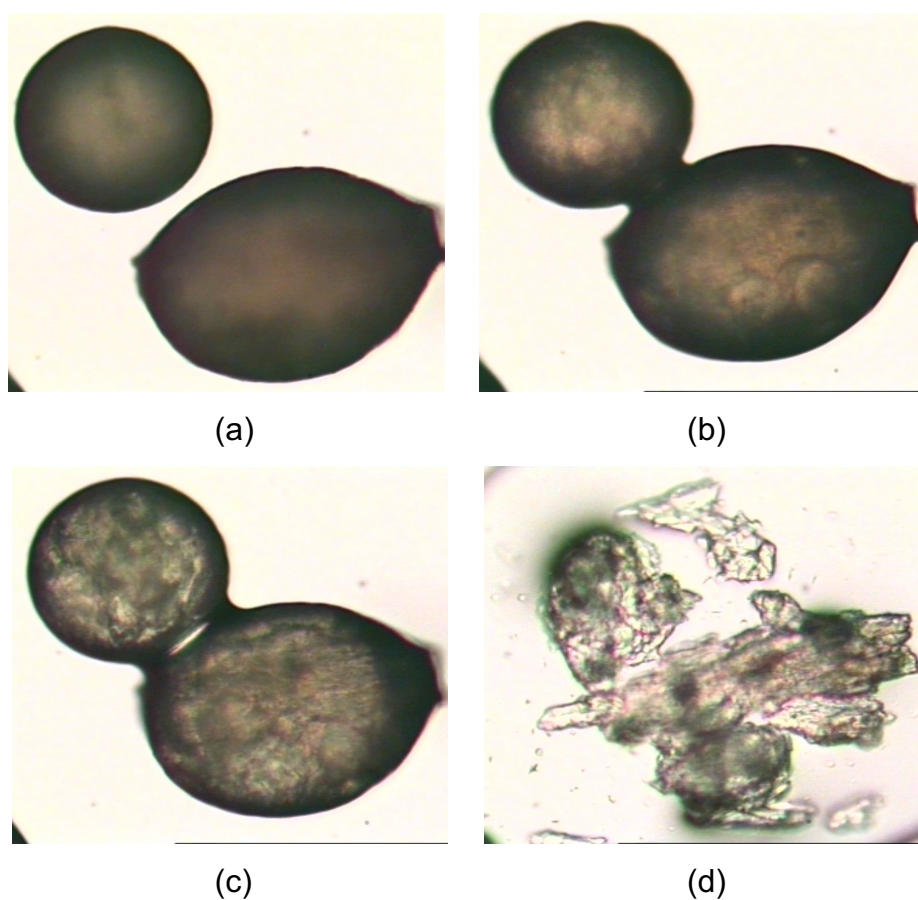


Figure 15. HSM Images of Formulation #3 (Cysteamine bitartrate/Carnauba wax/Stearin 40:30:30%) during heating: (a) 25°C, (b) 58°C, (c) 74 and (d) 83°C.

Then, from DSC and HSM analyses it was possible to assume that a lipid matrix of cysteamine bitartrate was obtained by means of spray congealing process. The drug was dispersed in the lipid carrier. In the case of lipid microparticles #1-3, in which the temperature of nozzle was about 90°C, the drug was partially dissolved in the melted lipid carrier.

#### 4.1.3 Odour masking efficiency

As one of the goal of the research thesis was to mask the bad taste of cysteamine bitartrate, the lipid microparticles were smelled by three operators, separately, to evaluate the taste masking efficiency of the formulations, according to the procedure described in Section 3.2.7. As it could be observed from the scores reported in Table VIII, Formulations #1, #5, #6 and #7 succeeded in the obtainment of an acceptable taste masking effect. It is important to underline that Formulations #1, #5 and #7 contain a lower percentage of the drug. Furthermore, Precirol ATO 5 seems to have a greater ability to mask the cysteamine bad smell even when the drug percentage is increased from 25 to 30%.

Table VIII. Smell of the drug lipid microparticles.

Formulations	Impression on smell		
	Operator 1	Operator 2	Operator 3
#1	0	0	0
#2	3	3	2
#3	1	2	2
#4	4	4	4
#5	0	1	1
#6	1	1	1
#7	0	0	0
#8	2	4	4

#### 4.1.4 *In vitro* dissolution studies

The *in vitro* dissolution studies were performed according to the procedure described in Section 3.2.5.1. The dissolution studies were set up to 60 minutes since, in agreement with the company, the interest was to investigate the controlled release of the drug over a period of time no longer than 1 hour, since the main goal of the modified release formulation was to mask the taste and the smell of cysteamine during the administration time. The dissolution profiles of the lipid microparticles obtained by spray congealing are shown in Figures 16-18. Cysteamine bitartrate raw material was completely dissolved in 10 minutes. The lipid microparticles containing carnauba wax (Formulation #1) or a mixture of carnauba wax and stearin (Formulations #2 and #3) showed a release of cysteamine of about 40–45% after 5 minutes and more than 80% after 30 minutes, independently from the drug amount loaded in the lipid carrier.

The Formulations #4, #5 and #6 contain Precirol ATO 5, a more lipophilic excipient. The *in vitro* dissolution profiles of Formulations #5 and #6 exhibited a rapid drug release (Figure 17), even faster than cysteamine bitartrate raw material in the first 5 minutes. On the other hand, there is an interesting result with Formulation #4 that met the drug release profile of 50% in the first 15 minutes and the rest in one hour. This could be associated to a smaller amount of the drug loaded in the lipid microparticles with respect to the other two formulations (#5 and #6).

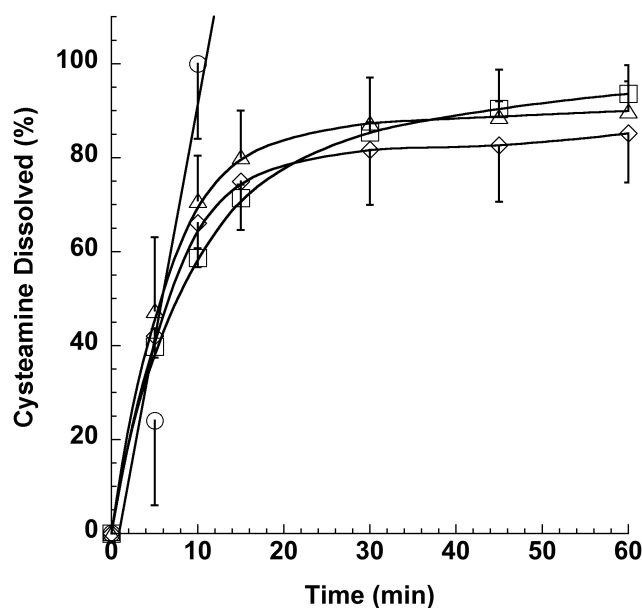


Figure 16. Dissolution profiles of cysteamine in simulated gastric fluid pH 1.2: (○) cysteamine bitartrate raw material, (□) Formulations #1 (Cysteamine bitartrate/Carnauba wax 25:75%), (◇) Formulation #2 (Cysteamine bitartrate/Carnauba wax/Stearin 30:35:35%) and (△) Formulation #3 (Cysteamine bitartrate/Carnauba wax/Stearin 40:30:30%). Results are expressed as mean value  $\pm$  standard deviation ( $n = 3$ ).

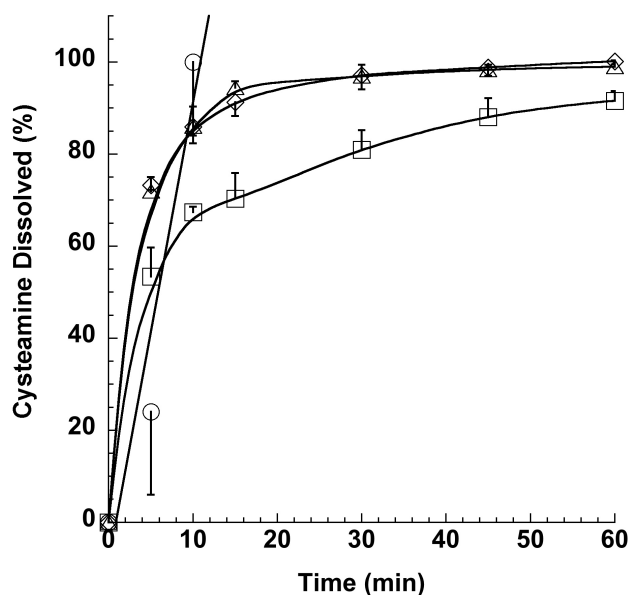


Figure 17. Dissolution profiles of cysteamine in simulated gastric fluid pH 1.2: (○) cysteamine bitartrate raw material, (□) Formulations #4 (Cysteamine bitartrate/Precirol ATO 5 25:75%, nozzle temp: 50°C), (◇) Formulation #5 (Cysteamine bitartrate/Precirol ATO 5 25:75%, nozzle temp: 70°C) and (△) Formulation #6 (Cysteamine bitartrate/Precirol ATO 5 30:70%). Results are expressed as mean value  $\pm$  standard deviation ( $n = 3$ ).

Moreover, at the nozzle temperature of 50°C for the lipid microparticles manufacturing, polymorph I of cysteamine is not dissolved but dispersed in the molten lipid carrier and this could affect the drug release from the lipid matrix.

The lipid microparticles #7 and #8, both containing Compritol HD 5 ATO as lipid carrier, showed a greater drug release control (Figure 18). In fact, about 20% of cysteamine was dissolved after 5 minutes. Less than 50% of drug dissolved in 15 minutes and the rest in one hour. In addition, Formulation #8, containing a drug loading of 30%, was characterized by a release of about 70% of cysteamine bitartrate after 45 minutes.

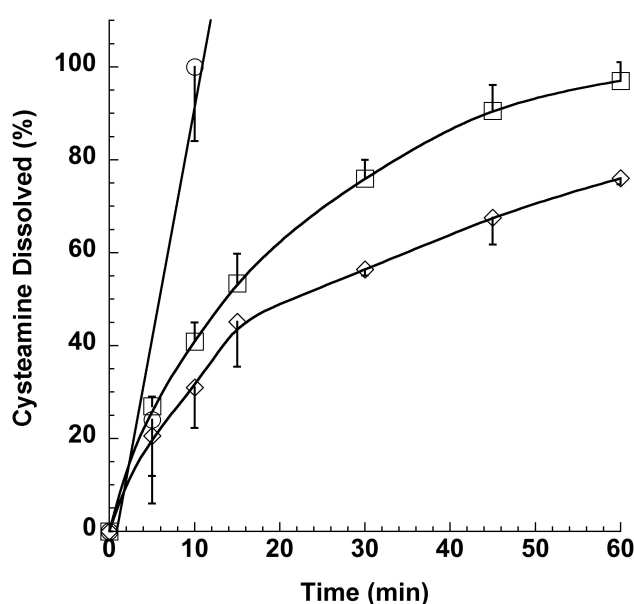


Figure 18. Dissolution profiles of cysteamine in simulated gastric fluid pH 1.2: (○) cysteamine bitartrate raw material, (□) Formulations #7 (Cysteamine bitartrate/Compritol HD 5 ATO 25:75%) and (◇) Formulation #8 (Cysteamine bitartrate/Compritol HD 5 ATO 25:75%). Results are expressed as mean value  $\pm$  standard deviation ( $n = 3$ ).

This laboratory scale investigation of cysteamine lipid microparticles evidenced that the lipid carrier Compritol HD 5 ATO (Formulations #7 and #8) showed the highest capacity, compared to the other lipid excipients, to control the release of cysteamine bitartrate in acid environment. However, due to the hydrophobic property of the lipid microparticles, they were not well dispersed in the dissolution medium but tended to remain on the surface thus affecting the dissolution process. In fact, as a consequence, a residue of the lipid microparticles was present in the dissolution vessel after 1 h of dissolution.

#### 4.1.5 Dry coating of cysteamine lipid microparticles with spray-dried excipients

Spray-dried mannitol/lecithin and sucralfate/lecithin microparticles were prepared according to the method described in Section 3.2.6. A hydrophilic layer of the spray-dried excipient microparticles was deposited on the surface of the cysteamine bitartrate lipid microparticles simply by mixing, with the purpose to increase the wettability of the lipid microparticles. Thus, mannitol/lecithin microparticles or sucralfate/lecithin microparticles were manufactured by spray drying and mixed with the lipid microparticles (1:9 ratio w/w%). This process, defined dry layering coating, is based on the affinity between mannitol/lecithin microparticles to the surface of lipid microparticles.<sup>54</sup>

The dry coating of the lipid microparticles with excipient microparticles nicely shows the capability of mannitol/lecithin microparticles, having round shape, to uniformly coat the surface of lipid particle (Figure 19). The microparticles with sucralfate are less uniformly coated (Figure 20).

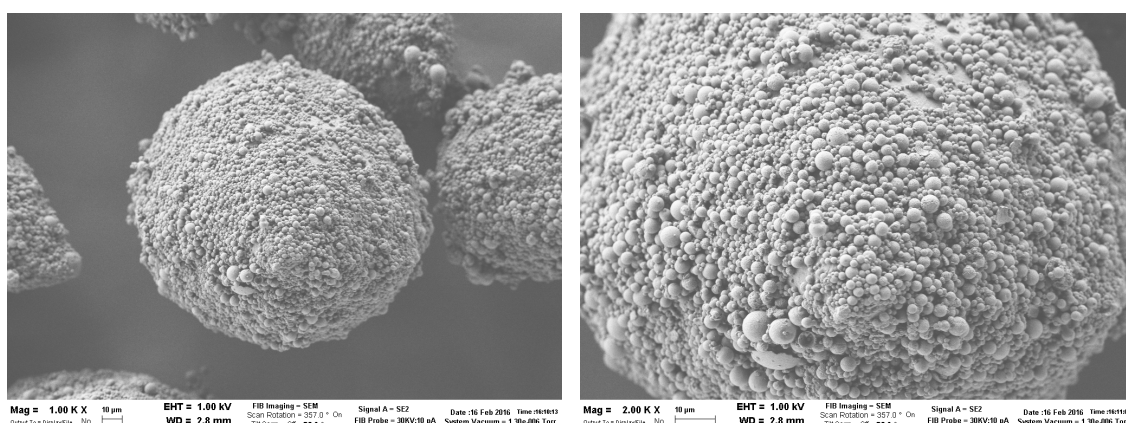


Figure 19. SEM Images of Formulation #7 (Cysteamine bitartrate/Compritol HD 5 ATO 25:75%) with mannitol/lecithin spray-dried microparticles (9:1 w/w%).

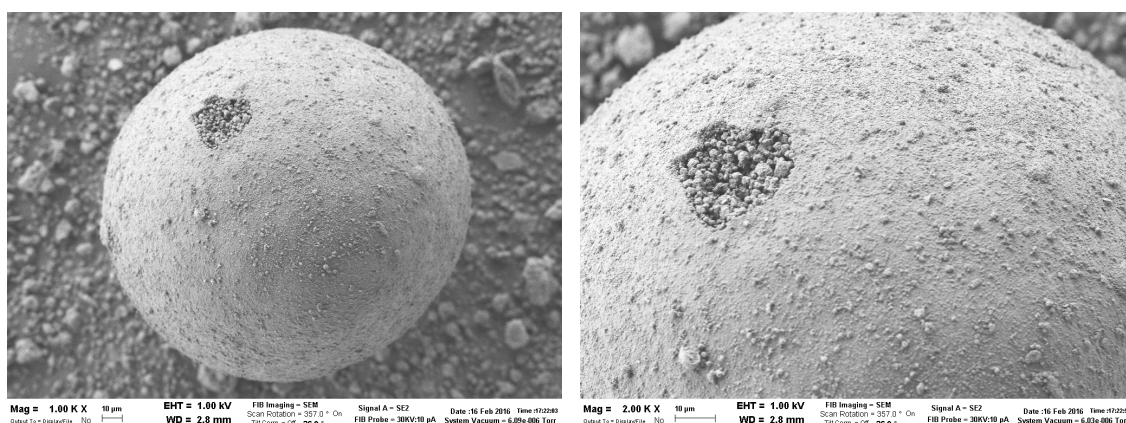


Figure 20. SEM Images of Formulation #7 (Cysteamine bitartrate/Compritol HD 5 ATO 25:75%) with sucralfate/lecithin spray-dried microparticles (9:1 w/w%).

By mixing, a hydrophilic layer of spray-dried excipient microparticles was then deposited on the surface of cysteamine bitartrate lipid microparticles, increasing their wettability. In fact, the drug release rate accelerates after the coating of the lipid microparticles with the excipient microparticles, as the Figures 21 and 22 clearly demonstrates. The use of microparticles containing sucralfate in the coating could also provide a solution to the problem of gastro-irritation of the drug.

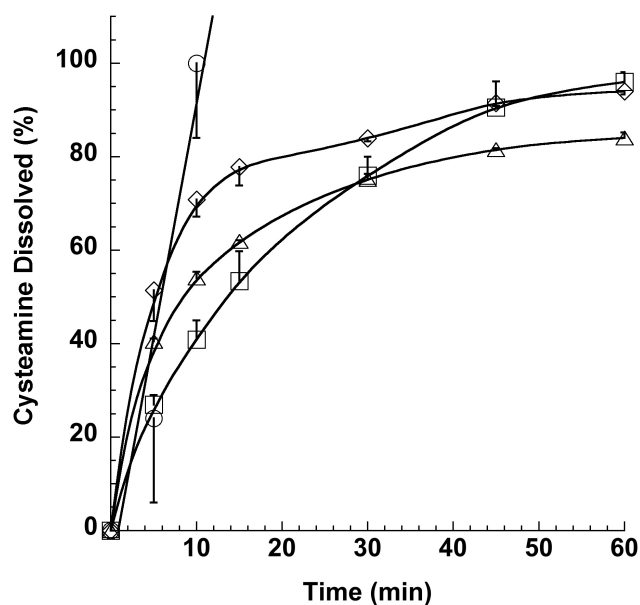


Figure 21. Dissolution profiles of cysteamine in simulated gastric fluid pH 1.2: (○) cysteamine bitartrate raw material, (□) Formulations #7 (Cysteamine bitartrate/Compritol HD 5 ATO 25:75%) and the corresponding layered lipid microparticles with (◇) mannitol/lecithin spray-dried microparticles or with (△) sucralfate/lecithin spray-dried microparticles. Results are expressed as mean value  $\pm$  standard deviation ( $n = 3$ ).

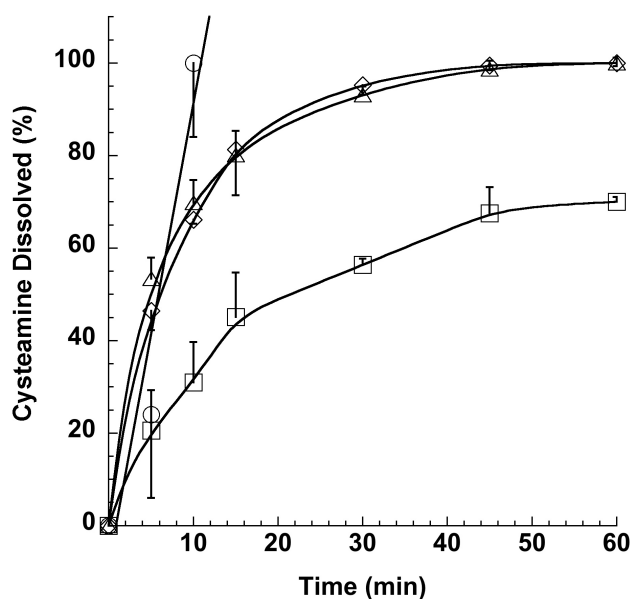


Figure 22. Dissolution profiles of cysteamine in simulated gastric fluid pH 1.2: (○) cysteamine bitartrate raw material, (□) Formulations #8 (Cysteamine bitartrate/Compritol HD 5 ATO 30:70%) and the corresponding layered lipid microparticles with (◇) mannitol/lecithin spray-dried microparticles or with (△) sucralfate/lecithin spray-dried microparticles. Results are expressed as mean value  $\pm$  standard deviation ( $n = 3$ ).

## 4.2 No-GMP scale-up production of Solid Lipid Microparticles of cysteamine bitartrate

### 4.2.1 Spray congealing manufacturing

Considering the capacity of Compritol HD 5 ATO to better control the drug release from the lipid matrix, this excipient was selected for the scale-up manufacturing of the cysteamine bitartrate lipid microparticles.

The scale-up production of cysteamine bitartrate lipid microparticles started with the manufacturing of three batches, corresponding to the replica of Formulations #7 and #8, both containing Compritol HD 5 ATO as lipid carrier, in a ratio 25:75% (w/w) and 30:70% (w/w), respectively. The instructions given to Xedev were to prepare batches of 100 g of drug lipid microparticles, with a particle size lower than 500 microns, keeping the same process parameters as the ones used in the laboratory scale manufacturing. It was not possible to keep the nozzle temperature used for the manufacturing of Formulations #7 and #8. This was mainly due to the high viscosity of the fluid after the dispersion of cysteamine bitartrate amount in the lipid molten mass. For this reason, it was necessary to increase the nozzle temperature up to 90°C. The composition and the process parameters of the scaled formulations are reported in Table IX.

Table IX. Composition of the formulations and process parameters used at Xedev facilities.

Lipid microparticles	Composition	Ratio (w/w %)	Nozzle Temperature (°C)	Atomization pressure (bar)	Yield (%)
#9	Cysteamine bitartrate/Compritol HD 5 ATO	25:75	90	1.7	81
#10	Cysteamine bitartrate/Compritol HD 5 ATO	25:75	90	2.5	91
#11	Cysteamine bitartrate/Compritol HD 5 ATO	30:70	90	1	85

Formulations #9 and #10 referred to the lipid microparticles theoretically containing cysteamine bitartrate and Compritol HD 5 ATO in a ratio 25:75% (w/w) whereas Formulation #11 was formulated in a ratio 30:70% (w/w). Moreover, Formulations #9 and #10 differed for the nozzle air and atomization pressure values. As it can be observed from Table IX, for all the three batches the yield was greater than 80%.

The drug content of the lipid microparticles of cysteamine bitartrate is reported in Table X. As it can be noticed, for all the three batches the experimental values obtained were higher than the theoretical ones.

Table X. Content (%) of cysteamine bitartrate in the lipid microparticles.

Results are expressed as mean value  $\pm$  standard deviation (n = 3).

Formulations	Drug content (%)
#9	28.7 $\pm$ 0.4
#10	30.9 $\pm$ 0.7
#11	34.9 $\pm$ 0.9

#### 4.2.2 Particle size distribution

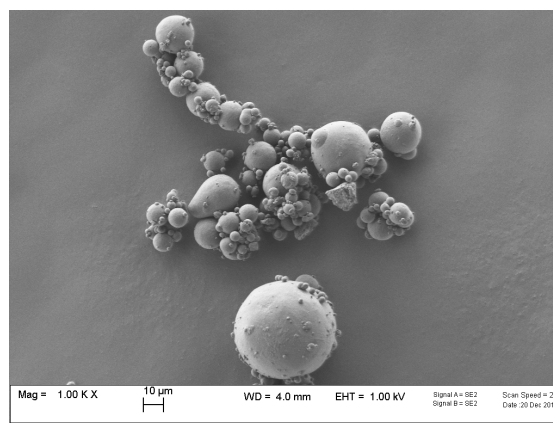
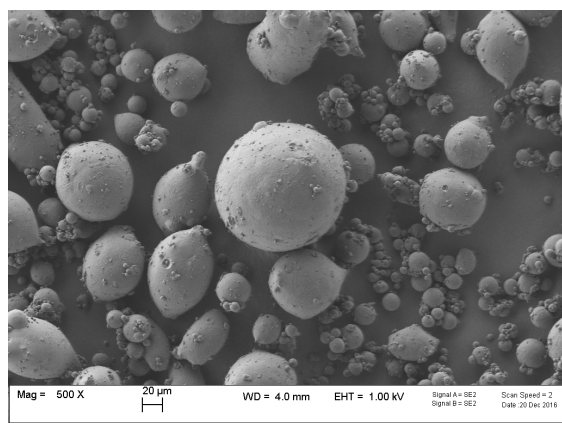
From the results related to the particle size distribution by means of a dry dispersion laser diffraction, Formulations #9 and #10 showed a  $d_{v50}$  value of about 39 and 69 microns, respectively (Table XI). Therefore, it was possible to conclude that the atomization pressure affected the particle size of the lipid microparticles.

Table XI. Particle size distribution of Formulations #9 - #11 (n = 3).

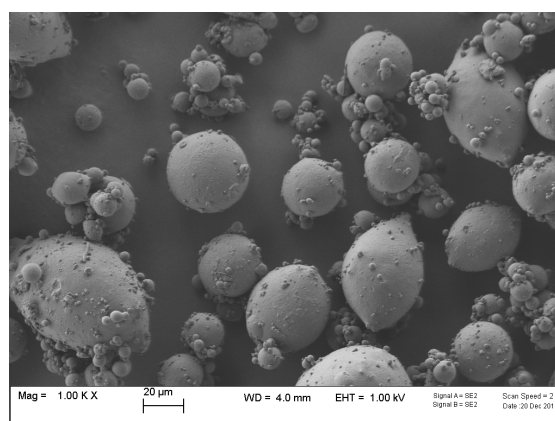
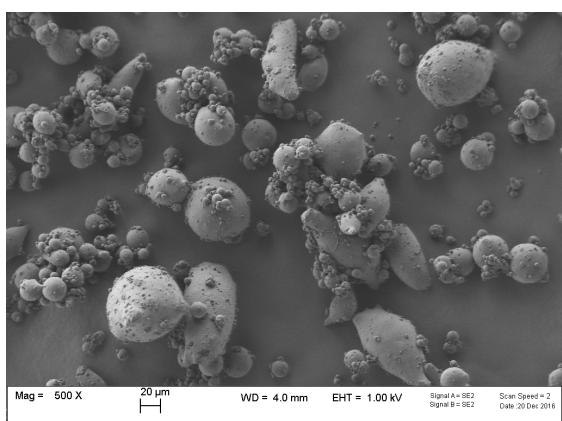
Formulations	Dv <sub>10</sub> (μm)	Dv <sub>50</sub> (μm)	Dv <sub>90</sub> (μm)
#9	13.63 $\pm$ 0.8	69.66 $\pm$ 0.7	191.92 $\pm$ 0.8
#10	5.74 $\pm$ 0.9	39.59 $\pm$ 0.6	175.93 $\pm$ 0.9
#11	7.51 $\pm$ 0.4	54.11 $\pm$ 0.6	160.01 $\pm$ 0.9

### 4.2.3 Scanning Electron Microscopy (SEM)

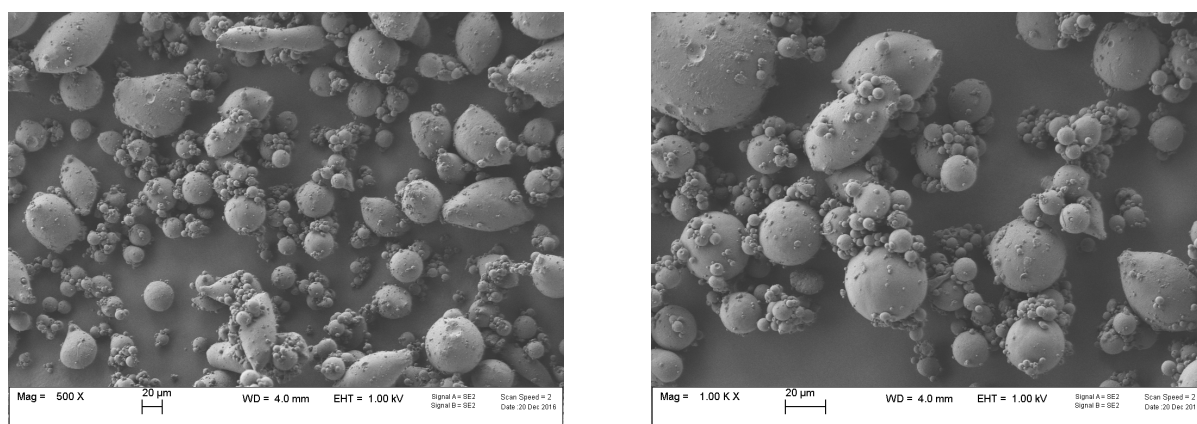
The morphological characterization of the lipid microparticles was performed with scanning electron microscopy (SEM). The lipid microparticles were almost spherical characterized with a smooth surface, as it can be seen from Figure 23. As expected from the particle size distribution analysis, two populations of microparticles were observed. Compared to the lipid microparticles manufactured with the laboratory scale facility, the shape and the surface characteristics are very similar.



(a)



(b)



(c)

Figure 23. SEM Images of cysteamine bitartrate lipid microparticles at two different magnifications (left side 500X and right side 1000X): (a) Formulation #9\_Cysteamine bitartrate/Compritol HD 5 ATO 25:75%, (b) Formulation #10\_Cysteamine bitartrate/ Compritol HD 5 ATO 25:75% and (c) Formulation #11\_Cysteamine bitartrate/ Compritol HD 5 ATO 30:70%.

#### 4.2.4 *In vitro* dissolution studies

The *in vitro* dissolution profiles at pH 1.2, performed according to the procedure described in Section 3.2.5.1. are shown in Figure 24. The lipid microparticles of Formulations #9 and #10 showed about 30 to 40% of drug dissolved in five minutes and 80% in one hour. The increase of drug loading in Formulation #11 led to a faster drug release; in fact, approximately 50% of the drug dissolved in five minutes and 80% in 15 minutes.

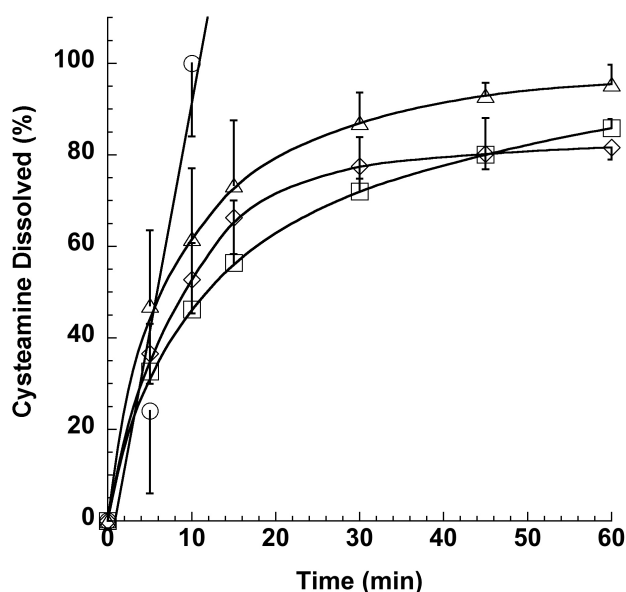


Figure 24. Dissolution profiles of cysteamine in simulated gastric fluid pH 1.2: (○) cysteamine bitartrate raw material, (□) Formulations #9 (Cysteamine bitartrate/Compritol HD 5 ATO 25:75%), (◇) Formulation #10 (Cysteamine bitartrate/Compritol HD 5 ATO 25:75%) and (△) Formulation #11 (Cysteamine bitartrate/Compritol HD 5 ATO 30:70%). Results are expressed as mean value  $\pm$  standard deviation ( $n = 3$ ).

The first scale-up of the laboratory preparation revealed that the product was feasible to be manufactured in higher amount and then suitable for industrial production. The release was not different despite the decrease of the particle size of the lipid microparticles.

From the results obtained during the first scale-up conducted by Xedev, it was decided to proceed with the manufacturing of batches of cysteamine bitartrate lipid microparticles containing at least 30% of drug and having higher particle size, mainly for reason of dissolution, flowability and taste masking. In addition, the attempt to increase the drug loading in the lipid microparticles to 40% was carried out.

For this reason, three batches with a theoretical drug loading of 30% were obtained. The composition and the process parameters of the formulations manufactured are summarized in Table XII.

Table XII. Composition of the formulations and process parameters used at Xedev facilities.

Lipid microparticles	Composition	Ratio (w/w %)	Nozzle Temperature (°C)	Atomization pressure (bar)	Yield (%)
#12	Cysteamine bitartrate/Compritol HD 5 ATO	30:70	90	1	45
#13	Cysteamine bitartrate/Compritol HD 5 ATO	30:70	95	2	55
#14	Cysteamine bitartrate/Compritol HD 5 ATO	30:70	90	1.5	56

There were critical issues related to the processability of the drug suspended lipid mass, mainly due to the tubing blocks during the test and the presence of residual suspension in the heated vessel. They clearly had a negative impact in the yield of the process, that was less than 60%, as it could be seen in Table XII. Moreover, it was not possible to process the formulation containing 40% of cysteamine bitartrate due to the high viscosity of the suspension, even at higher nozzle temperature (> 90 °C).

The drug content in the lipid microparticles was determined using the same procedure previously described (Section 3.2.3). In Table XIII the results are summarized.

Table XIII. Content (%) of cysteamine bitartrate in the lipid microparticles.

Results are expressed as mean value  $\pm$  SD (n=3).

Formulations	Drug content (%)
#12	29.6 $\pm$ 0.4
#13	23.3 $\pm$ 0.1
#14	27.4 $\pm$ 0.6

The measured drug content in Formulation #12 was in agreement with the theoretical value. On the contrary, cysteamine bitartrate content in Formulations #13 and #14 were significant lower; this was probably due to the problems observed during the manufacturing process.

#### 4.2.5 Particle size distribution

The particle size distribution of the three batches of cysteamine bitartrate lipid microparticles was performed by sieve analysis, according to the method described in Ph.Eur., following the procedure described in Section 3.2.4.1. As shown in the histograms illustrated in Figure 25, Formulation #13 showed different particle size distribution than Formulations #12 and #14. It was noticed that, during the sieve analysis, a partial agglomeration of the lipid microparticles was observed and then about 30% of lipid microparticles had a size greater

than 500  $\mu\text{m}$ . However, unlike the batches obtained in the first Xedev production (Formulations #9-11), the lipid microparticles size were greater than 125  $\mu\text{m}$ .

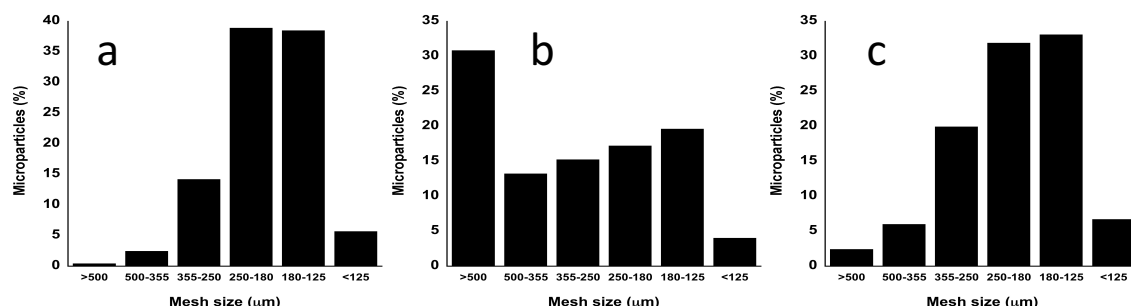
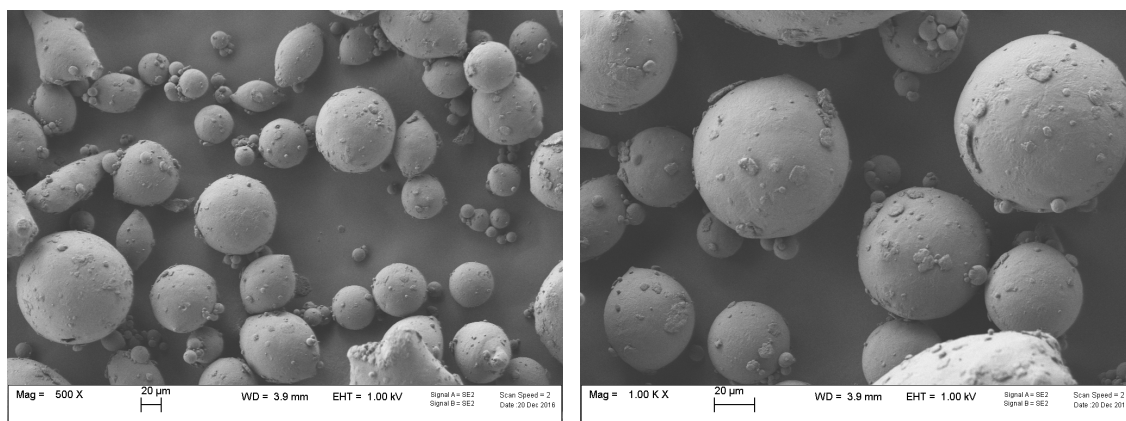


Figure 25. Particle size distribution of Formulations #12 (a), #13 (b) and #14 (c).

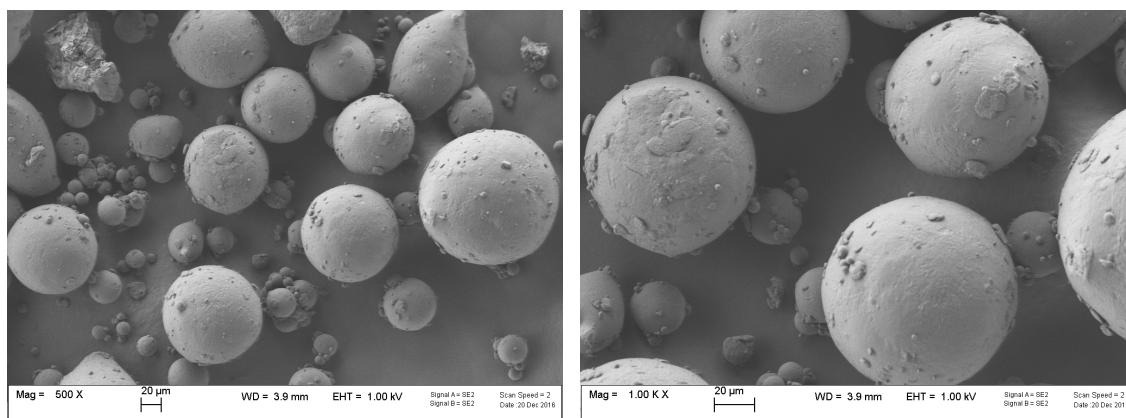
#### 4.2.6 Scanning Electron Microscopy (SEM)

The morphological characterization of the lipid microparticles was performed by means of scanning electron microscopy (SEM). From the images reported in Figure 26, it was possible to observe that the lipid microparticles showed a spherical structure and were characterized by a plain and regular surface.

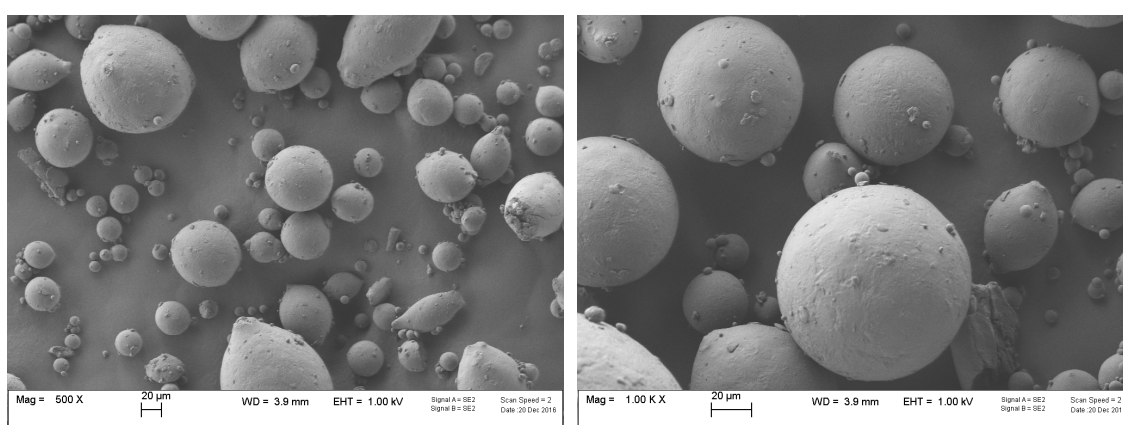
Concerning the results of the second production of lipid microparticles, it was possible to notice that there was an evident increase of particle size obtained by manipulating the process parameters. However, these modifications led to manufacturing problems that affected the yield of the process. The powders obtained were certainly more flowable, but the drug release rate appeared to be faster.



(a)



(b)



(c)

Figure 26. SEM Images of cysteamine bitartrate lipid microparticles at two different magnifications (left side 500X and right side 1000X): (a) Formulation #12\_Cysteamine bitartrate/Compritol HD 5 ATO 30:70%, (b) Formulation #13\_Cysteamine bitartrate/Compritol HD 5 ATO 30:70% and (c) Formulation #14\_ Cysteamine bitartrate/ Compritol HD 5 ATO 30:70%.

#### 4.2.7 Solid Lipid Microparticles characterization

##### 4.2.7.1 Differential Scanning Calorimetry (DSC)

The thermograms of the lipid microparticles, shown in Figures 27 and 28, were characterized by a broad endothermic band in the 50-70°C temperature range, due to the fusion of Compritol HD 5 ATO. In addition, a small peak at about 78°C (1<sup>st</sup> event) was observed, corresponding to the fusion of the polymorph I of cysteamine (see Section 4.1.2.2.) followed by a narrow peak at 120 °C (2<sup>nd</sup> event) characteristic of the fusion of polymorph II.

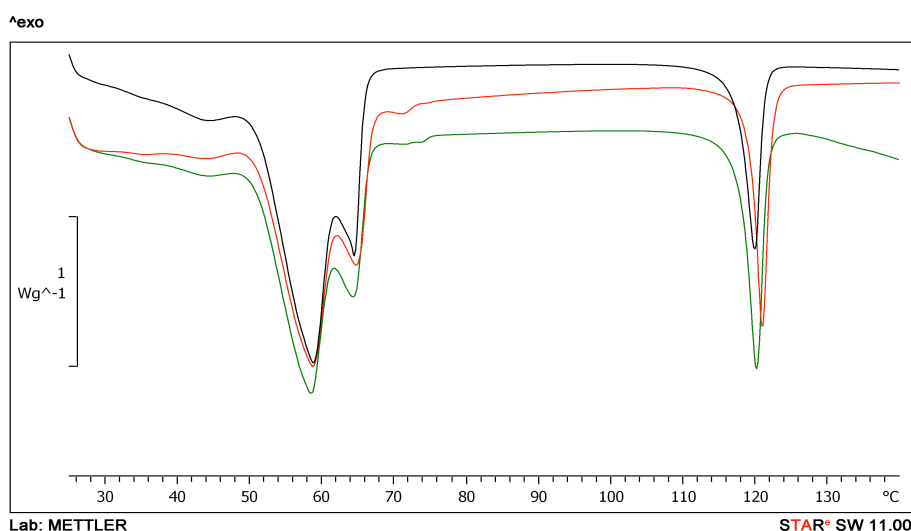


Figure 27. DSC thermograms of Formulation #9 (Cysteamine bitartrate/Compritol HD 5 ATO 25:75%, black curve), Formulation #10 (Cysteamine bitartrate/Compritol HD 5 ATO 25:75%, red curve) and Formulation #11 (Cysteamine bitartrate/Compritol HD 5 ATO 30:70%, green curve).

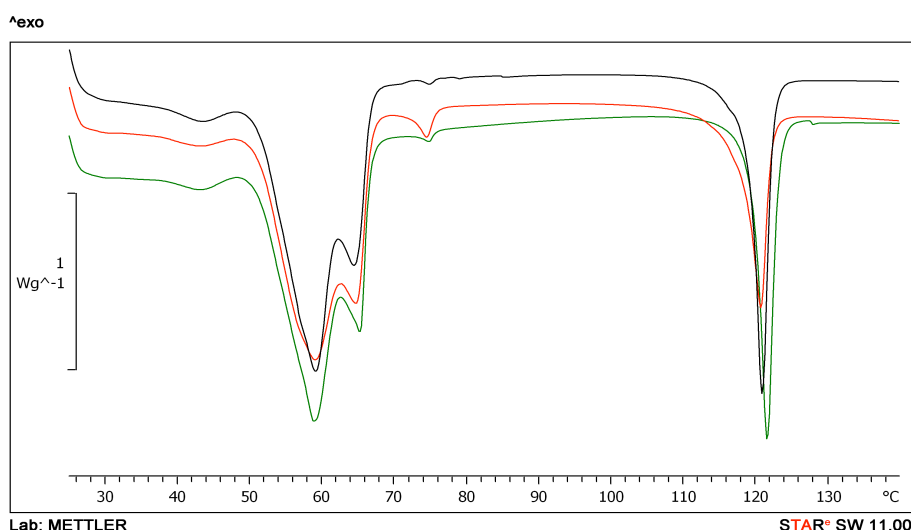


Figure 28. DSC thermograms of Formulation #12 (Cysteamine bitartrate/Compritol HD 5 ATO 30:70%, black curve), Formulation #13 (Cysteamine bitartrate/Compritol HD 5 ATO 30:70%, red curve) and Formulation #14 (Cysteamine bitartrate/Compritol HD 5 ATO 30:70%, green curve).

#### 4.2.7.2 Hot Stage Microscopy (HSM)

HSM analysis were conducted following the procedure described in Section 3.2.4.4. The most relevant HSM images are reported in Figures 29 and 30. The changes observed in the HSM images during the heating phase were in agreement with the thermal behaviour shown in Figures 27 and 28. In fact, the modifications at 58 and 85 °C were due to the melting of Compritol HD 5 ATO and cysteamine bitartrate (1<sup>st</sup> event), respectively. The crystals still

present at 85 °C are attributed to cysteamine bitartrate, which completely melts at 120°C (2<sup>nd</sup> event).

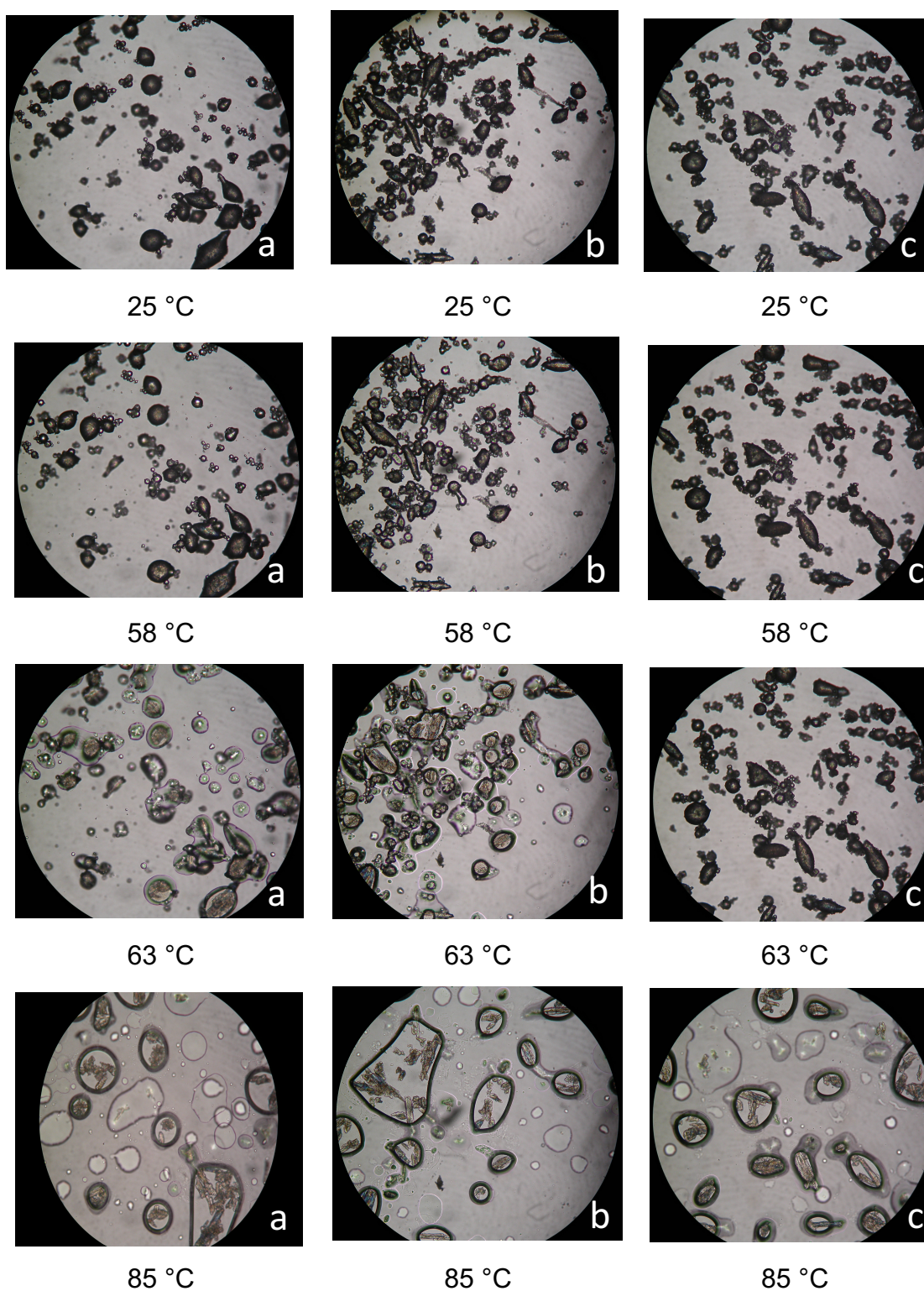


Figure 29. HSM Images of lipid microparticles: a) #9 (Cysteamine bitartrate/Compritol HD 5 ATO 25:75%), b) #10 (Cysteamine bitartrate/Compritol HD 5 ATO 25:75%) and c) #11 (Cysteamine bitartrate/Compritol HD 5 ATO 30:70%).

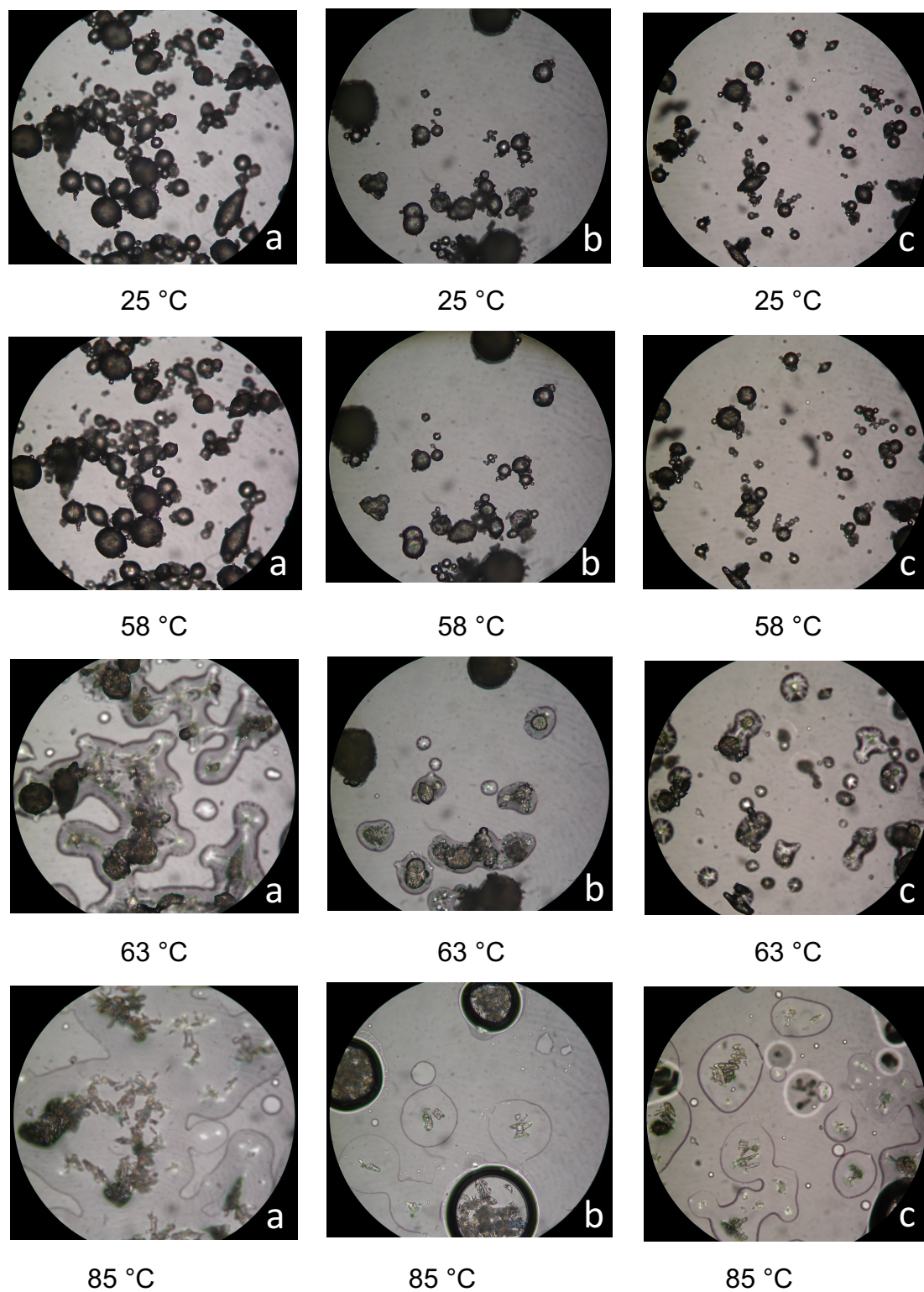


Figure 30. HSM Images of lipid microparticles a) #12 (Cysteamine bitartrate/Compritol HD 5 ATO 30:70%), b) #13 (Cysteamine bitartrate/Compritol HD 5 ATO 30:70%) and c) #14 (Cysteamine bitartrate/Compritol HD 5 ATO 30:70%).

#### 4.2.7.3 Microparticles X-ray Powder Diffraction (PXRD)

The PXRD diffractograms of cysteamine bitartrate raw material and Compritol HD 5 ATO are reported in Figures 31 and 32. In Figures 33 and 34 the diffractogram patterns of Formulations #9-11 and Formulations #12-14 are shown, respectively.

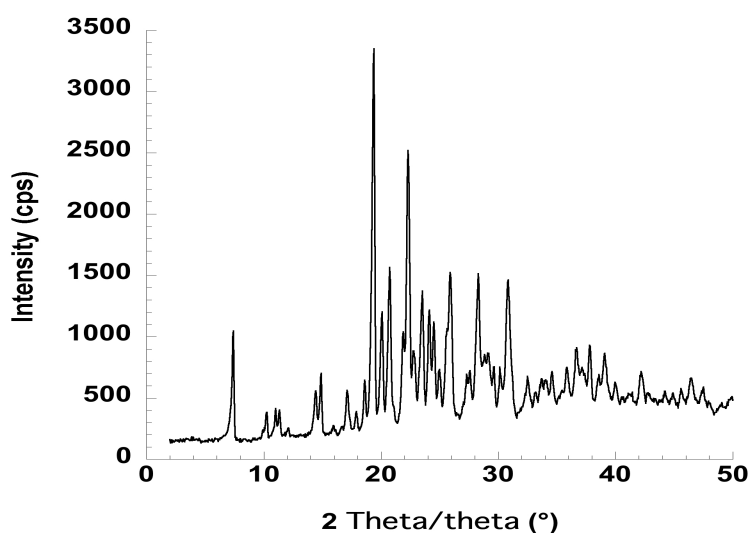


Figure 31. Powder X-ray diffraction pattern of cysteamine bitartrate raw material.

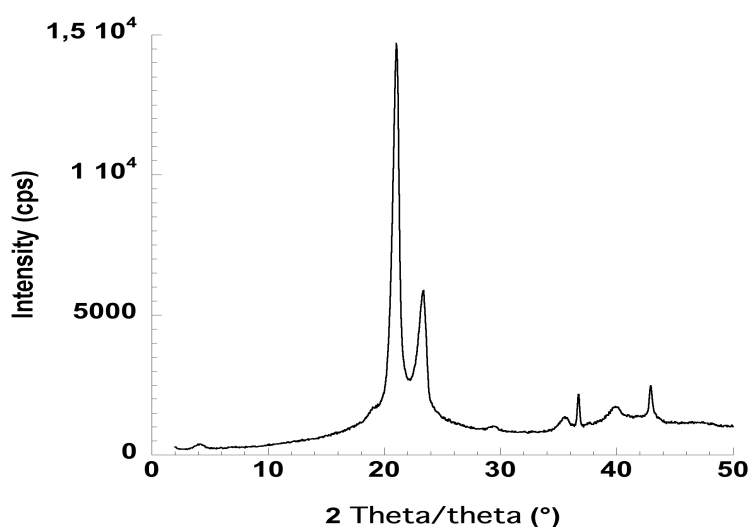


Figure 32. Powder X-ray diffraction pattern of Compritol HD 5 ATO.

In the diffractogram of the drug (Figure 31) and the lipid excipient (Figure 32) diffraction peaks typical of a crystalline structure were observed. These peaks were also present in the diffractograms of the lipid microparticles (Figures 33 and 34), confirming the thermal behaviour observed by DSC and HSM analyses. Moreover, no significant differences were detected in diffractogram patterns of the batches manufactured by Xedev.

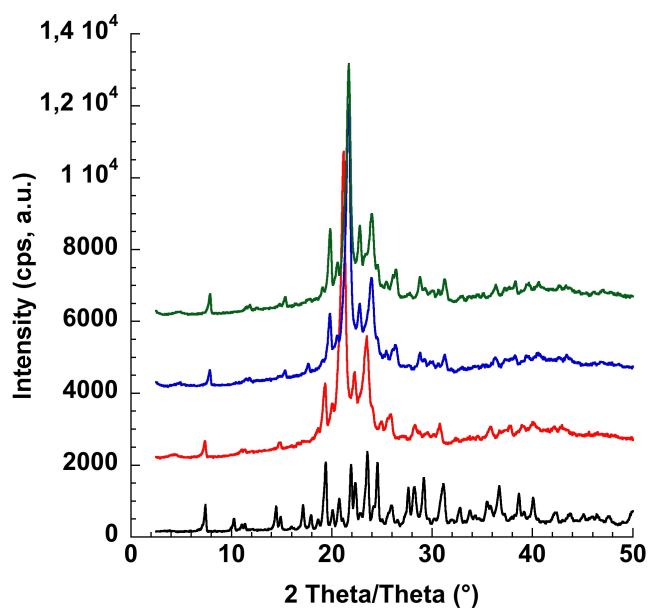


Figure 33. Powder X-ray diffraction pattern of cysteamine bitartrate (black curve), Formulation #9 (Cysteamine bitartrate/Compritol HD 5 ATO 25:75%, red curve), Formulation #10 (Cysteamine bitartrate/Compritol HD 5 ATO 25:75%, blue curve) and Formulation #11 (Cysteamine bitartrate/Compritol HD 5 ATO 30:70%, green curve).

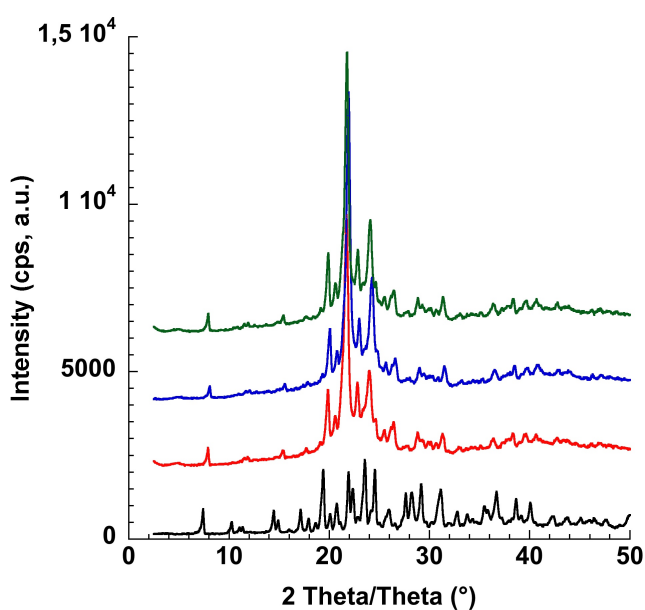


Figure 34. Powder X-ray diffraction pattern of cysteamine bitartrate (black curve), Formulation #12 (Cysteamine bitartrate/Compritol HD 5 ATO 30:70%, red curve), Formulation #13 (Cysteamine bitartrate/Compritol HD 5 ATO 30:70%, blue curve) and Formulation #14 (Cysteamine bitartrate/Compritol HD 5 ATO 30:70%, green curve).

#### 4.2.8 *In vitro* dissolution studies

The *in vitro* dissolution profiles were obtained following the procedure previously described in detail in Section 3.2.5.1. Formulations #12-14 showed a release profile similar to the one of Formulation #11, as it can be observed from Figure 35.

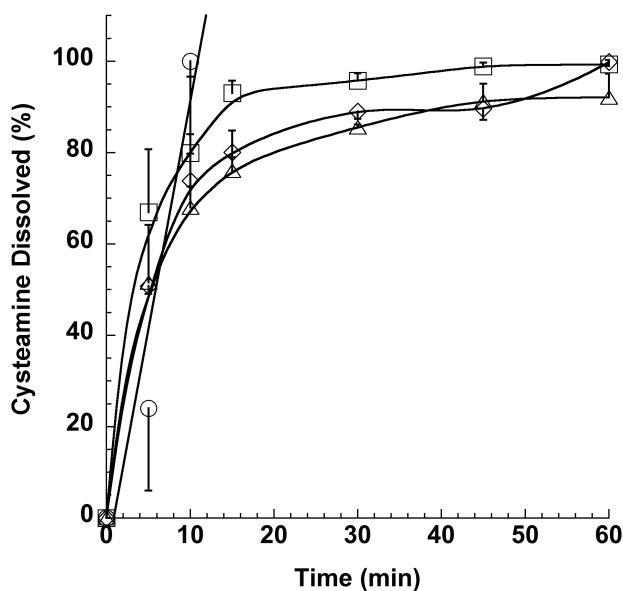


Figure 35. Dissolution profiles of cysteamine in simulated gastric fluid pH 1.2: (○) cysteamine bitartrate raw material, (□) Formulations #12 (Cysteamine bitartrate/Compritol HD 5 ATO 30:70%), (◇) Formulation #13 (Cysteamine bitartrate/Compritol HD 5 ATO 30:70%) and (△) Formulation #14 (Cysteamine bitartrate/Compritol HD 5 ATO 30:70%). Results are expressed as mean value  $\pm$  standard deviation ( $n = 3$ ).

#### 4.2.9 Odour masking efficiency

To evaluate the effectiveness of the taste masking, six operators have smelled the different lipid microparticles and compared the smell with the one of the raw drug. The results are reported in Table XIV.

Table XIV. Smell of the drug lipid microparticles (n = 6).

Formulations	Impression on smell					
<b>Cysteamine Bitartrate</b>	4	4	4	4	4	4
<b>#9</b>	1	1	1	2	2	3
<b>#10</b>	1	4	4	4	4	3
<b>#11</b>	3	3	3	3	4	4
<b>#12</b>	2	2	2	2	3	3
<b>#13</b>	2	2	2	2	3	3
<b>#14</b>	1	1	2	2	3	3

As it can be observed, there was an evident reduction of the smell of the API when manufactured together with the lipid carrier Compritol HD 5 ATO, suggesting that a good taste masking effect was obtained.

#### 4.2.10 Amount of product to be administered

To further proceed with the protocol development of cysteamine lipid microparticles, it is important to consider the amount of product to be introduced in a sachet in order to have the administration dose. The final drug product will be a powder to be filled in sachet to be readily dispersed in water. The daily dose for treatment of cystinosis in paediatric patients (Cystagon<sup>®</sup>) is 50 mg/kg per day, shared in three doses. In the case of a child weighing 25 kg we will have:

- daily dose of cysteamine (considered as free base):  
 $50 \text{ mg} \times 25 \text{ kg} = 1.250 \text{ g}$
- daily dose of cysteamine bitartrate:  
 $1.250 \text{ g} \times 3 = 3.750 \text{ g}$
- amount of lipid microparticles: considering the case of Formulation #8 plus 10% of the spray-dried excipient microparticles contains 27% of cysteamine bitartrate. Thus, 3.750 g of cysteamine bitartrate correspond to 13.9 g of coated lipid particles.

In total, the amount per day of lipid microparticles Formulation #8/spray-dried excipient microparticles is 13.89 g. This amount, shared in three sachets, will give a product amount of 4.63 g to be extemporaneously dispersed for administration.

A deep investigation on the excipients employed for the manufacturing of lipid microparticles of cysteamine bitartrate, and in particular on the daily admitted intake (ADI), demonstrated that the maximum amount of Compritol HD 5 ATO to be administered daily to patients is 1500 mg.<sup>56</sup> However, the percentage of Compritol HD 5 ATO in the lipid microparticles was superior to the ADI. For this reason, the attempt to increase the amount of cysteamine in the lipid microparticles up to 50% was performed without any positive results. Therefore, it was decided to replace Compritol HD 5 ATO with Compritol 888 ATO, for which there is no limit in the daily dose.

Based on the results of the excipient chemical-physical compatibility, the regulatory status and the evaluation of ADI, the prototype that was investigated for the spray congealing is listed in Table XV.

Table XV. Composition of the formulations and process parameters used at Xedev facilities.

Lipid microparticles	Composition	Ratio (w/w %)	Nozzle Temperature (°C)	Atomization pressure (bar)	Yield (%)
#15	Cysteamine bitartrate/Compritol 888 ATO/Gelucire 48/16	25:65:10	100	1	71

Gelucire<sup>®</sup>, which is an excipient that contain glycerides or a mixture of glycerides and PEG esters, is used in the preparation of sustained release formulations.<sup>57</sup> Gelucire 48/16 was selected since it is considered as a safe excipient and there is no limit for daily intake. Compritol 888 ATO was evaluated in replacement to Compritol HD 5 ATO even if chemical properties are different. Gelucire 48/16 is more hydrophilic and its use was investigated respectively at 10% in the core formation to reduce to risk of floating.

#### 4.2.11 Particle size distribution

The assessment of the particle size distribution was carried out by Xedev by means of a dry dispersion laser diffraction. The results of the particle size distribution are reported in Table XVI. As it can be observed, Formulation #17, containing Compritol 888 ATO as excipient for particle formation, showed a  $dv_{50}$  value of 46 microns.

Table XVI. Particle size distribution of Formulations #9 -11 (n = 3).

Formulations	Dv <sub>10</sub> (µm)	Dv <sub>50</sub> (µm)	Dv <sub>90</sub> (µm)
#17	5.99 ± 0.4	46.47 ± 0.9	130.10 ± 0.8

#### 4.2.12 Analysis of the cysteamine bitartrate spray congealing batches at t = 0

##### 4.2.12.1 Drug content determination and impurities assay

Cysteamine and cystamine content in the lipid microparticles were calculated and analyzed by means of HPLC according to the method described in Section 3.2.2.3. Data are reported in Table XVII, expressed in percent weight.

Table XVII. Cysteamine, Cystamine and impurities content (w/w %) in the lipid microparticles.

Results are expressed as mean value ± standard deviation (n=3).

Formulation #17	
Cysteamine (%)	24.7 ± 0.5
Cystamine Base (%)	0.31 ± 0.5
Unknown Impurities	0.09 ± 0.5

As it could be observed from Table XVII, the drug content was almost superimposable to the theoretical value of 25% of cysteamine bitartrate. The degradation products, such as cystamine and other unknown impurities, were present in a percentage below 1%.

#### 4.2.12.2 Scanning Electron Microscopy (SEM)

The morphological characterization of the cysteamine bitartrate lipid spray-congealing microparticles was performed by means of scanning electron microscopy (SEM). Spray-congealing lipid microparticles of Formulation #17 were almost spherical, with irregular surface (Figure 36). Two populations of microparticles were observed.

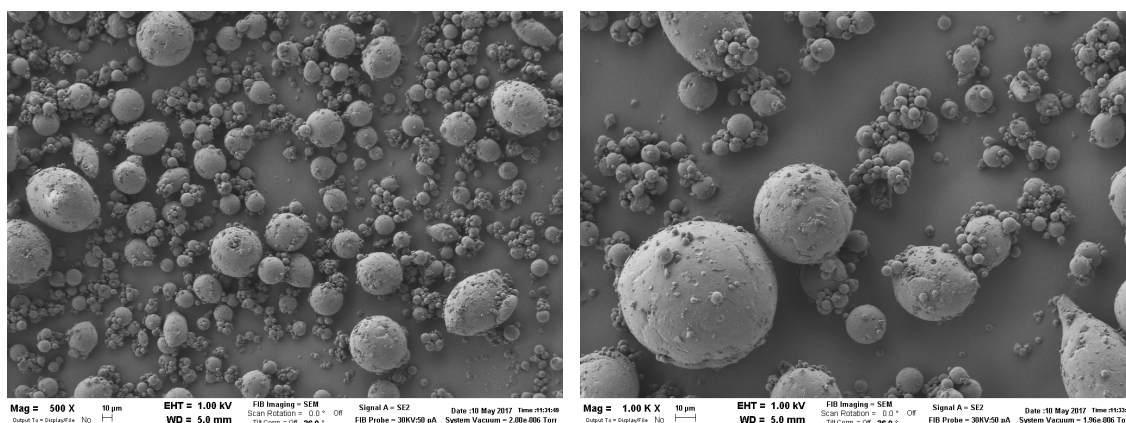


Figure 36. SEM Images of cysteamine bitartrate lipid microparticles of Formulation #17\_Cysteamine bitartrate/Compritol 888 ATO/Gelucire 48/16 (25/65/10%) at two different magnifications (left side 500X and right side 1000X).

Considering that the hydrophobicity of lipids caused the floating of particles on the dissolution medium during the *in vitro* dissolution tests and the drug release rate was slow down, the wettability of the cysteamine bitartrate lipid microparticles was improved by mixing them with the spray-dried excipient microparticles, as described in section 3.2.6. In particular, mannitol/lecithin spray-dried microparticles were mixed with the lipid microparticles in a ratio 1:9 (w/w %). As previously observed, by simple mixing, a hydrophilic layer of spray-dried excipient microparticles was deposited on the surface of cysteamine bitartrate lipid microparticles thus increasing their wettability and improving the taste masking (Figure 37).

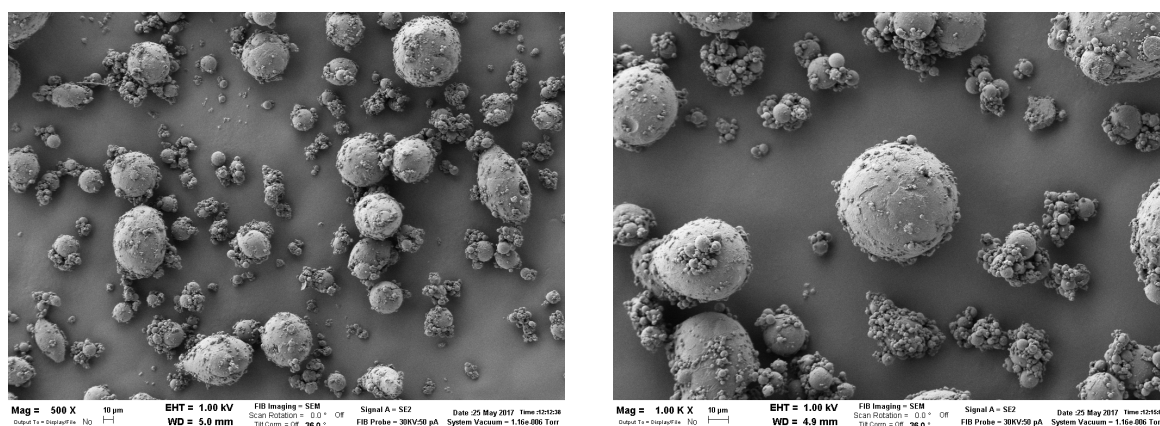


Figure 37. SEM Images of cysteamine bitartrate lipid microparticles of Formulation #17\_Cysteamine bitartrate/Compritol 888 ATO/Gelucire 48/16 (25/65/10%) with mannitol/lecithin spray-dried microparticles (9:1 w/w%), at two different magnifications (left side 500X and right side 1000X).

#### 4.2.13 Solid Lipid Microparticles characterization

##### 4.2.13.1 Differential Scanning Calorimetry (DSC)

The thermal behaviour of the cysteamine bitartrate spray-congealing microparticles and that of the placebo spray congealing batches was investigated by differential scanning calorimetry (DSC) according to the procedure described in Section 3.2.4.3. The DSC thermogram of Formulation #17 is shown below (Figures 38). The thermogram of cysteamine bitartrate raw material, reported Section 4.1.2.2., was characterized by a small peak at about 78°C (1st event), followed by a narrow peak at 120°C (2nd event), which corresponds to the melting point of the drug. In all the spray-congealing formulations, the thermal events attributed to the cysteamine bitartrate were present.

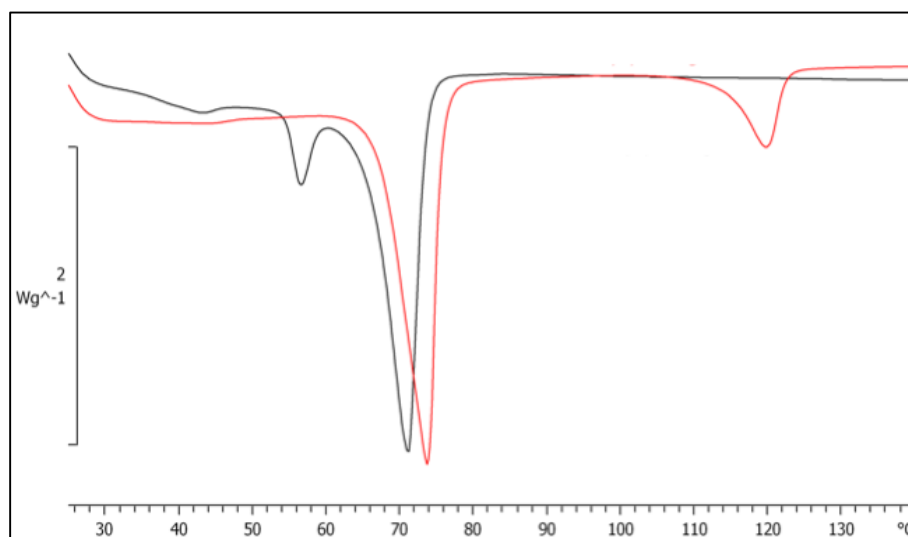


Figure 38. DSC thermograms of Placebo of Formulation #17 (Compritol 888 ATO/Gelucire 48/16, red curve) and Formulation #17 (Cysteamine bitartrate/Compritol 888 ATO/Gelucire 48/16 25/65/10%, black curve).

#### 4.2.13.2 Microparticles X-ray Powder Diffraction (PXRD)

Powder X-ray diffractometry (PXRD) patterns of the drug lipid spray-congealing microparticles and that of the placebo microparticles are shown in Figure 39. The spray congealing process and the presence of the Compritol 888 ATO didn't affect the crystallinity of the drug.

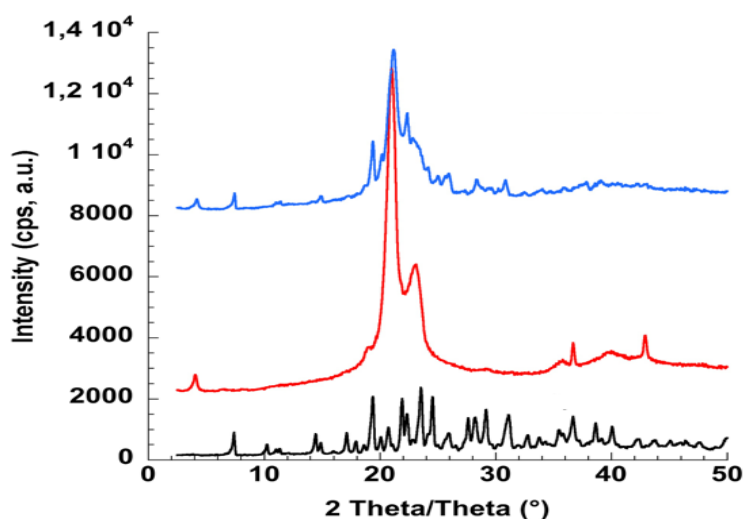


Figure 39. Powder X-ray diffraction pattern of Cysteamine bitartrate (black curve), Placebo of Formulation #17\_Cmpritol 888 ATO/Gelucire 48/16 (red curve) and Formulation #17\_Cysteamine bitartrate/Compritol 888 ATO/Gelucire 48/16 25/65/10% (blue curve).

#### 4.2.14 *In vitro* dissolution studies

*In vitro* dissolution studies were performed by means of the USP Apparatus II following the method described in Section 3.2.5.2. The drug dissolution profile is reported in Figure 40. As it can be observed, the dry layering coating process significantly improved the drug release, reaching about 100% of cysteamine bitartrate dissolved after 1 hour.

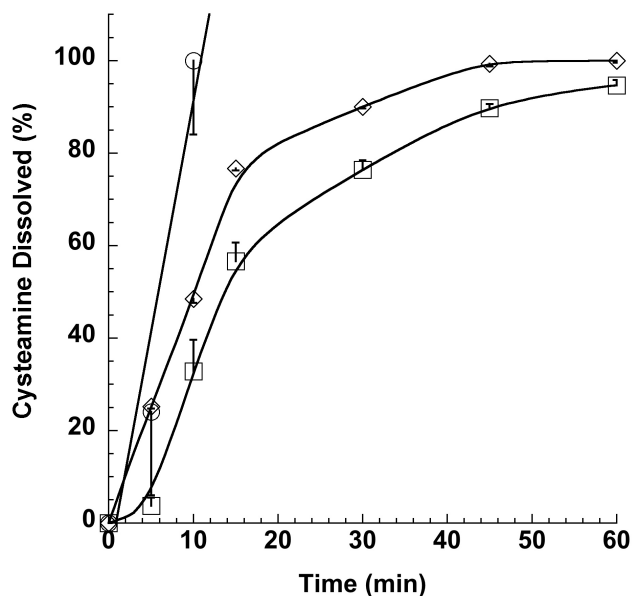


Figure 40. Dissolution profiles of cysteamine in HCl at pH 1.0: (○) cysteamine bitartrate raw material, (□) Formulation #17 (Cysteamine bitartrate/Compritrol 888 ATO/Gelucire 48/16 25/65/10%) and the corresponding layered lipid microparticles with (◇) mannitol/lecithin spray-dried microparticles (9:1 w/w%). Results are expressed as mean value  $\pm$  standard deviation ( $n = 3$ ).

#### 4.2.15 Analysis of the cysteamine bitartrate spray congealing batches after 2 weeks at 30°C and 65% RH

##### 4.2.15.1 Drug content determination and impurities assay

The drug content as well as the percentage of impurities present in the spray congealing prototypes were assessed after 2 weeks of storage at 30°C and 65% of relative humidity (RH) following the method deeply described in Section 3.2.2.3. The results of the HPLC analysis are shown in Table XVIII.

Table XVIII. Cysteamine, Cystamine and impurities content (w/w %) in the lipid microparticles after 2 weeks 30°C/65% RH. Results are expressed as mean value  $\pm$  standard deviation (n=3).

Formulation #17	
Cysteamine (%)	23.9 $\pm$ 0.5
Cystamine Base (%)	0.93 $\pm$ 0.5
Unknown Impurities	0.23 $\pm$ 0.5

#### 4.2.16 *In vitro* dissolution studies

*In vitro* dissolution profiles of the cysteamine bitartrate lipid spray congealing batches layered with mannitol/lecithin spray-dried microparticles, after 2 weeks' storage at 30°C and 65% RH, compared with those collected at t = 0, are reported in Figure 41. Before the *in vitro* dissolution analysis, cysteamine bitartrate lipid spray-congealing microparticles were dry coated with mannitol/lecithin spray-dried microparticles in a ratio 9:1 (w/w %). As it can be observed, after 2 weeks storage the drug dissolution increased up to 100% in about 30 minutes.

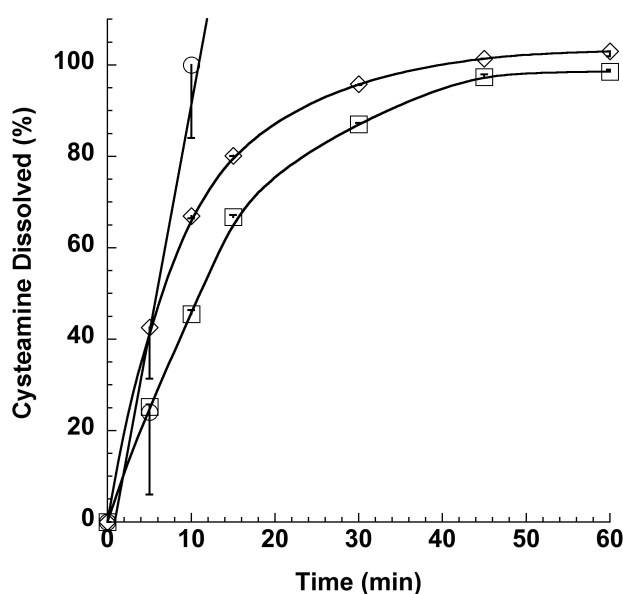


Figure 41. Dissolution profiles of cysteamine in HCl at pH 1.0: (○) cysteamine bitartrate raw material, (□) Formulations #17 (Cysteamine bitartrate/Compritol 888 ATO/Gelucire 48/16, 25/65/10%) at t=0, (◇) Formulations #17 (Cysteamine bitartrate/Compritol 888 ATO/Gelucire 48/16, 25/65/10%) after 2 weeks 30°C/65% RH. Results are expressed as mean value  $\pm$  standard deviation (n = 3).

## 5. CONCLUSIONS

Cysteamine was approved by the US Food and Drug Administration for the treatment of nephropathic cystinosis. In this Ph.D. thesis, an invention related to the preparation of novel cysteamine powders for oral administration was described. From the results obtained during the research project, it was possible to conclude that spray congealing was efficiently employed for the manufacturing of cysteamine bitartrate lipid microparticles.

In particular, by means of spray congealing technology, a lipid matrix of cysteamine bitartrate was prepared by spray congealing. The drug loading was between 25-30 (w/w %). Depending on the type of lipid excipients used, it was possible to obtain a release of drug of less than 50% in 5 min and 100% in 1 hour. Compritol HD 5 ATO was the lipid carrier that showed the best capacity of controlling the release of the drug in order to avoid the release of a huge amount of drug during the administration time. What is more, the application of a layering of the lipid microparticles with excipient spray-dried microparticles allowed the control of wettability of the lipid particles and also the taste masking of cysteamine bitartrate. A hydrophilic layer of spray-dried excipient microparticles was uniformly deposited on the entire surface of the lipid microparticles, as stated from the morphological analysis. In addition, combining the cysteamine with sucralfate in the layered powder could lead to a novel combination product.

The taste masking effect and the control on the release of the drug were carefully investigated in order to provide to patients a final product with proper organoleptic characteristics as well as an efficient controlled release of the API to avoid a high amount of cysteamine during the administration in water or other liquids.

Cysteamine lipid microparticles proved to be suitable for the scale-up manufacturing. During the laboratory scale preformulation study, conducted at the University of Bologna, a variability on the drug content, drug release rate and particle size distribution of lipid microparticles was observed. These drawbacks were reduced by scaling up the manufacturing at Xedev bvba (Zelzate, Belgium) production site, by performing a strictly control on the process parameters.

During the scale-up manufacturing, a deep investigation on the excipients compatibility based on the regulatory status and also the maximum dose permitted per day (ADI), was conducted. A spray congealing prototype was characterized immediately after the

manufacturing and after two weeks at 30°C and 65% RH. Compared to the dissolution profile of Formulation #17 at time 0, after 2 weeks an increase in the dissolution rate at 5 minutes was observed, reaching the 100% of the release after one hour.

The data obtained so far have shown that the lipid microparticles can be promising for the preparation of paediatric extemporaneous dosage form for taste masking and prolonged release of cysteamine bitartrate.

## REFERENCES

1. Gahl et al., "Early oral cysteamine therapy for nephropathic cystinosis", *European Journal of Pediatrics*, 2003, 162, p. 38-41.
2. Wilmer MJ et al., "The pathogenesis of cystinosis: mechanism beyond cysteine accumulation", *Am J Physiol Renal Physiol*, 2010, 299, p. 905-916.
3. Gahl et al., "Nephropathic cystinosis in adults: natural history and effects of oral cysteamine therapy", *Annals of Internal Medicine*, 2007, Vol. 147, No. 4.
4. Shams F et al., "Treatment of corneal cysteine crystal accumulation in patients with cystinosis", *Clinical Ophthalmology*, 2014.
5. Biswas et al., "Latest clinical approaches in the ocular management of cystinosis: a review of current practice and opinion from the ophthalmology cystinosis forum", *Ophthalmol Ther*, 2018, 7, p. 307-322.
6. Cherqui S., "Cysteamine therapy: a treatment for cystinosis, not a cure", *Kidney International*, 2012, 81, p.127-129.
7. "Cysteamine: an old drug with new potential", *Drug Discovery Today*, August 2013, Vol. 18, Issues 15-18, p. 785-792.
8. Tsilou E. et al., "Ophthalmic manifestations and histopathology of infantile nephropathic cystinosis: report of a case and review of the literature", *Survey of Ophthalmology*, 2007, Vol. 52, No. 1.
9. Taranta A. et al., "Pathogenesis of cell dysfunction in nephropathic cystinosis", *Advances in Metabolic and Kidney Diseases*.
10. Ariceta G. et al., "Cystinosis in adult and adolescent patients: recommendations for the comprehensive care of cystinosis", *Nefrologia*, 2015, 35 (3), p. 304-321.
11. Besouw M. et al., "The origin of halitosis in cystinotic patients due to cysteamine treatment", *Molecular Genetics and Metabolism*, 2007, 91, p. 228-233.
12. Sun L et al., "Effects of cysteamine on MPTP-induced dopaminergic neurodegeneration in mice", *Brain Research* 2010, 1335, p. 74-82.
13. Gibrat et al., "Potential of cystamine and cysteamine in the treatment of neurodegenerative diseases", *Progress in Neuro-Psychopharmacology & Biological Psychiatry*, 2011, 35, p. 380-389.
14. Besouw M. et al., "Halitosis in cystinosis patients after administration of immediate-release cysteamine bitartrate compared to delayed-release cysteamine bitartrate", *Molecular Genetics and Metabolism* 2012, 107, p. 234-236.

15. Dohil R. et al., "Enteric-coated cysteamine for the treatment of pediatric non-alcoholic fatty liver disease", *Aliment Pharmacol Ther*, 2011, 33, p. 1036-1044.
16. Markello T. et al., "Improved renal function in children with cystinosis treated with cysteamine", *The New England Journal of Medicine*, 1993, Vol. 328, No. 16.
17. Dohil R. et al., "Twice-daily cysteamine bitartrate therapy for children with cystinosis", *The Journal of Pediatrics*, January 2010, Vol. 156, No. 1.
18. Besouw M.T. "Cysteamine toxicity in patients with cystinosis", *The Journal of Pediatrics*, 2011, Vol. 159, No. 6.
19. Dohil R. et al., "Understanding intestinal cysteamine bitartrate absorption", *The Journal of Pediatrics*, June 2006.
20. Omran Z. et al., "Synthesis and in vitro evaluation of novel pro-drugs for the treatment of nephropathic cystinosis", *Bioorganic & Medical Chemistry* 2011, 19, p. 3492-3496.
21. Brodin-Sartorius A. et al., "Cysteamine therapy delays the progression of nephropathic cystinosis in late adolescents and adults", *International Society of Nephrology* 81, 2012, p. 179-189.
22. Stevenson C. et al., "Reservoir-based drug delivery systems utilizing microtechnology", *Adv Drug Del Rev.*, 2012, 64 (14), p. 1590-1602.
23. Colombo P. et al., "Principi di Tecnologie Farmaceutiche", Casa Editrice Ambrosiana.
24. Yang W. Et al., "Reservoir-based polymer drug release systems", *Journal of Laboratory Automation*, 2012, 17 (1), p. 50-58.
25. Dohil R. et al., "Long-term treatment of cystinosis in children with twice-daily cysteamine", *The Journal of Pediatrics*, May 2010, Vol. 156, No. 5.
26. WO2007/089670, Enterically Coated Cysteamine, Cystamine and Derivates thereof, PCT/US2007/002325, [patentscope.wipo.int](http://patentscope.wipo.int).
27. Langman C. et al., "Quality of life is improved and kidney function preserved in patients with nephropathic cystinosis treated for 2 years with delay-release cysteamine bitartrate", *The Journal of Pediatrics*, September 2014, Vol. 165, No. 3.
28. Nokhodchi A. et al., "The Role of Oral Controlled Release Matrix Tablets in Drug Delivery Systems", *BiolImpacts*, 2012, 2(4), p. 175-187.
29. Kaushik D. et al., "Recent patents and patented technology platforms for pharmaceutical taste masking", *Recent Patents on Drug Delivery & Formulation*, 2014, 8, p. 37-45.

30. Deepak S. et al., "Taste masking technologies: a novel approach for the improvement of organoleptic property of pharmaceutical active substance", *International Research Journal of Pharmacy*, 2012, 3 (4).
31. Anand V. et al., "The latest trends in the taste assessment of pharmaceuticals", *Drug Discovery Today*, 2007, Vol. 12, No. 5/6.
32. Joshi S. et al., "Film coatings for taste masking and moisture protection", *International Journal of Pharmaceutics*, 2013, 457, p. 395-406.
33. Al-kasmi B. et al., "Mechanical microencapsulation: the best technique in taste masking for the manufacturing scale – Effect of polymer encapsulation on drug targeting", *Journal of Controlled Release* 2017, 260, p. 134-141.
34. Sharma V. et al., "Role of taste and taste masking of bitter drugs in pharmaceutical industries – an overview", *International Journal of Pharmacy and Pharmaceutical Sciences*, 2010, Vol. 2, Suppl 4, p. 14-18.
35. Shet N. et al., "Taste masking: a pathfinder for bitter drugs", *International Journal of Pharmaceutical Sciences Review and Research*, 2013, 18 (2), No. 1, p. 1-12.
36. Sawan M.S., "Review on taste masking approaches in oral pharmaceutical dosage forms", *Lebda Medical Journal*, 2015, p. 33-43.
37. Chen M., "Lipid excipients and delivery systems for pharmaceutical development: a regulatory perspective", *Advanced Drug Delivery Reviews* 2008, 60, p. 768-777.
38. Kalepu S. et al., "Oral lipid-based drug delivery systems – an overview", *Acta Pharmaceutica Sinica B*, 2013, 3 (6), p. 361-372.
39. Feeney O. et al., "50 years of oral lipid-based formulations: provenance, progress and future perspectives", *Advanced Drug Delivery Reviews* 2016, 101, p. 167-194.
40. Jannin V. et al., "Approaches for the development of solid and semi-solid lipid-based formulations", *Advanced Drug Delivery Reviews*, 2008, 60, p. 734–746.
41. Albertini B. et al., "New spray congealing atomizer for the microencapsulation of highly concentrated solid and liquid substances", *European Journal of Pharmaceutics and Biopharmaceutics* 2008, 69, p. 348-357.
42. Rodriguez L. et al., "Description and preliminary evaluation of a new ultrasonic atomizer for spray-congealing process", *International Journal of Pharmaceutics* 1999, 183, p. 133-143.
43. Matos-Jr F. et al., "Development and characterization of solid lipid microparticles loaded with ascorbic acid and produced by spray congealing", *Food Research International* 2015, 67, p. 52-59.

44. Passerini N. et al., "Evaluation of melt granulation and ultrasonic spray congealing as techniques to enhance the dissolution of praziquantel", *International Journal of Pharmaceutics* 2006, 318, p. 92-102.
45. Yajima T. et al., "Particle design for taste-masking using a spray-congealing technique", *Chem. Pharm. Bull.* 1996, 44 (1), p. 187-191.
46. Dolci L.S. et al., "Spray-congealed solid lipid microparticles as a new tool for the controlled release of bisphosphonate from a calcium phosphate bone cement", *European Journal of Pharmaceutics and Biopharmaceutics* 2018, 122, p. 6-16.
47. Ilíc I. et al., "Microparticle size control and glimepiride microencapsulation using spray congealing technology", *International Journal of Pharmaceutics* 2009, 381, p. 176-183.
48. Maschke A. et al., "Development of a spray congealing process for the preparation of insulin-loaded lipid microparticles and characterization thereof", *European Journal of Pharmaceutics and Biopharmaceutics* 2007, 65, p. 175-187.
49. Di Sabatino M. et al., "Spray congealed lipid microparticles with high protein loading: preparation and solid state characterization", *European Journal of Pharmaceutical Sciences* 2012, 46, p. 346-356.
50. "Formulations of cysteamine and cysteamine derivatives", Application n: WO2017EP75801 20171010, Applicant: Recordati Industria Chimica e Farmaceutica S.p.a, Inventors: Barchielli M., Colombo P., Rossi A., Adorni G.
51. Bertoni S. et al., "Spray congealed lipid microparticles for the local delivery of  $\beta$ -galactosidase to the small intestine", *European Journal of Pharmaceutics and Biopharmaceutics* 2018, 132, p. 1-10.
52. Cordeiro P. et al., "Spray congealing: applications in the pharmaceutical industry", *Powder Technologies & Processing, Chemistry Today*, 2013, Vol. 31 (5).
53. EMEA/CHMP/ICH/730808/2009
54. Balducci A.G. et al., "Layered lipid microcapsules for mesalazine delayed-release in children", *International Journal of Pharmaceutics*, 2011, 421, p. 293-300.
55. Gana I. et al., "An Integrated View of the Influence of Temperature, Pressure and Humidity on the Stability of Trimorphic Cysteamine Hydrochloride", *Molecular Pharmaceutics* 2015, 12, p. 2276-2288.
56. Regulatory, Tox and Safety Overview, Compritol HD 5 ATO, Gattefossé.
57. Panigrahi K. et al., "Gelucire: a versatile polymer for modified release drug delivery system", *Future Journal of Pharmaceutical Sciences* 2018, 4, p. 102-108.

# Chapter II

## 1. INTRODUCTION

### 1.1 General aspect of pulmonary administration

Pulmonary delivery of drug has become an attractive and challenging target for the health care researchers since the lung is a suitable site both for local deposition and for systemic drug delivery.<sup>1,2</sup> The administration of aerosol therapeutics is a valid alternative to oral or invasive systemic delivery of drugs. In addition, recent advantages in aerosol technologies have led to the development of small-particle aerosols to be deposited in the alveolar region, thus being suitable for systemic absorption.<sup>3</sup>

The efficient delivery of an inhalable formulation to the lung basically depends on the aerodynamic particle size of the particles being inhaled. Particles in a range within 1 and 5  $\mu\text{m}$  are considered optimal for the treatment of most respiratory diseases, whereas larger particles ( $> 5 \mu\text{m}$ ) primarily deposited in the oropharynx region and are generally swallowed.<sup>4</sup> Compared to other routes of administration, drug delivery to the lungs offers several advantages. First, the need of a lower dose to achieve an equivalent therapeutic effect (i.e. 100–200  $\mu\text{g}$  dose by inhalation is therapeutically equivalent to 2–4 mg of oral dose of salbutamol sulfate) and the avoidance of the first pass metabolism, that allow to decrease the potential side effects and to achieve a rapid onset of action.<sup>5</sup> Furthermore, the inhalation route is characterized by rapid drug absorption because of the large surface area of the lung and consequently by high bioavailability. In addition, it is particularly useful due to the increasing number of proteins and peptide that can not be developed for conventional oral delivery. In fact, it is employed for the administration of drug poorly absorbed orally. Therefore, the pulmonary delivery of drugs is able to treat local respiratory diseases like asthma, local infectious diseases, pulmonary hypertension, cystic fibrosis, and it allows the systemic use of insulin, human growth hormones and oxytocin.

### 1.2 Mechanism of aerosol deposition

Based on the particle size, inhalation microparticles administered by the pulmonary route are typically classified in: coarse particles ( $\geq 5 \mu\text{m}$ ), fine particles (0.1–5  $\mu\text{m}$ ) and ultrafine particles ( $\leq 0.1 \mu\text{m}$ ).<sup>6</sup> A narrow particle size distribution or a monodisperse aerosol (with particles of equal size) is highly recommended for optimal deposition and specific pulmonary targeting.<sup>7</sup> The deposition of inhaled particles, intended as the process that involves the trapping of the particles that enter the respiratory tract being in contact with the wet respiratory surface, is of fundamental importance for pulmonary administration. The

deposition of the inhaled particles can occur according to three different mechanisms (Figure 42):

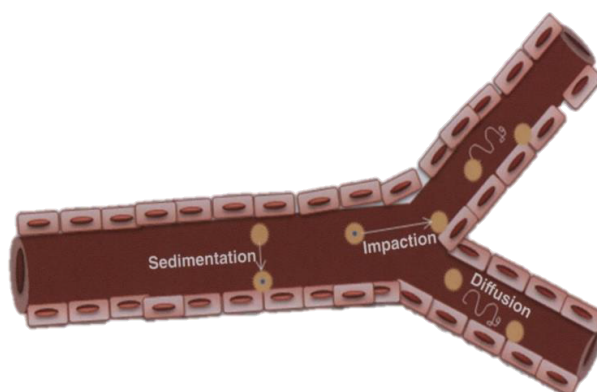


Figure 42. Mechanism of particle deposition in the respiratory tract.<sup>5</sup>

- inertial impaction: is a flow-dependent mechanism that influences the deposition of large particles ( $\geq 5 \mu\text{m}$ ) that do not follow the trajectory of the air stream, due to inertia, causing their impact as well as their deposit within the wall of the airways. This mechanism takes place especially in the upper respiratory tract where the airflow is mainly governed by turbulence and the air velocity is relevant;
- gravitational sedimentation: this mechanism is particularly relevant for particles having a particle size in the range  $0.5\text{-}5 \mu\text{m}$  since they may deposit by sedimentation in the bronchial and alveolar region. The sedimentation process is mostly caused by the gravitational force and the rate of sedimentation deposition increases when an increase in the particle size together with a decrease in the flow rate occurs;<sup>8</sup>
- Brownian diffusion: is a typical mechanism that involves particles of the lower airways and the alveolar zone having a size lower than  $0.5 \mu\text{m}$ . It is caused by Brownian motions that increase when the particle size and the airflow rate decrease. This phenomenon mainly depends on the geometry rather than the aerodynamic size of the particles.<sup>1</sup>

### 1.3 Factors affecting the therapeutic effect

The aerosol deposition mechanism strictly depends on several parameters, such as particles characteristics (particle size, shape, density and hygroscopicity)<sup>9</sup>, the geometry of the airways (age, gender and patient's health condition) and breathing pattern (frequency and breath-holding time).<sup>10,11</sup> The structure of the respiratory airways combined to specific defense mechanisms, like the mucociliary clearance, represent possible limitations imposed by the pulmonary route of administration.<sup>12</sup>

#### 1.3.1 Airway geometry

The deposition of the aerosol particles in the lungs is largely dependent on the structure of the airways.<sup>3</sup> In fact, parameters such as diameter, length as well as each bifurcation and branching contribute to the possibility of particle deposition by impaction hence causing a decrease in the aerosol fraction available to exert the therapeutic effect.<sup>1</sup>

#### 1.3.2 The physics and chemistry of an aerosol

An important measure of the deposition of aerosolized particles is provided by the aerodynamic diameter. The aerodynamic diameter is described as the diameter of a sphere of unitary density, which reaches in the air stream the same velocity pattern as a non-spherical particle of arbitrary density.<sup>11</sup> This parameter delineates the mechanism of particle deposition in the respiratory airways. The aerodynamic diameter ( $d_{ae}$ ) is well explained by the following equation in which the particle shape is considered:

$$d_{ae} = d_v \sqrt{\frac{\rho}{\rho_0 X}}$$

where:

$d_v$ : spherical equivalent volume diameter

$\rho$ : density of the solution

$\rho_0$ : density of 1 g/ml

$X$ : dynamic shape factor

The reported equation takes into account a factor ( $X$ ) that has a value equal to 1 for a sphere particle and, in addition, the density ( $\rho$ ) and the volume diameter ( $d_v$ ). The latter is of relevant

importance since it allows to establish the aerodynamic diameter of an aerosol using the equivalent volume diameter. Unfortunately, real particles do not correspond to spheres; therefore, they could present a lower aerodynamic diameter. Mass Median Aerodynamic Diameter (MMAD) of an aerosol is the particle size below which 50% of the population falls and is often denoted as  $d_{ae50}$ . Particle shape plays an important role in the deposition since irregular particles are cohesive, while spherical ones have a more smooth profile. Another relevant parameter is the hygroscopicity of inhalation powders, since it happens very frequently that many drugs absorb water in the respiratory tract, causing an increase in their size and, as a consequence, the deposition in the upper airways.<sup>13</sup>

### 1.3.3 Airflow rate

The different respiratory airflow rate has a considerable impact on the deposition of the aerosol through the respiratory system. In fact, rapid and turbulent airflow led to a reduction of the residence time of the particles in the airways promoting their deposition in the oropharynx and in the upper respiratory tract. On the contrary, slow inhalation flow rate results in the deposition in the lower respiratory regions. In addition, the increase of the tidal volume, defined as the volume of air exposed between a normal condition of inspiration and expiration, leads to an improved aerosol deposition in the lower airways.<sup>3</sup> For this reason, general practitioners are used to train patients to breathe deeply and slowly holding the breath while administering an inhalation product.

### 1.3.4 Particle clearance

The various clearance mechanisms that can occur in the respiratory airways can be summarized in:

- mucociliary clearance: due to its potential as a barrier for drug absorption, by means of the movement of the mucus through the action of ciliated epithelial insoluble inhalable products are removed from the respiratory tract within 24 h of inhalation;
- mechanical clearance: it involves coughing and swallowing of inhaled particles situated in the upper respiratory airways with expectoration that can eliminate many inhaled particles;
- alveolar macrophages: related to poorly soluble particles retained in the alveolar region, they are cleared away by the action of macrophages thus reducing the effectiveness of the treatment.<sup>1</sup>

### 1.3.5 Diseases

Obstructions of the airways and presence of a thick mucus layer can change the airways geometry modifying the airflow velocities and turbulences thus resulting in ineffective aerosol deposition in the respiratory system and drug efficacy.<sup>1</sup> In this thesis work the focus was on cystic fibrosis, which will be described in the Section 1.7.

## 1.4 Inhalation drug products

The development of an effective inhalation therapy depends not only on the active agent, but also on a well-designed delivery system and formulation. Since inhalation drug products are combination products, the optimization of the overall system (composed of drug, drug formulation and device) is mandatory for the successful development of inhalation therapies.<sup>14,15</sup> The formulation is intended to offer efficacy for patients, and for this to be truly achieved, it needs to be compatible and to work together with a device.<sup>16</sup> An inhalation product should be able to provide consistent dose content, along with suitable aerodynamic particle size distribution, to guarantee that the drugs can be efficiently delivered to the target sites in the lung. In order to achieve good patient compliance, a well-designed inhaler must also take into account the “human factor”, such as its usability for patients in terms of robustness, ease of use, portability, and suitability for all ages.

The commercially available devices for inhalation administration can be classified in nebulizers, metered dose inhalers, metered dose nebulizers and dry powder inhalers. In this thesis, only the dry powder inhalers are described, since they are used for the *in vitro* assessment of manufactured spray-dried powders for inhalation.

### 1.4.1 Dry powder inhalers

Dry powder inhalers (DPIs) are considered the most popular inhalation devices due to several factors, such as their convenience and compliance. In DPIs, the formulation to be administered to patients is present in form of a dry powder. Whether compared to liquid formulations, DPI drug inhalation products present improved chemical stability, even if assuring an easy aerosolization and alveolar delivery is more challenging.<sup>17</sup> They provide a fast administration, requiring limited maintenance and cleaning procedures. DPIs necessitate of a minimum inspiratory effort to effectively dispense and disperse the formulation.<sup>18</sup> In addition, they require the least patient coordination between breathing and actuation of the device to deliver the formulation.<sup>17</sup> Hence, they can be used by different categories of patients having distinct inspiratory capability. However, DPIs are best suited

for adult patients, in which a better dose uniformity is guaranteed, rather than young or geriatric patients.

DPIs can be distinguished as single-unit dose, multi-unit dose, and multi-dose reservoirs. In single-dose DPIs, the dose is delivered in previously filled capsules. Before the administration, patients manually load the capsule into the device. In Figure 43, a representation of one among the most used single-dose DPIs, the RS01 (Plastiapè® S.p.A, Osnago LC, Italy) dry powder inhaler, is reported. Multi-unit dose DPIs use pre-metered doses already packaged in a blister so that the device can hold multiple doses at the same time without the need to be reloaded. Finally, in multi-dose reservoir DPIs the powder is contained in bulk and have a built-in mechanism to properly meter the doses before the actuation.<sup>17</sup>

According to the mechanism of powder aerosolization, DPIs can be classified as passively or actively actuated devices.<sup>17</sup> Most of the DPIs are passive actuated devices, also called breath-actuated devices. They are entirely based on the patient's inspiration flow to provide the sufficient energy for dispersing and deaggregating the powder from the device.

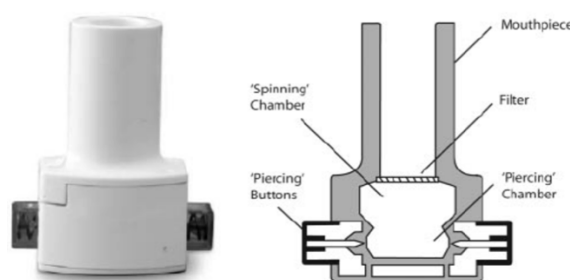


Figure 43. Representation of a RS01 (Plastiapè® S.p.A, Osnago LC, Italy) dry powder inhaler.

The inspiration should be rapid and energetic in order to achieve a high fraction of respirable microparticles.<sup>1</sup> Among the commercially available passive DPIs there are Rotahaler™ and Spinhaler™, both of them single-dose devices. In the Rotahaler™, a capsule containing the formulation is loaded into the device. Before the actuation, the capsule is pierced and an impeller rotates the powder released from the capsule by the inspiratory flow of the patient.<sup>17</sup>

### 1.5 Production of inhalation products

The manufacturing of inhalation drug products is aimed at the obtainment of microparticles with suitable characteristics such as size, shape, density and morphology.<sup>1</sup> Spray drying is a widely used particle engineering technique for the manufacturing of inhalable

microparticles.<sup>19</sup> This technology has been efficiently used in the past for the preparation of antibiotic, anti-inflammatory and insulin dry powders.<sup>20</sup> This process provides many advantages; in fact, it is a rapid, reproducible and continuous operation process, suitable for industrial scale-up manufacturing.<sup>21</sup> Starting either from a solution or a suspension, spray drying technology allows to obtain a dry powder by atomization through a hot drying gas stream.<sup>4</sup> The process mainly consists of four steps:

- atomization of the feed solution or suspension, containing the drug, into droplets;
- drying of the droplets in contact with hot air that circulates inside the drying chamber;
- formation of dry particles due to the rapid solvent evaporation;
- separation of the dried particles from the collector.<sup>22</sup>

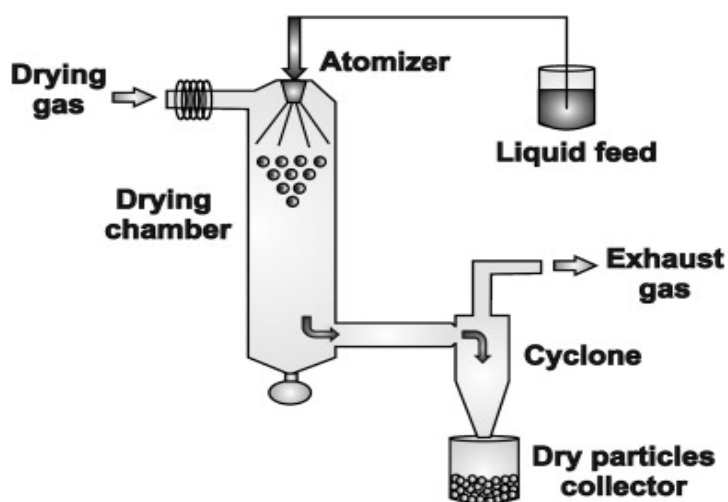


Figure 44. Schematic representation of the spray drying process.<sup>4</sup>

The capacity of spray drying process to incorporate multiple components into a particle through a single step process has been deeply employed over the years. In fact, by means of the spray drying, particles can be engineered to enclose different components useful in improving drug stability and aerosolization properties.<sup>23</sup>

In Figure 44, an illustration of a classic spray drying process and the related steps involved, is described. The drug is either solubilized or suspended in water and/or organic solvent.<sup>24</sup> Through the action of a peristaltic pump, the solution is pumped into a nozzle where it is atomized into small droplets in the drying chamber. The small droplets are then quickly dried due to the rapid solvent evaporation with the consequent formation of dried particles that are separated from the gas stream by means of a cyclone and finally collected. There are different types of atomizers that can be employed. Among the most common used, there

are the two-fluid and three-fluid (or coaxial) nozzle. The latter is composed of two concentric nozzles, from which two solutions are atomized (one outside and one inside). Generally, the solution used for coating flows outside, while the one containing the active ingredient and any other excipients inside. The two fluids are then mixed and the liquid is atomized in droplets. In the research project here described, both nozzle's types were employed; in particular, the coaxial nozzle considering the high instability of the drug.

### 1.6 *In vitro* models of pulmonary drug absorption

The latest developments in the pulmonary delivery of drugs require the need for *in vitro* methods to study the cellular mechanism involved in drug permeation and transport towards the airway epithelia.<sup>25</sup> In addition, *in vitro* models would be useful in studying the pathogenesis of diseases and in developing new therapies. The significant characteristics of airway epithelia for the study of drug delivery are: cell differentiations, the formation of a polarized tight cell layers, the presence of mucus and the expression of transporters and metabolic systems.<sup>26</sup> To investigate the interactions between drugs and airway epithelium, *in vitro* models have been employed using excised tissues, primary cell cultures as well as immortalized cell lines.

In recent years, the high predictability and the prompt throughput provided by cell cultures have driven the interest of pharmaceutical industries and companies.<sup>26</sup> Primary cultures of human airway epithelia resulted to be useful in the study of the defective Cl<sup>-</sup> secretion in cystic fibrosis patients.<sup>27</sup> However, primary cells present some drawbacks. First, the access to the tissues is limited; then, primary cultures are characterized by short lifespans, heterogeneity within and between cultures and unpredictable reproducibility. For this reason, several immortalized cell lines, deriving from carcinomas or having been transformed by means of viral genes, were developed since they guarantee a high degree of reproducibility and are easily maintained in culture.<sup>28</sup> Among other advantages, they guarantee a predictive, rapid and cost-effective approach to investigate the bioavailability across the pharmacological barriers.<sup>29</sup> Every cell line has different phenotype and characteristics thus necessitating of different requirements. A proper cell culture practice together with a deep knowledge on factors such as passage numbers, seeding density, composition of culture medium, is mandatory for the well-being of the cells and for the reliability of the experiments conducted.<sup>30</sup>

The airway epithelium of the lung represents a physical barrier to drug absorption and is constituted of various cell types having different properties. Among them, Calu-3 cell line

expresses a suitable respiratory epithelium cell-like phenotype and is considered, so far, the most appropriate cell line for the study of the mechanism of drug absorption through bronchial epithelium due to the close similarity to this epithelium *in vivo*.<sup>29,31</sup> In fact, Calu-3 cells are capable of expressing the cystic fibrosis transmembrane conductance regulator (chloride ion channel); in addition, Calu-3 form functional tight junctions and, when cultured under air-liquid interface conditions, they are able to secrete a thick mucus layer on the surface of the epithelium.<sup>32</sup> What is more, they grow rapidly and persistently and can be trustworthy over a wide range of passages.<sup>25</sup> NuLi-1 cell line is developed from healthy human isolated airway epithelia transformed by reverse transcriptase component of telomerase (hTERT) and by human papillomavirus (HPV-16 E6/E7).<sup>33</sup> Cultures of this cell line form tight junctions and are used for the studies of active and passive drug transport.<sup>34</sup> Apart from Calu-3 and NuLi-1 cell lines, a model of cystic fibrosis airway epithelium was employed. Different cell lines have been originated by transformation of bronchial epithelial cells of cystic fibrosis patients. Primary lung cells from cystic fibrosis lung transplant recipients were infected with hTERT and HPV-16 E6/E7 to originate CuFi-1 cell lines. This cell line conserves the capability of developing polarized differentiated epithelia active in Na<sup>+</sup> and Cl<sup>-</sup> transport that express trans epithelial resistance and maintain the ion channel physiology expected of each genotype.

## 1.7 Cystic Fibrosis

### 1.7.1 Pathogenesis of Cystic Fibrosis

Cystic Fibrosis (CF) is an autosomal recessive genetic disorder that include several medical conditions caused by mutations of the cAMP/PKA-dependent CFTR (Cystic Fibrosis Transmembrane Conductance Regulator) gene protein located on chromosome 7 (7q31.2).<sup>35</sup> The estimated prevalence of this genetic disorder is calculated to be 1 in 2500-4500 live births among Caucasians.<sup>36</sup> CFTR is a phosphorylation-regulated transmembrane channel for chloride ions exchange, typically present in the majority of the apical membrane of epithelial tissues such as lungs, gut, kidney and uterus.<sup>37</sup> The altered chloride membrane conductance in the epithelial cells impairs the physiological osmotic fluid movement thus leading to the presence of greasy mucus in the respiratory and intestinal tract, pancreatic insufficiency, increased sweat salt concentration, infertility in male patients and liver malfunctions (Figure 45).<sup>38</sup>

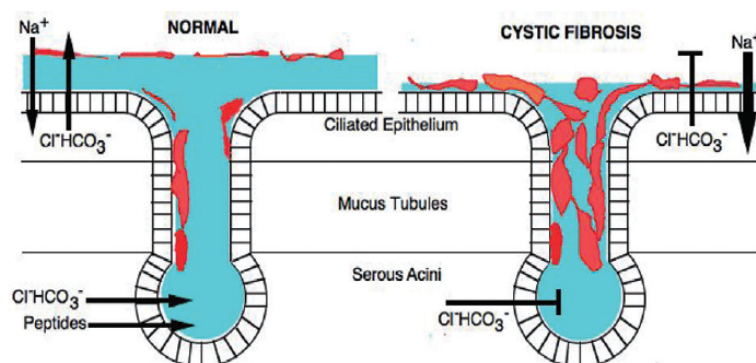


Figure 45. Representation of the mechanism of transport of salts in healthy and CF airways.<sup>1</sup>

More than 2000 different mutations of CFTR gene have been found to be responsible of the clinical manifestation of the pathology that can therefore be variable in terms of intensity and quality of the symptoms from patient to patient.<sup>39,40</sup> In addition, mutations of the gene encoding for alfa-1-antitrypsin and air pollution have been considered as co-factor in determining symptoms and pathology outcome.<sup>41</sup> Mutations of CFTR in heterozygotes Caucasians have been proposed as responsible of the resistance to Tuberculosis infections and this could at least explain why the mutations are maintained over time.<sup>42</sup> Anyway, despite the typology of mutation, the chronic obstructive lung disease is a condition that affect the 70% of CFTR homozygotes at the age of seventeen and lung chronic infections are the main causes of death among patients.<sup>43</sup>

Since Cystic Fibrosis is a genetic disorder, the cure of this pathology would require a genetic therapy that is not available so far. CFTR modulators are drugs able to improve the production, transport and functions of chloride defecting channels. The introduction of these drugs in therapy started in 2011 with the approval of Ivacaftor (Kalydeco<sup>®</sup>), a CFTR enhancer that was proved to efficiently increase the secretion of chloride ions.<sup>44</sup> Apart from Ivacaftor, there are now two combination pharmaceutical forms approved for CF treatment i.e. Lumacaftor/Ivacaftor (Orkambi<sup>®</sup>) and Tezacaftor/Ivacaftor (Symdeko<sup>®</sup>). Unfortunately, CFTR modulators are available only for specific mutations and can't be used *a priori*. The treatment of Cystic Fibrosis is focused therefore on symptoms relieving and usually requires a therapeutic plan tailored on the needs of the patient. The main target of the treatments available are the lungs and the exocrine pancreas. As for the latter, usually patients are recommended to take pancreatic enzyme supplements and vitamins to increase the amount of essential compounds introduced and absorbed.<sup>45</sup> The symptoms in the respiratory tract are often the major factors impacting the quality of the life of CF patients being the loss of pulmonary functionality the main cause of death among this population.

### 1.7.2 Bacterial infections by *Pseudomonas Aeruginosa*

Due to the lack of fluidity of the mucus, the mucociliary clearance mechanism, responsible for the clearance of bacteria as well as other microorganisms from the respiratory tract, is impaired and altered.<sup>46</sup> This is associated with chronic infections by pathogens. Infections of the lower airways by *Staphylococcus Aureus* and *Pseudomonas Aeruginosa* (*P. Aeruginosa*) are the most occurring in CF patients.<sup>47</sup> Chronic infections, associated to sustained and prolonged inflammation, are the main causes of pulmonary function declination. The presence of a thick and viscous mucus can lead to a decrease of the effectiveness of the drug delivery towards the respiratory tract.<sup>48</sup> *P. Aeruginosa* infections are challenging to treat since it is shown to be a resilient and resistant bacterium. In the lungs of CF patients, *Pseudomonas* is capable of producing a biofilm mucoid strain. The slow growth of the biofilm in CF patients is associated with an enhanced frequency of mutations and an adapting bacteria mechanism to the conditions in the lungs, and to resistance towards antibiotic therapy.<sup>49</sup>

### 1.7.3 Antibiotic treatments

The pharmacological treatment usually consists of an association of one or more antibiotics and anti-inflammatory drugs.<sup>50</sup> It has been reported that intravenous antibiotic treatments against *P. Aeruginosa* decreases the concentration of proteinase in secretions, thus improving lung function. For this reason, the administration of intravenous antibiotics should be given at regular intervals in a planned pharmacological regime in order to reduce lung inflammation presumably by reducing the bacterial activity.<sup>51</sup> Tobramycin intravenous administration is the only alternative during exacerbations.<sup>43</sup> Colistin (administered as colistimethate sodium) is usually used whenever tobramycin is not tolerated or with the tobramycin-resistant *Pseudomonas Aeruginosa* strains.<sup>52</sup> However, since the penetration of tobramycin through the viscous mucus is low following intravenous administration, high doses are necessary to obtain the minimum effective inhibitory concentration towards *P. Aeruginosa*. Due to the intravenous high posology, adverse side effects, including ototoxicity and nephrotoxicity, are very frequent.<sup>50</sup>

Since the concentration of antibiotic at the infection site is of relevant importance, delivering high concentrations of antibiotics directly to the lungs by inhalation is convenient, considering that inhalation therapy has several advantages over the systemic administration.<sup>53</sup> First, the side effects of the systemic exposure can be mitigated thus increasing the adhesion to therapy and patient compliance. Moreover, the drug can be

released directly to the site of action, i.e. the lung, avoiding the first pass effect. These aspects must be accurately evaluated in CF patients since the chronic colonization of the airways by microorganisms requires a chronic therapy with all the related inconveniences.<sup>54</sup> Several antibiotics have been studied for the management of pulmonary infections in CF patients; among these, the most prescribed are the aminoglycosides in combination with a  $\beta$ -lactam or a quinolone.<sup>55,56</sup> In fact, clinical trials delivering multiple APIs in combination demonstrated a significant improvement in the efficacy of the treatment of the common respiratory diseases, including asthma and COPD.<sup>57</sup>

Tobramycin is the aminoglycoside of first choice. It is available for inhalation administration either as solution for nebulization either as dry powder inhaler. Nebulized antibiotics like tobramycin (TOBI<sup>®</sup>) and aztreonam (Cayston<sup>®</sup>) have proven to be efficient in the treatment of CF patient's infections; nevertheless, they are easily cleared away from the lungs.<sup>58</sup> What is more, nebulization products generally require an administration time of approximately 20 minutes.<sup>59</sup> Apart from tobramycin, other antibiotics such as gentamicin, amikacin and colistimethate sodium (Colobreathe<sup>®</sup>) are generally used in the management of CF patient's exacerbations.<sup>60</sup>

In order to keep sufficiently high levels of antibiotics for antimicrobial efficacy, multiple doses of high concentration of antibiotics are mandatory each day.<sup>61</sup> Dry powder inhalers (DPI), since they are activated by patient inspiration flow, are a significant alternative because of rapid dose administration and high local drug concentration.<sup>62,63</sup> TOBI<sup>®</sup> Podhaler<sup>™</sup> (Novartis Pharmaceuticals Corporation, East Hanover, NJ, USA) is the dry powder pharmaceutical product of the inhaled antibiotic tobramycin. It is a low resistance device, which allows to generate a high inspiratory flow thus achieving a predictable dose delivery.<sup>64</sup>

#### 1.7.4 Mucolytic agents in the treatment of cystic fibrosis

Antibiotics represent the mainstay pharmacological treatment in the management of cystic fibrosis patients' infections. However, the increasing antibiotic resistance is an issue that must be addressed. In the last years, the urgent need for research into new antimicrobial agents able to target the biofilm enhancing the success of antibiotic treatments was emphasised.<sup>65</sup> Due to the thickness of the dehydrated mucus and sputum creating an ideal environment for microbial colonization and infections, the co-administration of mucolytic as well as osmotic agents is highly recommended.<sup>66</sup> Drug products containing Dornase alfa (Pulmozyme<sup>®</sup>, Roche), N-acetylcysteine (Mucomyst<sup>®</sup>) or mannitol (Bronchitol<sup>®</sup>) have been proved to be effective in reducing the viscosity and elasticity of the mucus thus increasing

the effectiveness of the antibiotic treatment. N-acetylcysteine has been previously described in literature as mucolytic agent with antimicrobial properties.<sup>67</sup> In fact, it is able to decrease the formation of the biofilm made up by several bacteria promoting at the same time the disruption of the already formed biofilms.

### 1.8 Cysteamine (Lynovex<sup>®</sup>) in the treatment of cystic fibrosis

In relatively recent times, cysteamine has been granted an orphan designation for the treatment of cystic fibrosis in Europe and USA in 2011 and 2014, respectively. Furthermore, cysteamine gained a Fast Track designation for CF exacerbations by the FDA in March 2018.<sup>68</sup> Cysteamine, as experimental antibacterial drug NM001 (Lynovex<sup>®</sup>), was proved to advantageously treat CF symptoms being an effective mucolytic and disrupter/preventer of the biofilm formed by *P. Aeruginosa*.<sup>66</sup> Cysteamine also acted towards other CF pathogens. The mucolytic effect of cysteamine was attributed to the thiol moiety that reduces the disulphide bond in mucus proteins, thus breaking up their ligand bonding and structure.<sup>65</sup> In addition, cysteamine was surprisingly found to exercise a direct antimicrobial effect against *P. Aeruginosa*. In fact, the administration of Lynovex<sup>®</sup> improved the efficacy and potency of tobramycin, ciprofloxacin, colistin and other antibiotics commonly employed in the treatment of the disease.<sup>65,66</sup> A recent paper described the favorable effect of cysteamine administered in combination with epigallocatechin gallate (a well know antioxidant agent) in re-establishing CFTR function and expression in nasal brushing from CF patients.<sup>69</sup> Lynovex<sup>®</sup> (NM001) is being developed by NovaBiotics in both oral and inhaled dosage forms. The oral capsules were designed as a first high dose and short term intervention in order to address the infectious exacerbations of CF patients. At the same time, an inhaled form of Lynovex<sup>®</sup>, as dry powder inhaler, was developed as low dose for long term maintenance of symptoms in CF's patients.<sup>68</sup> Lynovex<sup>®</sup>, intended as adjunct treatment alongside primary antibiotic therapy, due to the overall multi-active properties of cysteamine, was found to be therapeutically beneficial in CF patients. The co-administration of cysteamine could improve the lifespan of conventional antibiotics increasing their efficacy and reducing the frequency of dose administration.<sup>66</sup> In 2014, Lynovex<sup>®</sup> oral capsules successfully completed a phase IIa clinical trial in UK. The following phase IIb has started in 2019. The inhaled formulation was recently optimized and clinical trials will initiate in 2020, due to the very encouraging efficacy and safety data obtained from the preclinical phase.<sup>68</sup>

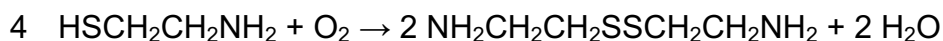
### 1.8.1 Inhalable cysteamine formulations for the treatment of lung diseases

Inhalable formulations of cysteamine for the treatment of lung diseases were developed after the orphan drug designation granted to Lynovex<sup>®</sup>. To guarantee the effectiveness of cysteamine in the lungs, the drug has to be administered as an aerosol in order to reach the respiratory tract and exercise the therapeutic effect. Patent US 2017/0348254 discloses spray-dried microparticles of cysteamine bitartrate alongside stabilizing agents such as trehalose and leucine.<sup>70</sup> However, the aerodynamic performance of the obtained powders was poor and the fine particle doses showed low values. In view of the inhalation administration, an important issue to face is the instability of the raw material in environmental conditions. In fact, cysteamine base and the related salts are hygroscopic, deliquescent and prone to oxidative degradation. Nevertheless, cysteamine bitartrate has shown to be the most stable salt of cysteamine. Furthermore, the commercially available raw drugs, such as cysteamine bitartrate and hydrochloride, have not a proper particle size for being administered as dry powder formulation. All these factors clearly confirm the need for a new stable inhalation product of cysteamine with a suitable particle size for inhalation administration.

### 1.8.2 Cysteamine base

Cysteamine base ( $\beta$ -mercaptoethylamine) is a decarboxylation product of cysteine, characterized by the presence of a thiol as well as an amino group. The chemical structure is reported in Figure 3.

In the human organism it is present at very low concentrations as part of the metabolic pathway of coenzyme A. The residue -SH can bind an acetyl group in the acetyl-CoA through a thioester bond. In presence of oxygen, cysteamine turns into its dimeric degradation product, cystamine, according to the following reaction:



## 1.9 Hyaluronic acid

HA is a natural occurring biopolymer, ubiquitously distributed throughout the body, governing many important biological functions in humans.<sup>71</sup> It consists of a linear chain of D-glucuronic and N-acetyl D-glucosamine (Figure 46) linked together by glycosidic bond  $\beta$ <sub>1,3</sub> and  $\beta$ <sub>1,4</sub>.<sup>72</sup> It is an abundant constituent of the extracellular matrix of connective tissue, synovial fluid, embryonic mesenchyme and vitreous humor. The lungs, together with skin

and intestine, enclose more than 50% of HA of the body.<sup>73</sup> It possesses high hydrating properties thus contributing to cellular growth and tissue repair, inhibition of migration, chemotaxis and aggregation of leucocytes and monocytes.<sup>73</sup>

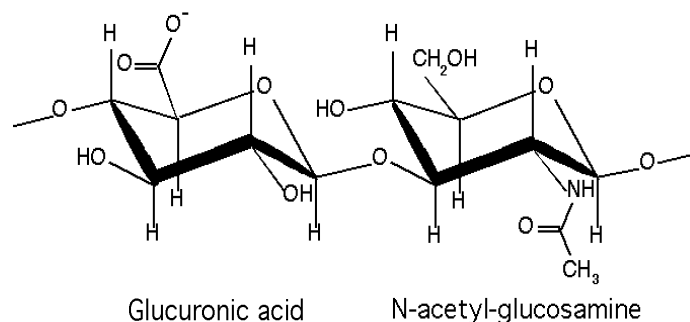


Figure 46. Chemical structure of hyaluronic acid.

It is a highly hydrophilic molecule and when not bound to other molecules it tends to bind water molecules assuming a viscous consistency similar to a gel.<sup>73</sup> Hyaluronic acid is commercially available as sodium hyaluronate; it appears as a white powder that must necessarily be stored at temperatures between 2-8 ° C. Some studies have shown that the HA, at a certain molecular weight, has an important role in inflammation.<sup>74</sup> High-molecular weight ( $\geq 1$  MDa) HA is a component of the normal airway secretions and is involved in the homeostasis of the entire respiratory system.<sup>75</sup> In particular, it has been observed that fragments with a high molecular weight (400-20.000 kDa) have anti-inflammatory properties due to the hydrophilic nature of hyaluronic acid, which binds large quantities of water. On the contrary, low molecular weight fragments (180-370 kDa) tend to accumulate at sites of inflammation and therefore stimulate the production of pro-inflammatory cytokines.<sup>76,77</sup> This pro-inflammatory activity is thought to be associated with the high affinity of HA for the CD44 receptor, since activation of this receptor on leukocytes promotes the transfer of pro-inflammatory cells into lesion sites, while the interaction with that located on macrophages induces the transcription of pro-inflammatory genes.<sup>78</sup> If properly formulated, hyaluronic acid can be used in pharmaceutical preparations for its antibacterial properties and its compatibility with tissues and the ability to regenerate them.<sup>79</sup> In addition, hyaluronic acid can also be used to increase the stability of the drug in solution and to promote the absorption of drugs and proteins through the mucus tissue.<sup>80</sup>

### 1.10 L-Leucine

Leucine is an essential branched-chain amino acid and appears as a white crystalline solid powder. The chemical structure is shown in Figure 47.

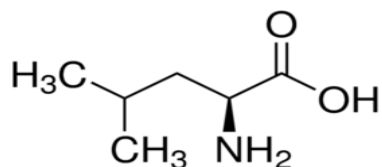


Figure 47. Chemical structure of L-Leucine.

L-leucine is soluble in water, ethanol and acetic acid whereas being insoluble in ether. It is widely used in the development of spray-dried formulations since it is considered an effective excipient in the manufacturing of inhalation powders. In fact, L-leucine demonstrated to efficiently increase the aerosolization performance of a dry powder inhaler, acting as a “dispersing enhancer” for respirability purposes.<sup>81,82</sup> This property is the result of L-leucine forming low density hollow microparticles with a rough coating surface being in this way suitable for inhalation administration.<sup>83</sup> In particular, it is reported that L-leucine used in a concentration range of 5-20% (w/w), is capable of improving the yield of the process as well as the aerosolization properties.<sup>84</sup> The incorporation of L-leucine as excipient in a spray-dried formulation is promising in order to obtain a more dispersible powder.<sup>84</sup> In addition, L-leucine is reported to provide a moisture protection effect, reducing the humidity of the powder thus acting as anti-hygroscopic agent.<sup>85</sup>

### 1.11 Trehalose

Trehalose is a sugar with different properties, including flavor enhancer, wetting agent, sweetening agent, stabilizer and thickener. It appears as a white crystalline solid with a sweet taste (45% of sweetness of sucrose) and odorless.<sup>86</sup> It is soluble in water, scarcely soluble in ethanol and insoluble in ether. The chemical structure is reported in Figure 48.

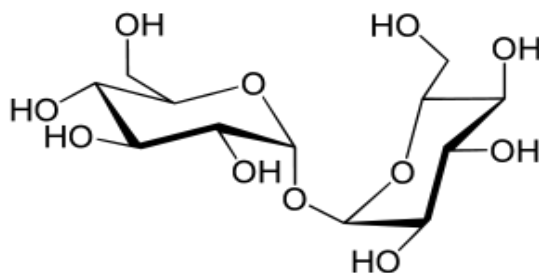


Figure 48. Chemical structure of trehalose.

Trehalose is often employed due to its ability to stabilize biological active pharmaceutical drugs and to increase their shelf life.<sup>87</sup>

### 1.12 Polyvinylpyrrolidone

Polyvinylpyrrolidone (PVP) is part of the lactam family. It is a vinyl polymer, produced through the radicalic vinyl polymerization. It appears as odorless and white granular powder. PVP is used as a disintegrating excipient as well as a stabilizer and coating agent, especially in solid formulations.<sup>88</sup> Its chemical structure is reported in Figure 49.

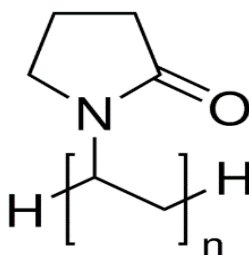


Figure 49. Chemical structure of Polyvinylpyrrolidone.

### 1.13 Ascorbic acid

Ascorbic acid (Figure 50) is an anti-oxidant agent; it appears as a white crystalline solid, odorless and hygroscopic. It presents two dissociation constants:  $pK_{a1} = 4.17$  and  $pK_{a2} = 11.57$ .

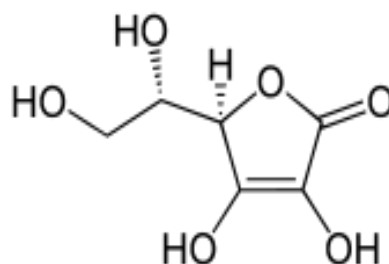


Figure 50. Chemical structure of ascorbic acid.

### 1.14 Cyclodextrins

Cyclodextrins (CD) are enzymatic degradation products of starch obtained by means of the cyclodextrin-glycosyl-transferase (CGT). From the chemical point of view, CD are cyclic oligosaccharides containing at least six units of D-(+)-glucopyranose attacked with a  $\alpha$ -1,4-glucosidic bond. The three natural cyclodextrins  $\alpha$ ,  $\beta$  and  $\gamma$  (Figure 51) differ from each other by their ring size and solubility in water. Cyclodextrins appear as white, fine and odorless powders, with a slightly sweet taste. They are used in the manufacturing of inhalation powders as stabilizing and solubilizing agents.

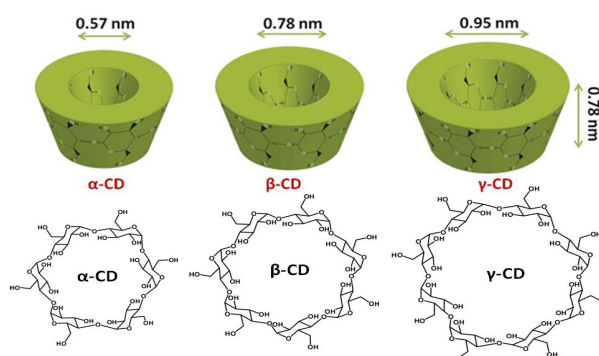


Figure 51. Chemical structure of the natural cyclodextrins.

Cyclodextrins form a truncated cone in which the central cavity varies in size depending on the type of cyclodextrin. The interior of the cavity is hydrophobic, while the exterior is hydrophilic, due to the arrangement of the hydroxyl groups. This feature allows the cyclodextrins to host a molecule to form an inclusion complex. In this way, CD can be used to form inclusion complexes with many drugs, improving their chemical and physical stability, dissolution profile, bioavailability. CD are sometimes used to mask the unpleasant taste of drugs.

## 2. AIM

Cystic fibrosis (CF) is a hereditary disease that affects the cells in the lungs and the glands in the intestine/pancreas which secrete fluids such as mucus or digestive juices, respectively. As a consequence, these fluids become thick and viscous, blocking both the airways and the flow of digestive juices. Due to the decline in lung function, exacerbations or episodes of acute worsening of CF lung symptoms, often as a result of bacterial infection, are the principle cause of morbidity and mortality.-To date, lung diseases in cystic fibrosis patients are mainly treated with a combination of antibiotics, anti-inflammatory agents, bronchodilators and mucolytic agents.

In the latest years, cysteamine has obtained an orphan designation for the treatment of cystic fibrosis. Cysteamine was shown to advantageously treat CF symptoms by reducing the thickness of mucus allowing it to be cleared away more easily and, at the same time, by acting directly against the bacteria in the lungs, thus exercising both a mucolytic as well as an antibacterial activity.

Therefore, the research project aimed at the design and development of cysteamine spray-dried powders to be used for inhalation administration as an aerosol directly in the patient's airways. Formulation studies of cysteamine spray-dried powders for inhalation has been conducted starting either from cysteamine free base or from cysteamine bitartrate.

The project, that led to the submission of the European Patent Application EP18425038, successfully aimed at identifying an inhalation powder of cysteamine, either as cysteamine free base or cysteamine bitartrate, for the eradication of CF patients' infections.<sup>89</sup> Thus, novel cysteamine inhalable powders, advantageously obtained for making highly respirable microparticles, have been manufactured by spray drying. The novel formulation idea was based on the development of spray-dried cysteamine hyaluronate salts. Hyaluronic acid is well known in literature for its anti-inflammatory activity, but has never been considered as counterion for making a salt of cysteamine. Hyaluronic acid was selected since, to date, such polymeric substance has never been employed for the preparation of spray-dried cysteamine salts. In view of the inhalation administration, additional excipients such as L-leucine and trehalose were added to the formulation for respirability and stability improvement. The use of hyaluronic acid in combination with the active agent led to the obtainment of a stable salt with good aerodynamic properties for inhalation drug delivery.

The spray-dried inhalable cysteamine hyaluronate microparticles were characterized in terms of drug content and particle size distribution in parallel with FT-IR spectroscopy and  $^{13}\text{C}$  NMR analysis to verify the interaction between the API and hyaluronic acid during the spray drying process. The *in vitro* aerodynamic characterization was first assessed by means of Fast Screening Impactor; then, a deep investigation was conducted with Next Generation Impactor, according to Ph.Eur.

Cell cultures studies on *in vitro* respiratory epithelia were performed to investigate cell toxicity. Finally, rheology studies were carried out to verify the mucolytic properties of cysteamine reported in literature.

### 3. MATERIALS AND METHODS

#### 3.1 MATERIALS

- Cysteamine base (batch n. 605/05, Recordati, Milan, Italy);
- Cysteamine base (batch n. BCBT3349, Sigma Aldrich, Switzerland);
- Cysteamine bitartrate (batch n. 13100571, Recordati, Milan, Italy);
- Sodium hyaluronate 900 kDa (batch n. 850P-0023, Novozymes, Cina);
- Sodium hyaluronate EP ALTERGON PM 349 kDa (batch n. 1000004605, Altergon, Italy.);
- Dowex<sup>®</sup>Monosphere 650C (batch n. 419642/1, Fluka, Germany);
- Ethylenediaminetetraacetic acid (batch n. 61930, Riedel-de-Haën, Germany);
- L-leucine (batch n. M0096005, A.C.E.F., Fiorenzuola d'Arda (PC), Italy);
- Trehalose (batch n. 07/4801, A.C.E.F., Fiorenzuola d'Arda (PC), Italy);
- Acetic acid (batch n. 12H020503, VWR, Milan, Italy);
- Ascorbic acid (batch n. STBB0358, Sigma-Aldrich, Germany).

All materials and reagents used were of analytical grade according to Ph.Eur. and USP.

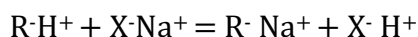
## 3.2 METHODS

### 3.2.1 Development process for the obtainment of cysteamine hyaluronate microparticles

In the preformulation study, the instability of the cysteamine base in the environmental conditions was considered. In the market, hyaluronic acid is available as sodium hyaluronate at different molecular weights. The molecular range used in this study was between 30 kDa and 1 MDa. In particular, we employed a sodium hyaluronate having a molecular weight of 0.35 MDa and 0.9 MDa.

#### 3.2.1.1 Preparation of hyaluronic acid solution by ion exchange method

In view of preparing a cysteamine salt, it was necessary to convert the sodium salt of hyaluronic (NaHA) in the acid form, able to interact in solution with the cysteamine base free. An ion exchange method was used to obtain hyaluronic acid starting from sodium hyaluronate solution, exploiting the ability of a resin to exchange  $\text{Na}^+$  ions with  $\text{H}^+$  ions, according to the following reaction:



Thus, a strong cationic resin (Dowex Monosphere™ 650C (H) matrix of styrene-DVB gel and sulfonic acid as functional group) was employed in “batch” mode: the solution to be treated was put in direct contact with the resin for the time necessary to complete the reaction. A representation of the matrix of a cationic resin is reported in Figure 52.

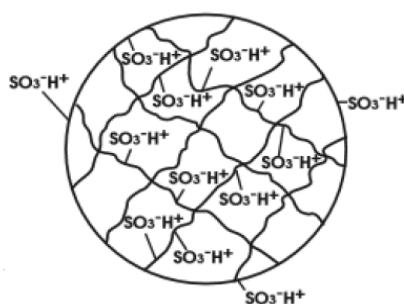


Figure 52. Schematic representation of a cationic resin with a matrix negatively charged to exchange positive ions.

The total capacity of the resin (the total number of available sites for the exchange), is the amount of active groups per weight or volume unit; theoretically, for each active group corresponds an exchange site. The total capacity was expressed in meq/ml.

In detail, in case of a formulation having a solid content of 0.25% (w/v), the solution of hyaluronic acid (HA) was prepared by introducing 500 mg of sodium hyaluronate (MW 0.35-0.9 MDa), depending on the cysteamine base/hyaluronic acid ratio to be used (see Section 3.2.1.2), in a flask containing 170 ml of MilliQ grade water. The flask was heated at 50°C until a solution of sodium hyaluronate was obtained. The pH values of the sodium hyaluronate solutions were measured. Then, considering that the capacity of the Dowex Monosphere™ 650C (H) resin is 2 meq/ml (density: 1.22 g/ml), 500 mg of resin were added to the hyaluronate solution. To increase the contact between sodium hyaluronate and the resin, the solution was kept under magnetic stirring at room temperature for a length of time, usually between 2 - 3 hours, until the value of pH was stable. An acid pH value indicates the complete transformation of sodium hyaluronate into hyaluronic acid (HA).

The solution containing HA was filtered by Buchner funnel and collected in a 200 ml volumetric flask. The remaining resin on the filter was washed with 10 ml of MilliQ grade water to extract the residual hyaluronic acid deposited on the surface of the resin.

### 3.2.1.2 Acid-base titration for the determination of hyaluronic acid/cysteamine base ratio for the preparation of spray-dried microparticles

The capacity of hyaluronic acid solution (expressed as meq) to titrate the cysteamine free base was determined. In details, 25 ml of hyaluronic acid solution, containing 63.25 mg of sodium hyaluronate (NaHA 0.35-0.9 MDa), were titrated, dropwise, with a solution of NaOH 0.01 N, contained in a 25 ml graduated burette. Bromothymol blue, used as indicator, was added to the flask containing the hyaluronic acid solution. The indicator change color from yellow to blue (pH around 7.0) was index of neutralization of the acid solution by the basic solution. As a function of the ml of basic solution added, it was possible to calculate the normality of the solution of hyaluronic acid according to the following equation:

$$N_a \times V_a = N_b \times V_b$$

where:

$N_a$  and  $V_a$  are the normality and the volume of the acid solution, respectively;

$N_b$  and  $V_b$  are the normality and the volume of the basic solution, respectively.

### 3.2.1.3 Manufacturing of cysteamine hyaluronate microparticles by spray drying

An accurately weighed amount of cysteamine base was added into the solution of HA, obtained with the method previously described in Section 3.2.1.1. Considering that cysteamine undergoes to degradation in presence of oxygen, the raw material was weighed under a nitrogen atmosphere within a humidity percentage lower than 10%. Cysteamine base was dissolved in the flask, containing the HA solution, under stirring, and then the volumetric flask was brought to the final volume of 200 ml with MilliQ grade water. The solid content in the formulations was between 0.25 - 1% (w/v).

Finally, the solution was sprayed by means of the spray dryer (Büchi Mini Spray Dryer B-290, Büchi Labortechnik AG, Switzerland). In addition to the spray-dried cysteamine microparticles, a spray-dried powder of hyaluronic acid was prepared by spraying a hyaluronic acid solution, obtained following the procedure previously described in Section 3.2.1.1, that involved the use of an ion exchange resin to obtain hyaluronic acid starting from sodium hyaluronate.

### 3.2.1.4 Two fluid and three fluid nozzles to produce cysteamine hyaluronate microparticles

Among the different nozzle types available for the manufacturing of microparticles by spray drying, the two-fluid and three-fluid (coaxial) nozzles were selected. In Figure 53, a representation of a two-fluid and a three-fluid nozzle is shown, respectively.

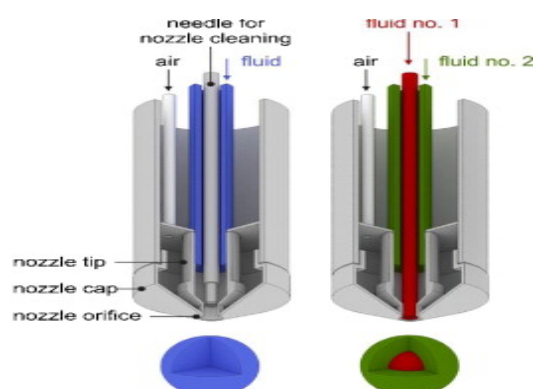


Figure 53. Representation of a two-fluid (left) and three-fluid nozzle (right).

The two-fluid nozzle is commonly used in spray drying technology. It consists of an inner and outer orifice. During the process, the liquid containing the drug is pumped through the inner channel until the nozzle tip where it is atomized by means of a compressed gas that

flows through the outer channel. On the contrary, by using the three-fluid nozzle system, three separate channels are available, enabling the spraying of two different solutions that meet at the tip of the nozzle where they form a concentric liquid, which is then atomized and dried due to compressed gas (generally hot air). In this way, it was possible to concurrently spray two separated solutions. Concerning the formulations in which the coaxial nozzle was employed, the outer orifice was feed with a 100 ml water solution of the excipients, while the inner orifice was feed with a 100 ml solution containing the cysteamine free base and hyaluronic acid. By means of a peristaltic pump, the two solutions were then separately sprayed at the same time through the nozzle allowing to obtain spray-dried coated microparticles with uniform characteristics.

### 3.2.2 Formulation study of cysteamine bitartrate spray-dried microparticles

In addition to cysteamine base, spray-dried microparticles containing cysteamine bitartrate were produced by spray drying technique. The percentage of the solid in each formulation was 1% (w/v). At first, a solution of cysteamine bitartrate in water was sprayed, by means of the two-fluid nozzle, simply by weighing an accurately amount of cysteamine bitartrate that was then dissolved in MilliQ grade water. Then, several excipients, compatible with the inhalation route of administration, were employed. The ratio between cysteamine bitartrate and the excipients was 70:30% (w/w). In all spray dryer experiments the coaxial nozzle was used. In this way, the outer orifice was feed with a water solution containing L-leucine, while the inner orifice was feed with a solution containing cysteamine bitartrate and other excipients, such as PVP, trehalose and cyclodextrins to enhance the stability of the drug. The inner orifice solution was prepared by weighing in a volumetric flask the excipients that were then solubilized in water. Finally, before the spraying, cysteamine bitartrate was weighed and dissolved in the flask containing a water solution of the excipients.

### 3.2.3 HPLC quantification of cysteamine

A Shimadzu chromatograph (LC-10AT, Shimadzu Europe GmbH, Duisburg, Germany) equipped with an isocratic LC-10AS pump and a SPD-10A UV-VIS spectrometer set at a fixed wavelength of 210 nm was employed. For the stationary phase, a Jupiter C18 column (4.6 x 150 mm, 5  $\mu$ m, 300 Å; Phenomenex, USA) set at 50°C was used. The composition of the mobile phase was as follows: 620 ml of Millipore Grade water, 330 ml of acetonitrile, 50 ml of methanol, 1.4 ml of H<sub>3</sub>PO<sub>4</sub> 85% (v/v) and 11.52 g of sodium dodecyl sulphate. The HPLC analysis was conducted at a flow rate of 1.6 ml/min, with an injection volume of 20  $\mu$ l (Waters 717 plus Autosampler, Waters Corporation, Milford, USA). The run time was 6

minutes, since the retention time of the peak corresponding to cysteamine was around 4 minutes. The method was validated for linearity in the range 0.005-1 mg/ml ( $R^2$ : 0.9992), precision (RSD% <2%), LOD (1.1 µg/ml) and LOQ (3.5 µg/ml).

#### 3.2.4 Drug content determination of cysteamine

The determination of cysteamine base and cysteamine bitartrate content in the spray-dried microparticles was carried out according to the following procedure. 5 mg of spray-dried microparticles were accurately weighed on an analytical balance. The powder was then transferred in a 10 ml volumetric flask and dissolved using a water solution containing 0.1% of EDTA and 0.8% of acetic acid. Since cysteamine is stable in acidic environment, the addition of acetic acid was able to guarantee the stability of the drug during the experiments performed. The flasks were sonicated for 5 minutes and then samples were analyzed by HPLC according to the analytical method described in Section 3.2.3. Standard solution was prepared weighing 10 mg of cysteamine bitartrate that were dissolved in a 10 ml volumetric flask using a water solution containing 0.1% of EDTA and 0.8% of acetic acid. Concerning the spray-dried cysteamine hyaluronate microparticles, considering that the molecular weight of cysteamine base is 77.15 g/mol and the one of cysteamine bitartrate 227.15 g/mol, the quantity of cysteamine base contained in the standard solution was calculated. The analyses were conducted in triplicate.

#### 3.2.5 Characterization of the cysteamine hyaluronate microparticles

##### 3.2.5.1 Determination of the particle size distribution

The dimensional analysis of the spray-dried cysteamine microparticles was determined by means of a laser light diffractometer (SprayTec, Malvern, Worcestershire, United Kingdom) equipped with a 300 mm focal lens, which measures particle size in the range of 0.1 and 900 microns. Samples were prepared by suspending 10 mg of spray-dried formulations in 10 ml of a solution of Span 85% (0.1% w/v) in cyclohexane. The suspension was sonicated for 10 minutes to avoid the formation of aggregates. Measurements were performed in triplicate. The assessment of the particle size distribution of the powders was also carried out by means of a Mastersizer laser light diffractometer (Mastersizer 3000, Malvern, Worcestershire, United Kingdom) equipped with a dry dispersion unit. Roughly 10 mg of powder was deposited in the feeder and dispersed in air through the Aero-S dry dispersion unit (Malvern, Worcestershire, United Kingdom), with a pressure of 4 bar with a total time of analysis set at 10 seconds. Each analysis was conducted in triplicate.

### 3.2.5.2 Scanning Electron Microscopy (SEM)

Morphological analysis was carried out by scanning electron microscopy (SEM). The microscope (SUPRA 40, Carl Zeiss NTS GmbH, Oberkochen, Germany) was operated under high vacuum conditions with 1.5 kV accelerating voltage, at different magnifications. Each powder was gently deposited on a double-sided adhesive black carbon tape pre-mounted on aluminum stubs and imaged without the need of a metallization process.

### 3.2.5.3 Thermogravimetric Analysis (TGA)

The thermal behaviour of cysteamine bitartrate lipid microparticles was also studied by thermogravimetric analysis (TGA) using a TG50 STARE system (Mettler Toledo, USA). Samples of about 4–5 mg were inserted in alumina crucibles under a dynamic nitrogen atmosphere ( $100 \text{ ml}\cdot\text{min}^{-1}$ ) and subjected to specific thermal program ( $25 - 140 \text{ }^\circ\text{C}$ ,  $10 \text{ }^\circ\text{C}/\text{min}$ ).

### 3.2.5.4 FT-IR spectroscopy analysis

The FT-IR spectral measurements were performed at room temperature using a Jasco FT/IR-460 Plus (Tokyo, Japan) instrument, equipped with a *Spectra Manager* software, in transmittance mode in the wavenumber range of  $4000\text{-}650 \text{ cm}^{-1}$ . Cysteamine base, hyaluronic acid spray-dried powder and cysteamine hyaluronate spray-dried microparticle formulations were prepared by dispersing the spray-dried powders with KBr in a ratio 1:9 (w/w) in a mortar and then compacting the blend in a thin tablet by a hydraulic press.

### 3.2.5.5 $^{13}\text{C}$ NMR analysis

The formation of the novel cysteamine hyaluronate salt was further investigated by  $^{13}\text{C}$ -NMR analysis in solid state. The spectra of cysteamine free base, sodium hyaluronate, hyaluronic acid spray-dried powder and cysteamine hyaluronate spray-dried powder were collected by means of a JNM-ECZR 400 NMR spectrometer (Jeol, Peabody, USA).

## 3.2.6 *In vitro* aerodynamic characterization

### 3.2.6.1 Fast Screening Impactor (FSI)

A Fast Screening Impactor (Copley Scientific Ltd, Nottingham, UK) was used to assess the aerodynamic performance of cysteamine spray-dried powders. FSI is constituted of a Coarse Fraction Collector (CFC) that captures particles with an aerodynamic diameter larger than 5 microns and a Fine Fraction Collector (FFC) that collects particles with an

aerodynamic diameter smaller than 5 microns. The respirable fraction was calculated as the ratio between the amount of powder collected in the FFC and the loaded dose. In detail, 20 mg of spray-dried powders were manually loaded into a size 3 HPMC capsule and aerosolized using a RS01 (Plastiapè® S.p.A, Osnago LC, Italy) powder inhaler device. A representation of the dry powder inhaler employed is reported in Figure 54.



Figure 54. RS01 (Plastiapè® S.p.A, Osnago LC, Italy) powder inhaler device.

The capsule was inserted into the holder chamber of the device and pierced. The device was connected to the FSI and passed by the air stream for 4 s at 60 L/min. The particles not captured in the CFC kept following the airstream and deposited in the FFC where a filter captured all of them.

### 3.2.6.2 Next Generation Impactor (NGI)

The aerodynamic characterization of the spray-dried formulations was also investigated by means of a Next Generation Impactor (NGI, Westech, Model: 7201, Westech Innovative Sampling Technologies, Bedfordshire, UK).

NGI allowed to determine the dimensional distribution in terms of aerodynamic diameter ( $d_{ae}$ ) and to calculate the particle fraction that reaches the lower stages considered critical for the respirable fraction (lower than 5  $\mu\text{m}$ ). By assaying the amount of the product deposited on the different stages, it is possible to calculate parameters such as Delivered Dose (DD), fine particle fraction (FPF), Median Mass Aerodynamic Diameter (MMAD) and Geometric Standard Deviation (GSD). The Delivered Dose (DD) is the amount of drug leaving the device and reaching the impactor. The Fine Particle Fraction (FPF) denotes the percentage that has a size equal to or less than 5  $\mu\text{m}$ . The MMAD corresponds to the diameter of the particles deposited in the impactor for which 50% w/w has a lower diameter and 50% w/w has a higher diameter.

The NGI is a high performance, precision, particle classifying cascade impactor consisting of a lid, seal body, nozzle pieces, collection cups, cup tray and bottom frame. There are

inside seven pierced stages and a micro-orifice collector (MOC), in which a filter (glass microfiber filter 934-AH TM, 82.6 mm, GE Healthcare Whatman, UK) is deposited to trap the finest particles. There are also two other accessories: the induction throat and the pre-separator. The USP 42<sup>th</sup> edition and Ph. Eur. 9<sup>th</sup> edition report the use of a pre-separator only for dry powders with large solid carrier in order to retain the large particles.

NGI was coupled with a Westech Flow Regulator (Model N.: F0330, Westech Innovative Sampling Technologies, Bedfordshire, UK) and a Flow Control Valve (Model N.: WP-CFC-01, Westech Innovative Sampling Technologies, Bedfordshire, UK). The air-flow rate was set at 60 L/min by a flow meter (DFM 2000, Copley Scientific, Nottingham, UK). 20 mg of spray-dried powder was loaded into a size 3 HPMC capsule. The inhalation device was then connected to the mouthpiece adapter of the induction port and passed by the airstream for 4 seconds at 60 L/min. The amount of spray-dried powder deposited on different component (mouthpiece adaptor, throat, stages and MOC) was recovered with a water solution containing 0.1% of EDTA and 0.8% of acetic acid. The amount of cysteamine was determined by HPLC analysis. Each formulation was analyzed in triplicate.

### 3.2.7 Stability studies

The stability assessment of the spray-dried cysteamine hyaluronate microparticles was investigated. Formulations were stored into HPMC size 3 capsules in a glass vial sealed with teflon plug and ring nut at two different conditions for one month to assess the physical and chemical stability: 4°C and at 25°C/60% RH and then analysed. The results were compared to those collected at time 0.

### 3.2.8 *In vitro* cell culture studies on the cysteamine hyaluronate microparticles

A range of *in vitro* cell culture models of the respiratory epithelia are employed to investigate the interaction between drugs and the lung. Among the airway epithelia cell lines, the attention was focused on three different cell lines.

#### 3.2.8.1 Calu-3 cell line

The Calu-3 cell line is an epithelial and adherent cell line obtained from the human lung adenocarcinoma. Calu-3 were cultured between passages 27 and 35 in sterile 75 cm<sup>2</sup> flasks (Corning Incorporated, Life Sciences, NY, USA) and grown in Dulbecco's Modified Eagle's medium/F-12 with 10% (v/v) fetal bovine serum, 1% (v/v) L-Glutamine solution and 1% (v/v) non-essential amino acids solution. Cells were maintained in an incubator (Binder C170,

Brightside Scientific Pty Ltd, Tuggerah, NSW, Australia) at 37°C in a 95% air and 5% CO<sub>2</sub> atmosphere until confluency was obtained. The medium was refreshed every two days, and cells were passaged according to American Type Culture Collection (ATCC) recommended guidelines. For all the experiments, Calu-3 cells were seeded at a cell density of 2 x 10<sup>5</sup> cells/ml.

#### 3.2.8.2 NuLi-1 and CuFi-1 cell lines

The NuLi-1 cell line is a normal human airway epithelial cell line immortalized with E6/E7 and hTERT derived from normal lung. On the contrary, CuFi-1 cell line is a normal human airway epithelial cell line immortalized with E6/E7 and hTERT derived from lung of a cystic fibrosis patient.

NuLi-1 and CuFi-1 cell lines were cultured between passages 31 and 33 in sterile 75 cm<sup>2</sup> flasks in BEGM (Bronchial Epithelial Growth Medium, Serum-free) (BEGM<sup>®</sup> SingleQuots<sup>®</sup>, Lonza, USA). The flasks were first coated with a 60 µg/mL solution of Human Placental Collagen Type IV (Sigma Cat. No. C-7521) at least 24 hours in advance, then let dried in air atmosphere and rinsed 2-3 times with Dulbecco's Phosphate Buffered Saline. Medium was refreshed every two/three days. Once confluency was reached, cells were passaged following the American Type Culture Collection (ATCC) recommended guidelines. For all the experiments, NuLi-1 and CuFi-1 cells were seeded at a cell density of 4 x 10<sup>5</sup> cells/ml and 8 x 10<sup>5</sup> cells/ml, respectively.

#### 3.2.8.3 MTS Assay

To assess cell viability and eventually cytotoxicity, MTS assays were performed on the previously described cell lines, according to the protocol here reported. MTS assay is a colorimetric method based on the reduction of the tetrazolium compound into formazan by viable cells. This enzymatic reaction occurs only in cells in which the metabolic activity is preserved.

In detail, cells were seeded into sterile 96-well plates at a density of 2 x 10<sup>4</sup> cells/ml in case of Calu-3, 8 x 10<sup>5</sup> cells/ml and 4 x 10<sup>5</sup> cells/ml for CuFi-1 and NuLi-1 cell lines, respectively. After the seeding, the 96-well plates were kept in the incubator overnight to allow the attachment of the cells. The following day treatments were added by preparing a stock solution having the concentration of 2 mg/ml. The stock solution was prepared by dissolving 2 mg of formulation in DMEM medium, then filtered by means of a sterile membrane filter (Millex<sup>®</sup> GP, Filter unit 0.22 micron, sterile, Merck Millipore Ltd, Cork, Ireland) and finally,

starting from the stock solution, dilutions were performed. In this way, cells were exposed to a range of drug concentrations. In particular, 100  $\mu$ l of treatments were added into each well and the 96-well plates were incubated for 48 h at 37°C. Then, 20  $\mu$ l of MTS solution was added into each well and incubated for another 4 h. The absorbance of the wells was measured at 490 nm by means of a microplate reader (SpectraMax M2, Bio-strategie delivering technologies). In each experiment, DMEM and DMSO 20% solution were employed as positive and negative controls, respectively. Each experiment was performed in triplicate.

### 3.2.9 Airways mucus mimetic models

An already developed model to formulate a series of airway mucus mimetics, having the chemical composition and concentration, viscoelastic properties and the surface tension matched to that of native and non-diseased tracheal mucus, was followed.<sup>90</sup> Rheological measurements were performed by means of an AR-2000 advance rotational rheometer (TA Instruments AR-2000, TA Instruments Ltd, UK) with a parallel plate geometry. The plate diameter was set at 20 mm. The mucus mimetic was prepared by dissolving bovine serum albumin (Lot.N.: SLBX2362, Sigma Aldrich Co, USA) and mucin from porcine stomach Type III (Batch n. 116K7002, Sigma Aldrich) in a buffer solution (154 mM NaCl, 3 mM CaCl<sub>2</sub>, 15 mM NaH<sub>2</sub>PO<sub>4</sub>/Na<sub>2</sub>HPO<sub>4</sub> in water; pH 7.4) that was kept under magnetic stirring at 4°C for at least 6 days. To control the viscoelastic properties of the airways mucus mimetic models, glutaraldehyde (GA) (EM grade distillation purified, batch n. 2130911, Electron Microscopy Sciences, Hatfield, PA) was added as crosslinking agent. In detail, samples at 4%, 5.3% and 6.5% of GA were prepared. Once the glutaraldehyde was added, the solution was kept under stirring at 4°C for 3 days. Then, treatments were prepared at a concentration of 10 mg/ml in DMEM. In detail, cysteamine base and cysteamine hyaluronate spray-dried powders were dissolved in DMEM. Then, 4  $\mu$ l of each treatment solution were added to 100  $\mu$ l of mucus samples and incubated for 16 h at 37  $\pm$  0.5 °C. After the incubation, 100  $\mu$ l of samples were finally loaded on the plate of the rheometer by means of a Gilson Microman precision displacement microliter pipette (Gilson, Paris, France), allowed to relax and equilibrate for 1 minute at room temperature. Dynamic frequency sweep experiments were conducted in the frequency range of 0.1-100 rad/s. Oscillatory rheological tests, which better reproduce the *in vivo* stress conditions in the airways, were conducted. Frequency dependent parameters, such as the elastic (G') and the viscous (G'') moduli, were evaluated.

## 4. RESULTS AND DISCUSSION

### 4.1 Preformulation study of spray-dried cysteamine microparticles

The aim of this research project was the design and preparation of cysteamine spray-dried powders for inhalation administration. In the preliminary phase of the project, explorative formulation studies of cysteamine spray-dried powders for inhalation were conducted, starting either from cysteamine base or from cysteamine bitartrate.

#### 4.1.1 Cysteamine hyaluronate spray-dried microparticles

The spray-dried microparticles of cysteamine hyaluronate salt were obtained following the procedure described in Section 3.2.1.1. The neutralization of HA solution required 12.13 ml of NaOH 0.01 N (i.e. 0.1213 meq). Thus, 63.25 mg of NaHA on average contained 0.1213 milliequivalents of HA. The exact ratio between the cysteamine base and HA was determined by means of an acid-base titration, as reported in Section 3.2.1.2. From the experiments carried out the optimal weight ratio of cysteamine base/hyaluronic acid (as sodium hyaluronate) in the solution was found to be 1:7 (w/w). Since cysteamine is stable at pH lower than 5, the stability of the API during the experimental processes was guaranteed by keeping the pH below this value. Thus, the pH of the solutions to be sprayed were measured and the values are reported in Table XIX.

Table XIX. pH values of the spray-dried solutions: before the addition of the resin, after the filtration of the resin and after the addition of cysteamine base free.

<b>Formulations</b>	<b>pH of sodium hyaluronate solution before the addition of resin</b>	<b>pH of hyaluronic acid solution after the filtration of resin</b>	<b>pH of hyaluronic acid solution after the addition of cysteamine base and other excipients</b>
<b>#1</b>	6.20	3.22	3.90
<b>#2</b>	6.18	2.43	3.86
<b>#3</b>	6.68	2.57	3.68
<b>#4</b>	6.30	2.60	3.86
<b>#5</b>	6.19	2.56	3.16
<b>#6</b>	6.33	2.59	3.98
<b>#7</b>	6.34	2.61	4.60
<b>#8</b>	6.13	2.41	4.18
<b>#9</b>	6.37	2.69	4.39
<b>#10</b>	6.52	2.62	4.30
<b>#11</b>	6.58	2.70	4.25
<b>#12</b>	6.40	2.47	3.68

The solutions were sprayed by means of the spray dryer according to the process parameters reported in Table XX.

Table XX. Spray dryer process parameters employed during the preformulation study of cysteamine hyaluronate microparticles.

Formulations	Spray-dryer	Inlet Temperature (°C)	Feed Rate (ml/min)	Atomizing Air Rate (L/h)	Nozzle Type
#1	B191	150	5 ml/min	500	Two fluid nozzle (0.7 mm)
#2	B191	150	5 ml/min	500	Two fluid nozzle (0.7 mm)
#3	B191	120	5 ml/min	500	Two fluid nozzle (0.7 mm)
#4	B191	120	5 ml/min	600	Two fluid nozzle (0.7 mm)
#5	B290	120	5 ml/min	600	Two fluid nozzle (0.7 mm)
#6	B290	120	5 ml/min	600	Two fluid nozzle (0.7 mm)
#7	B290	120	5 ml/min	600	Two fluid nozzle (0.7 mm)
#8	B290	120	4 ml/min	600	Three fluid (coaxial) nozzle
#9	B290	120	5 ml/min	600	Two fluid nozzle (0.7 mm)
#10	B290	120	4 ml/min	600	Three fluid (coaxial) nozzle
#11	B290	150	4 ml/min	600	Three fluid (coaxial) nozzle
#12	B290	150	4 ml/min	600	Three fluid (coaxial) nozzle

In Table XXI are reported the composition of each formulation and the yield of the spray drying process.

Table XXI. Composition and yield of the spray-dried powders of cysteamine base.

Formulations	Composition	Yield (%)
#1	13.1 % cysteamine/86.9 % sodium hyaluronate	27.5
#2	12.7 % cysteamine/87.3 % sodium hyaluronate	38.0
#3	12.2 % cysteamine/87.8 % sodium hyaluronate	68.1
#4	12.7 % cysteamine/87.1 % sodium hyaluronate/0.2 % ascorbic acid	24.6
#5	15 % cysteamine/85 % sodium hyaluronate/0.8 ml acetic acid	64.2
#6	12.9 % cysteamine/86.6 % sodium hyaluronate/0.4 % ascorbic acid	67.0
#7	13.0 % cysteamine/84.3 % sodium hyaluronate/2.7 % trehalose	67.3
#8	13.1 % cysteamine/78.2 % sodium hyaluronate/8.7 % L-leucine	44.3
#9	12.8 % cysteamine/78.5% sodium hyaluronate/8.7 % L-leucine	66.1
#10	13.4 % cysteamine/69.1% sodium hyaluronate/17.5 % L-leucine	61.1
#11	12.1 % cysteamine/70.2% sodium hyaluronate/17.7 % L-leucine	60.8
#12	10.9 % cysteamine/79.3 % sodium hyaluronate/9.8 % L-leucine	60.4

As it can be noticed from Table XXI, initially solutions containing only hyaluronic acid and cysteamine base (Formulations #1-3) were spray dried. Then, with the goal of improving particle shaping and increasing drug stability, other excipients, compatible with the inhalation administration route, were selected. In particular, amino acids such as L-leucine, sugars like trehalose and ascorbic acid or acetic acid were used. Furthermore, in some experiments the coaxial nozzle was employed according to the procedure described in Section 3.2.1.4. In detail, in case of Formulations #8, #10, #11 and #12 the outer orifice was feed with the solution containing L-leucine, while the inner orifice was feed with the solution containing the cysteamine base and hyaluronic acid. L-leucine, externally deposited, could play a protective action over cysteamine hyaluronate thus increasing the physical-chemical stability of the cysteamine hyaluronate microparticles. Moreover, L-leucine was able to counteract both the adhesiveness of HA and the hygroscopicity of cysteamine base.

#### 4.1.2 Drug content determination

The drug content determination of cysteamine in the cysteamine hyaluronate spray-dried microparticles was performed according to the HPLC method described in Section 3.2.4. The results obtained are summarized in Table XXII.

Table XXII. Drug content of the spray-dried formulations of cysteamine hyaluronate microparticles.

<b>Formulations</b>	<b>Theoretical drug content (%)</b>	<b>Experimental drug content (%)</b>
<b>#1</b>	13.1	11.1
<b>#2</b>	12.7	10.8
<b>#3</b>	12.2	10.4
<b>#4</b>	12.7	10.8
<b>#5</b>	15.0	12.7
<b>#6</b>	12.9	11.0
<b>#7</b>	13.0	11.0
<b>#8</b>	13.1	11.2
<b>#9</b>	12.8	10.9
<b>#10</b>	13.4	11.4
<b>#11</b>	12.1	10.3
<b>#12</b>	10.9	8.4

As it can be observed, the experimental drug content was around the 80% of the theoretical value. This was mainly attributed to the high instability of the raw material in environmental conditions.

#### 4.1.3 Characterization of the cysteamine hyaluronate microparticles

##### 4.1.3.1 Thermogravimetric analysis (TGA)

The residual water content in the spray-dried microparticles was measured by thermogravimetric analysis using the method reported in Section 3.2.5.3. The results are reported in Table XXIII.

Table XXIII. Water content determination of the spray-dried formulations of cysteamine hyaluronate microparticles.

Formulations	Residual water content (%)
#1	7.9
#2	8.2
#3	8.4
#4	7.9
#5	7.5
#6	8.5
#7	7.0
#8	7.3
#9	5.9
#10	6.0
#11	5.8
#12	5.9

Spray-dried microparticles of cysteamine base and hyaluronic acid showed a water content of between 6 and 8.5%.

#### 4.1.3.2 Scanning Electron Microscopy (SEM)

The morphological characterization of the cysteamine/hyaluronic acid spray-dried microparticles was performed by scanning electron microscopy (SEM), according to the procedure described in Section 3.2.5.2. In Figures 55-60 are reported the images of some formulations manufactured. As it can be noticed, spray-dried microparticles showed roundish structures characterized by a small shrunken surface.

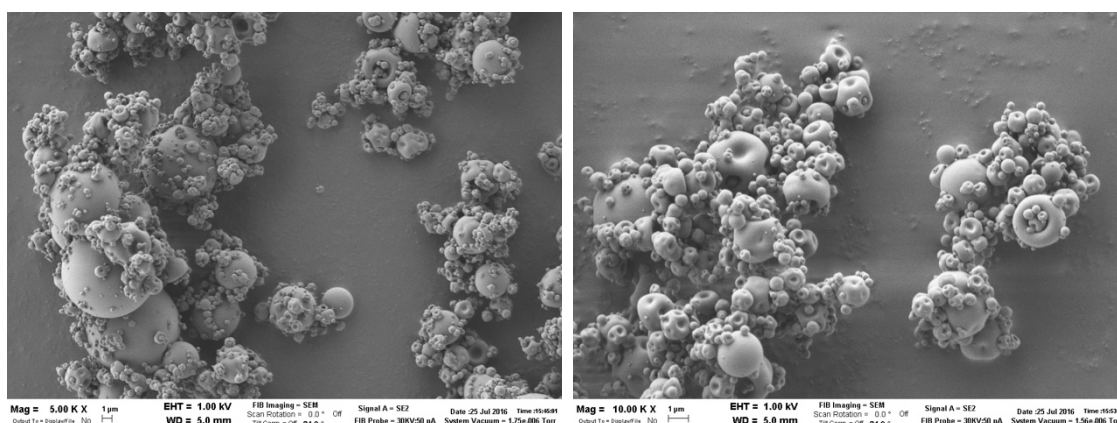


Figure 55. SEM Images of Formulation #1 (13.1% cysteamine/86.9% sodium hyaluronate).

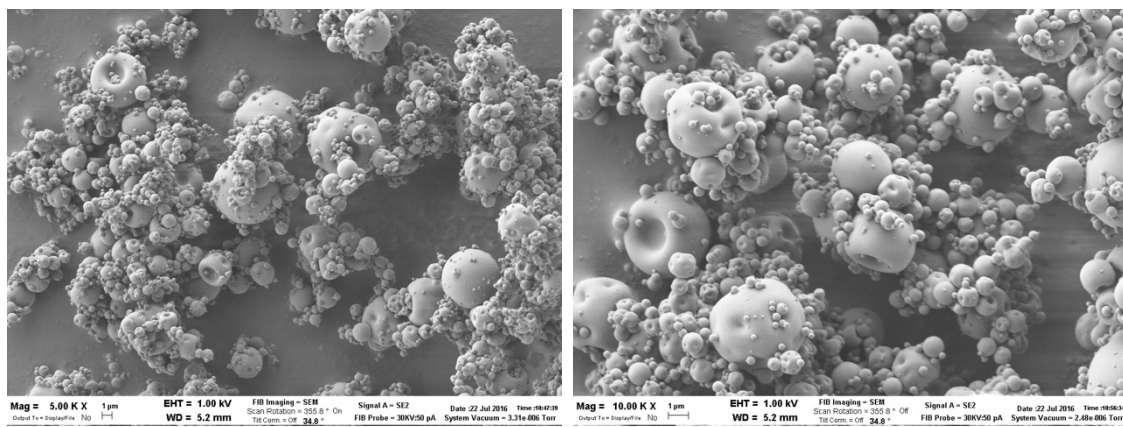


Figure 56. SEM Images of Formulation #7 (13.0 % cysteamine/84.3 % sodium hyaluronate/ 2.7 % trehalose).

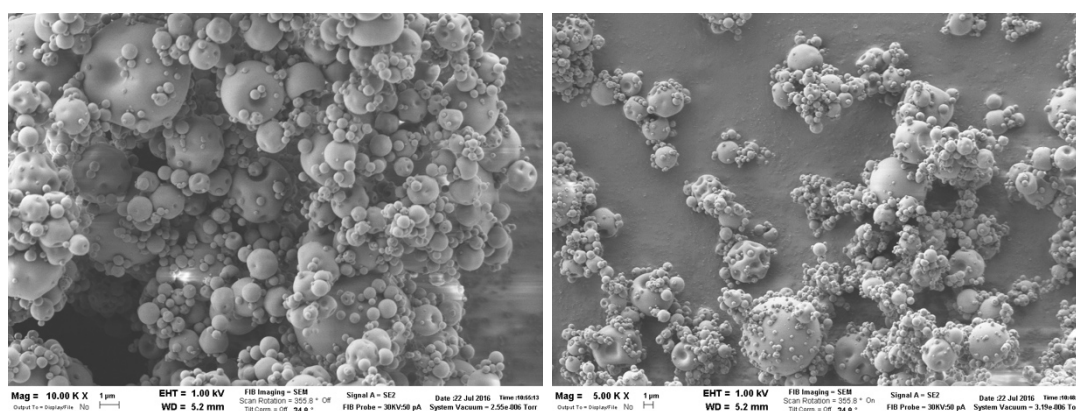


Figure 57. SEM Images of Formulation #8 (13.1 % cysteamine/78.2 % sodium hyaluronate/ 8.7 % L-leucine).

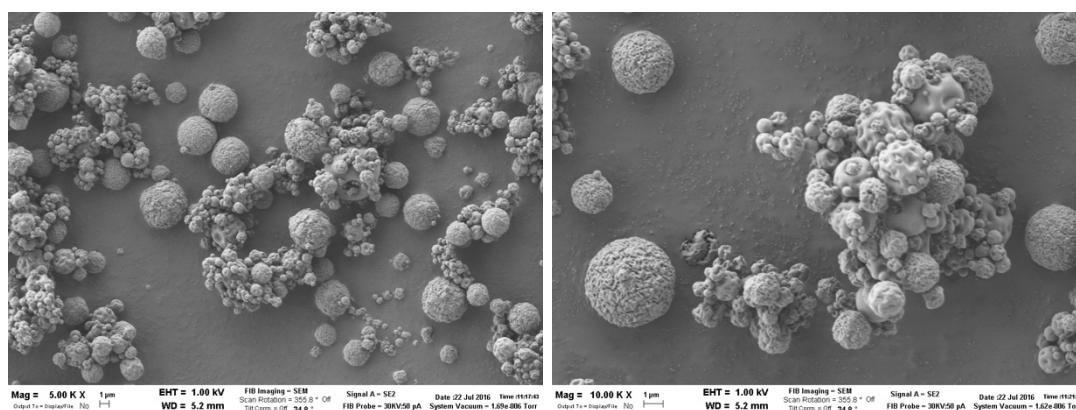


Figure 58. SEM Images of Formulation #10 (13.4 % cysteamine/69.1 % sodium hyaluronate/ 17.5 % L-leucine).

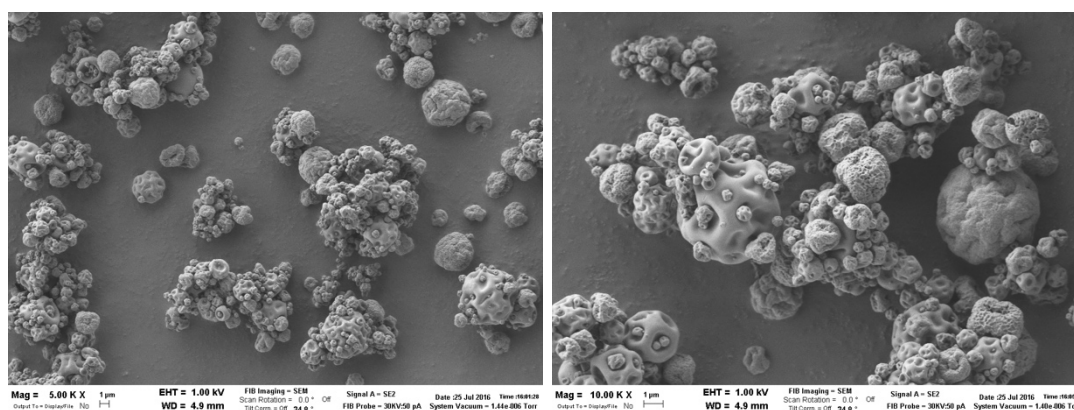


Figure 59. SEM Images of Formulation #11 (12.1 % cysteamine/70.2 % sodium hyaluronate/ 17.7 % L-leucine).

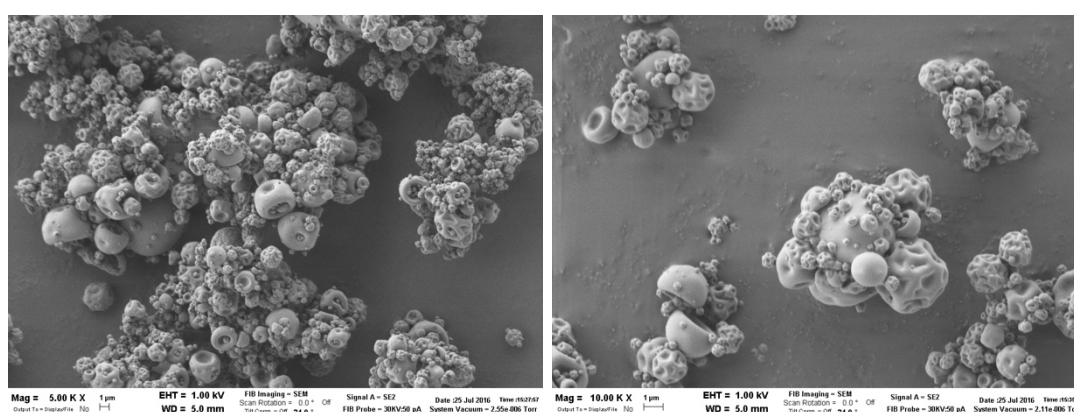


Figure 60. SEM Images of Formulation #12 (10.9 % cysteamine/79.3 % sodium hyaluronate/ 9.8 % L-leucine).

When L-leucine was present in an amount of about 17% (Formulations #10 and #11) and its solution was sprayed from the outer orifice of the coaxial nozzle, spongy microparticles were observed (Figures 58 and 59). The structure of the spray-dried microparticles revealed a low value of powder bulk density, thus providing an important advantage for respirability.

#### 4.1.3.3 Determination of the particle size distribution

The assessment of the particle size distribution was performed according to the procedure described in Section 3.2.5.1. As representative of all the formulations produced, the results of Formulation #2 (cysteamine base/hyaluronic acid 1:7) and Formulation #8 (cysteamine base/hyaluronic acid/L-leucine) are reported below, in Figures 61 and 62, respectively.

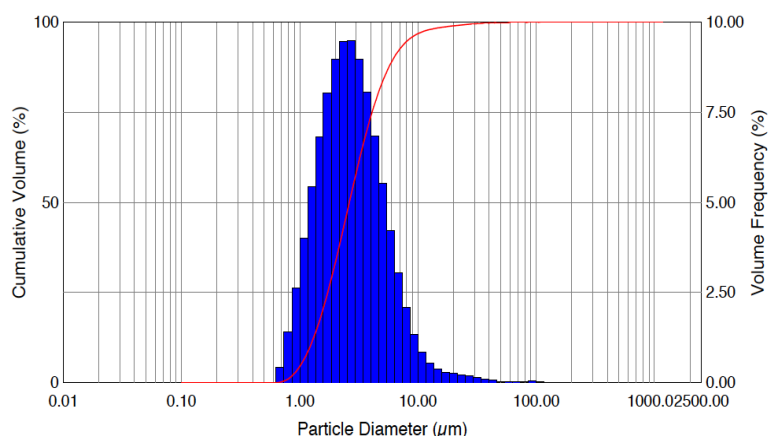


Figure 61. Particle size distribution of Formulation #2 (12.7 % cysteamine/87.3 % sodium hyaluronate).

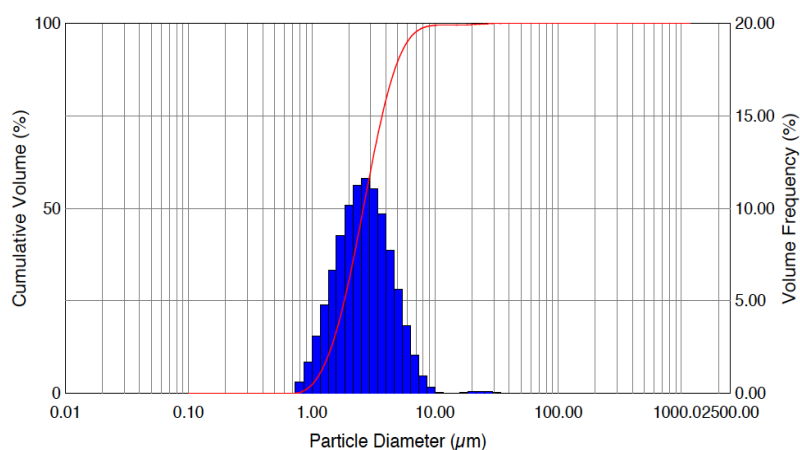


Figure 62. Particle size distribution of Formulation #8 (13.1 % cysteamine/78.2 % sodium hyaluronate/ 8.7 % L-leucine).

Parameters such as  $Dv_{50}$  were evaluated. From the results reported in Table XXIV, Formulations #2 and #8 showed a geometrical size suitable for inhalation administration. In fact,  $Dv_{50}$  values were  $2.66 \pm 0.03$  and  $2.57 \pm 0.06$ , respectively.

Table XXIV. Particle size distribution of Formulation #2 (12.7 % cysteamine/87.3 % sodium hyaluronate) and Formulation #8 (13.1 % cysteamine/78.2 % sodium hyaluronate/8.7 % L-leucine). Results are expressed as mean value  $\pm$  standard deviation (n=3).

	$Dv_{10}$ ( $\mu\text{m}$ )	$Dv_{50}$ ( $\mu\text{m}$ )	$Dv_{90}$ ( $\mu\text{m}$ )	Span
<b>Formulation #2</b>	$1.23 \pm 0.02$	$2.66 \pm 0.03$	$6.52 \pm 0.26$	$1.99 \pm 0.07$
<b>Formulation #8</b>	$1.31 \pm 0.04$	$2.57 \pm 0.06$	$5.04 \pm 0.06$	$1.45 \pm 0.05$

These results were confirmed by the assessment of the aerodynamic behavior of the formulations.

#### 4.1.4 *In vitro* aerodynamic characterization

In the preformulation study of the spray-dried cysteamine hyaluronate microparticles, the determination of the *in vitro* aerodynamic performances of the manufactured formulations was investigated by means of the Fast Screening Impactor (FSI) following the procedure described in Section 3.2.6.1. The FPF (fine particle fraction) values of each formulation are reported in Figure 63.

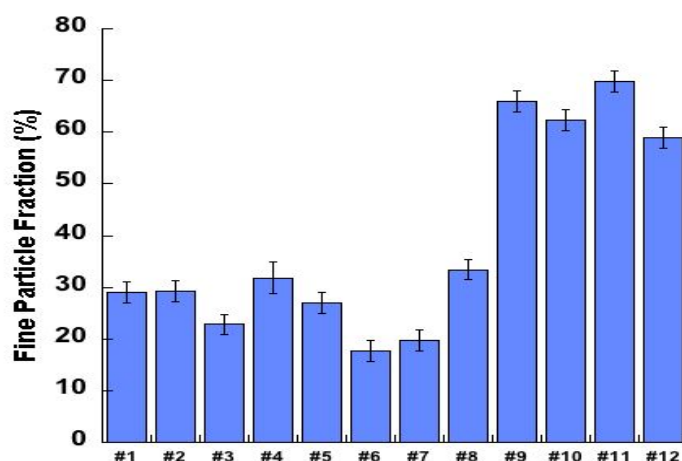


Figure 63. Fine Particle Fraction (FPF %) values of the spray-dried cysteamine base microparticles.

Formulations #1-3, containing only the API and the hyaluronic acid, showed a low FPF value, of about 29%. On the contrary, Formulations #9-12, in which L-leucine was present as disaggregating excipient, showed good FPF values between 60 and 70%.

#### 4.1.5 FT-IR spectroscopy analysis

The formation of the novel cysteamine hyaluronate salt through the process of the present invention was demonstrated by Fourier transform infrared (FT-IR) spectroscopy. The typical absorption bands of cysteamine free base (Figure 64) are:

- $\sim 3450\text{ cm}^{-1}$ : -  $\text{NH}_2$  group (medium intensity);
- $\sim 2920\text{ cm}^{-1}$  and  $\sim 2850\text{ cm}^{-1}$ : -  $\text{CH}_2$  group (strong intensity);
- $\sim 1650\text{ cm}^{-1}$ : -  $\text{NH}_2$  group stretching (medium intensity).

At  $\sim 2600\text{ cm}^{-1}$  a very weak band of the -SH group were observed.

Concerning sodium hyaluronate, the most characteristic absorption bands (Figure 65) are as follows:

- $\sim 3390\text{ cm}^{-1}$ : - OH group;
- $\sim 1640\text{ cm}^{-1}$ : stretching of the C = O peak, superimposed on the peak of secondary amide group (strong intensity);
- $\sim 1580\text{ cm}^{-1}$ : shoulder, - NH group stretching (weak intensity);
- $\sim 1400\text{ cm}^{-1}$ : bending of - CH<sub>2</sub> group and asymmetrical bending of - CH<sub>3</sub> group;
- $\sim 1370\text{ cm}^{-1}$ : stretching of the methyl group (medium intensity).

The FT-IR spectrum of hyaluronic acid spray-dried microparticles (Figure 66) differed from that of sodium hyaluronate powder (Figure 65) by the presence of a fork band, made of three peak, attributed to the stretching vibration of the C=O peak of carboxylic group ( $1734\text{ cm}^{-1}$ ), stretching vibration of the C=O peak of secondary amide group ( $1641\text{ cm}^{-1}$ ) and NH deformation (II amide) ( $1561\text{ cm}^{-1}$ ). Moreover, a variation in terms of intensities and shifts of the peaks at  $1417$ ,  $1378$  and  $1320\text{ cm}^{-1}$ , with respect to the sodium hyaluronate, was observed. Finally, a difference appeared evident in the band at  $1043\text{ cm}^{-1}$ , where the shoulder at  $1077\text{ cm}^{-1}$  became a peak.

Concerning the FT-IR spectrum of cysteamine hyaluronate spray-dried powder (Figure 67), the band at  $\sim 1645\text{ cm}^{-1}$  corresponded both to the stretching of the -NH<sub>2</sub> group of cysteamine and the stretching of C=O of the carboxylic group of the hyaluronic acid. Compared to the FT-IR spectra of cysteamine free base (Figure 64) and hyaluronic acid (Figure 66), a difference indicating an interaction of these functional groups in the cysteamine hyaluronate spray-dried powder was evident. Moreover, from the analysis of the FT-IR spectrum of cysteamine hyaluronate salt spray-dried powder, a reduction of intensity of the peak at  $1370\text{ cm}^{-1}$  (stretching vibration of the methyl group of hyaluronate), becoming the shoulder of the band at  $1410\text{ cm}^{-1}$ , was observed. The intensity of the peak at  $1077\text{ cm}^{-1}$ , corresponding to the stretching vibration of C-O of carboxylic group, was reduced as demonstrated by its transformation in a shoulder (as in the spectrum of the sodium hyaluronate). This further supported the interaction between cysteamine base and hyaluronic acid at the level of the carboxylic group of the hyaluronic acid and the amino group of the cysteamine.

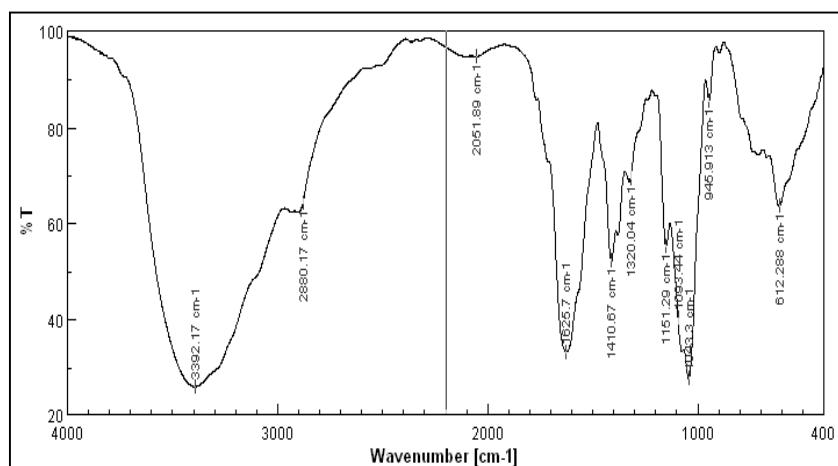


Figure 64. FT-IR spectrum of cysteamine base raw material.

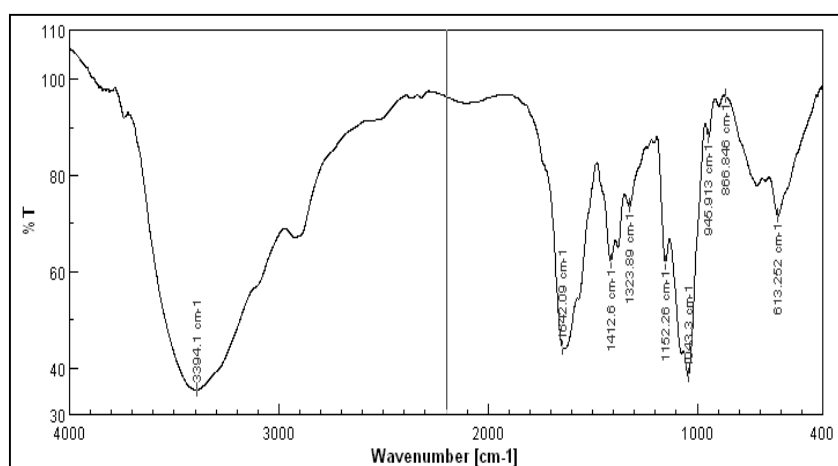


Figure 65. FT-IR spectrum of sodium hyaluronate raw material.

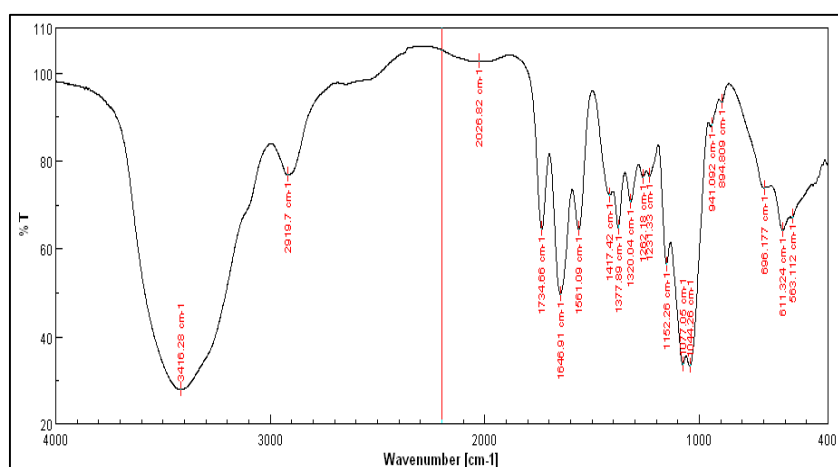


Figure 66. FT-IR spectrum of spray-dried hyaluronic acid microparticles.

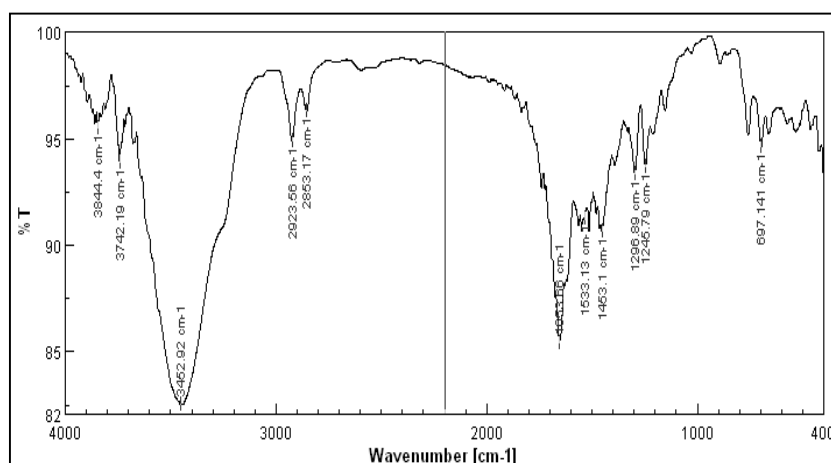


Figure 67. FT-IR spectrum of cysteamine hyaluronate spray-dried formulation.

#### 4.1.6 $^{13}\text{C}$ NMR analysis

To confirm the formation of a cysteamine hyaluronate salt, a further investigation, by using  $^{13}\text{C}$ -NMR analysis in solid state, was performed. The spectra of the raw materials and the spray-dried cysteamine hyaluronate microparticles are reported in Figure 68.

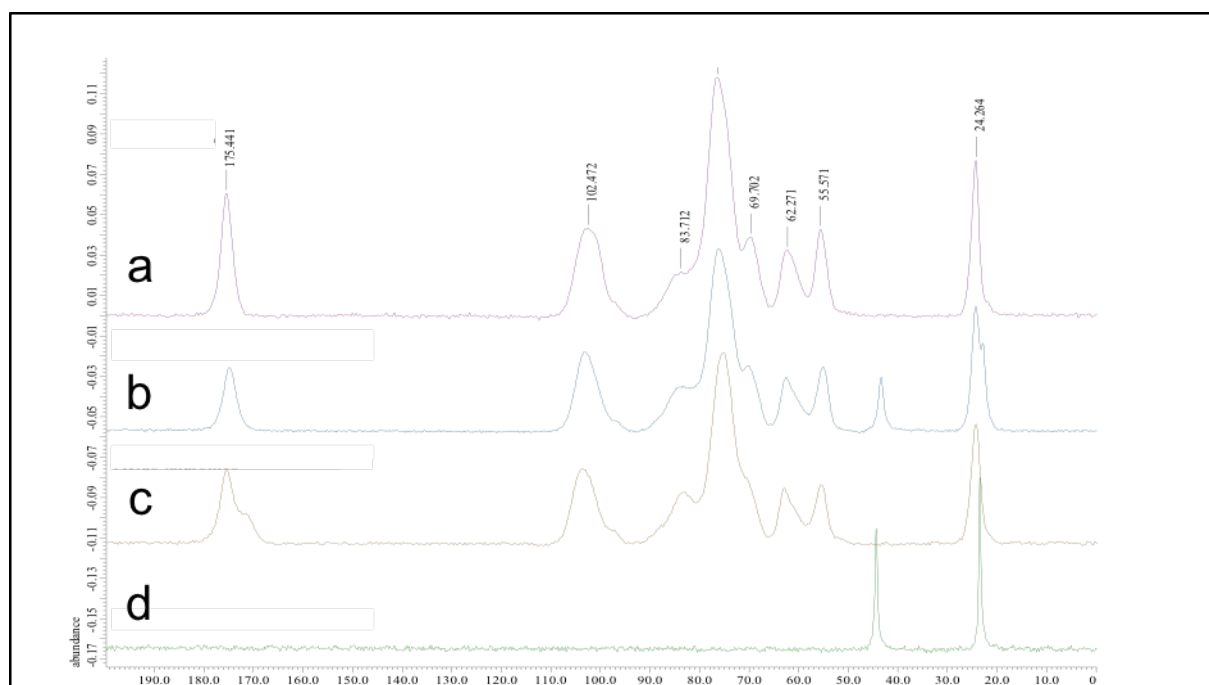


Figure 68.  $^{13}\text{C}$  NMR spectra of sodium hyaluronate (a), spray-dried cysteamine hyaluronate salt (b), spray-dried hyaluronic acid (c) and cysteamine base (d).

Comparing the spectrum of cysteamine hyaluronate with the others, the salt formation was evidenced by the presence of peaks of both the counterions (Figure 68), with a small shift of these peaks due to the influence of the different neighbors compared to the counterions alone (spray-dried hyaluronic acid and cysteamine). Moreover, significant differences were observed in the spectra of sodium hyaluronate and hyaluronic acid. In particular, in the spectrum of spray-dried hyaluronic acid, a shoulder appeared on the peak at about 175 ppm and the peak at about 69 ppm, that was present in the sodium hyaluronate spectrum, disappeared.

#### 4.1.7 Stability studies

The stability studies were performed by storing the spray-dried microparticles for a month at two different conditions, as reported in Section 3.2.7. Cysteamine hyaluronate proved to be stable at environmental conditions, not prone to oxidative degradation, non-hygroscopic and non-deliquescent. In fact, after a month at 4°C and 25° C with 60% R.H., the chemical stability by HPLC analysis and the physical stability by *in vitro* respirability test were assessed. No variation, with respect to cysteamine hyaluronate spray-dried powders at time 0, was observed in terms of content of cysteamine (Table XXV) and fine particle fraction (Table XXVI).

Table XXV. Drug content determination for the stability assessment.

	<b>Formulation #1</b>	<b>Formulation #11</b>
<b>T = 0</b>	89.2 ± 1.2%	91 ± 0.8 %
<b>1 M 4 °C</b>	88 ± 1.0 %	89.5 ± 1.0 %
<b>1 M 25 °C 60% RH</b>	86.6 ± 1.2 %	88 ± 1.2%

Table XXVI. FSI aerodynamic assessment at t=0, t=1 month 4 °C and t=1 month 25 °C.

	<b>Formulation #1</b>	<b>Formulation #11</b>
<b>FPF (%) T=0</b>	20.8 ± 1.1%	66.5 ± 2.0 %
<b>FPF (%) 1 M 4°C</b>	27.3 ± 0.8%	65.1 ± 1.6%
<b>FPF (%) 1 M 25°C</b>	27.8 ± 1.4 %	63.1 ± 1.3 %

#### 4.2 Formulation development of cysteamine hyaluronate microparticles

Based on the results obtained from the preliminary studies, it was decided to focus the attention on Formulations #3, #9, #10 and #11 thus being the formulations with the best drug content and respirability values. New batches of the selected formulations were manufactured by spray drying, following the same process parameters used in the preformulation study (Section 3.2.1.). In Table XXVII the yield of the spray drying process, as well as the results obtained from the drug content determination, are reported. The drug content was determined following the procedure described in Section 3.2.4.

Table XXVII. Yield and drug content determination of the new batches of cysteamine hyaluronate microparticles.

<b>Formulations</b>	<b>Yield (%)</b>	<b>Theoretical drug content (%)</b>	<b>Experimental drug content (%)</b>
<b>#3</b>	59.1	13.4 ± 0.8	13.1 ± 0.9
<b>#9</b>	57.3	14.0 ± 0.9	13.5 ± 0.8
<b>#10</b>	60.1	12.9 ± 1.0	10.3 ± 1.2
<b>#11</b>	61.2	13.1 ± 1.0	10.6 ± 1.5

For all the formulations, the yield was around 60%. Concerning the drug content determination, Formulation #3 showed an experimental drug content almost superimposable to the theoretical one. In a similar way, Formulation #9, containing 10% of L-leucine, resulted in a drug content value of 96% of the theoretical value. Formulations #10 and #11, containing 20% of L-leucine, but manufactured with different process parameters, showed a drug content higher than 80%.

##### 4.2.1 Particle size distribution

The determination of the particle size distribution was assessed by means of a Mastersizer laser light diffractometer. Samples were prepared and analyzed according to the procedure described in Section 3.2.5.1. In Figure 69, a representation of the results obtained is shown.

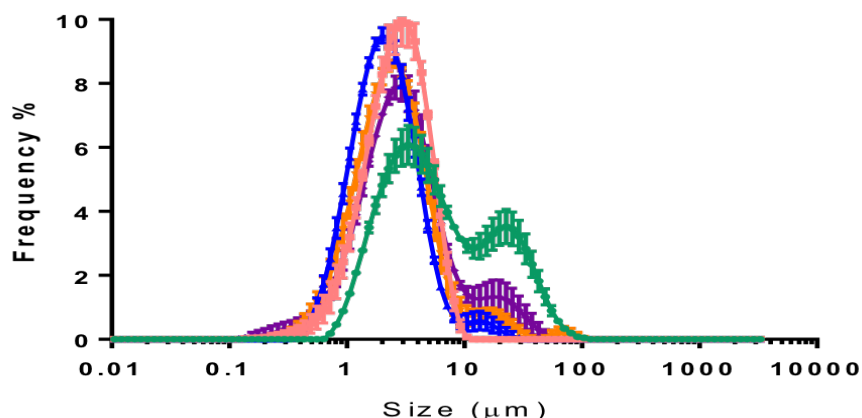


Figure 69. Particle size distribution of Formulation #3 (12.2 % cysteamine/87.8 % sodium hyaluronate) (green), #9 (12.8 % cysteamine/87.5 % sodium hyaluronate/8.7 % L-leucine) (pink), #10 (13.4 % cysteamine/69.1 % sodium hyaluronate/17.5 % L-leucine) (blue) and #11 (12.1 % cysteamine/70.2 % sodium hyaluronate/17.7 % L-leucine) (orange).

As it can be appreciated from the Figure 69, in Formulation #3 it can be observed the presence of two population of particles, probably due to the agglomeration of the powder. Differently, in Formulations #9-11 the particle size distribution showed that these powders had a good geometrical size and a quite narrow distribution around the median value; in fact, as it can be appreciated from Table XXVIII, the  $Dv_{50}$  values of each formulation tested were around 2.6 microns.

Table XXVIII. Particle size distribution of Formulation #3 (12.2 % cysteamine/87.8 % sodium hyaluronate), #9 (12.8 % cysteamine/87.5 % sodium hyaluronate/8.7 % L-leucine), #10 (13.4 % cysteamine/69.1 % sodium hyaluronate/17.5 % L-leucine) and #11 (12.1 % cysteamine/70.2 % sodium hyaluronate/17.7 % L-leucine). Results are expressed as mean value  $\pm$  standard deviation (n=3).

Formulations	$Dv_{10}$ ( $\mu\text{m}$ )	$Dv_{50}$ ( $\mu\text{m}$ )	$Dv_{90}$ ( $\mu\text{m}$ )	Span
#3	$1.72 \pm 0.05$	$5.61 \pm 0.89$	$28.6 \pm 1.50$	$1.42 \pm 0.01$
#9	$1.14 \pm 0.15$	$2.84 \pm 0.17$	$5.53 \pm 0.43$	$1.74 \pm 0.22$
#10	$0.98 \pm 0.07$	$2.58 \pm 0.06$	$6.48 \pm 0.26$	$2.00 \pm 0.70$
#11	$0.99 \pm 0.07$	$2.78 \pm 0.19$	$5.23 \pm 0.17$	$2.10 \pm 0.70$

#### 4.2.2 *In vitro* aerodynamic characterization

The determination of the *in vitro* aerodynamic performances of the formulations was investigated by means of the Next Generation Impactor (NGI), according to the method described in Section 3.2.6.2. Figure 70 showed the results obtained from the aerodynamic assessment of the spray-dried microparticles.

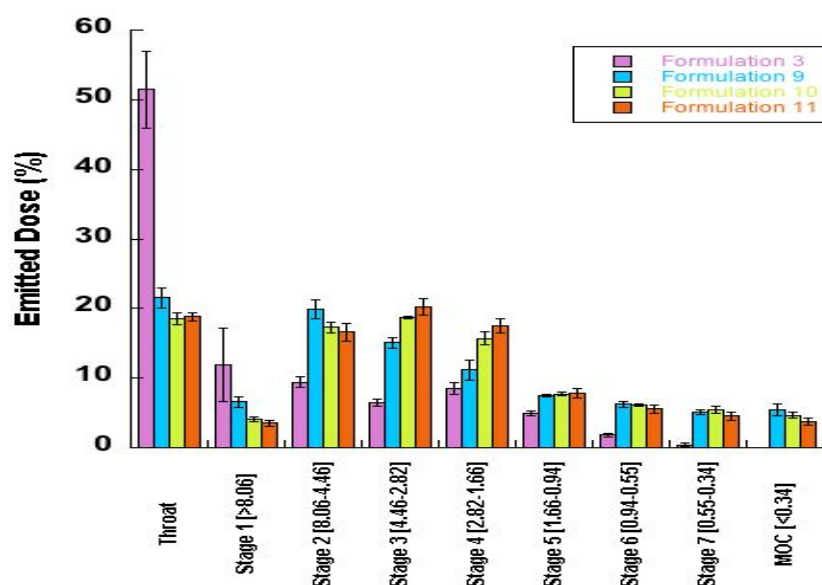


Figure 70. *In vitro* aerosol stage deposition of Formulation #3 (12.2 % cysteamine/87.8 % sodium hyaluronate) (pink), #9 (12.8 % cysteamine/87.5 % sodium hyaluronate/8.7 % L-leucine) (light-blue), #10 (13.4 % cysteamine/69.1 % sodium hyaluronate/17.5 % L-leucine) (green) and #11 (12.1 % cysteamine/70.2 % sodium hyaluronate/17.7 % L-leucine) (orange). Results are expressed as mean value  $\pm$  standard deviation (n=3).

For all the powders the recovery was higher than 85%, in agreement with pharmacopoeia specifications. As it can be observed from Table XXIX, Formulation #3 was the one that showed a high amount of powder deposited in the throat and a very low fine particle fraction (about 25%). On the contrary, formulations containing leucine as deaggregating agent showed MMAD values between 2.8 and 3 with a fine particle fraction between 55 and 65%.

Table XXIX. FPF (%), MMAD ( $\mu\text{m}$ ) and GSD (%) values obtained from the assessment of the *in vitro* aerodynamic performance by means of NGI. Results are expressed as mean value  $\pm$  standard deviation ( $n=3$ ).

	Formulation #3	Formulation #9	Formulation #10	Formulation #11	Formulation #12
<b>FPF (%)</b>	25.4 $\pm$ 1.38	56.4 $\pm$ 1.70	64.3 $\pm$ 0.48	65.22 $\pm$ 0.79	59.13 $\pm$ 0.31
<b>MMAD (<math>\mu\text{m}</math>)</b>	4.30 $\pm$ 0.93	3.08 $\pm$ 0.03	2.82 $\pm$ 0.04	2.83 $\pm$ 0.11	2.83 $\pm$ 0.11
<b>GSD (%)</b>	2.62 $\pm$ 0.30	2.08 $\pm$ 0.07	1.96 $\pm$ 0.01	1.89 $\pm$ 0.05	1.99 $\pm$ 0.06

#### 4.2.3 MTS cytotoxicity assays

MTS *in vitro* cytotoxicity assays were performed in order to identify the optimal range of concentrations suitable for use on pulmonary cell lines. Experiments were conducted according to the method deeply described in Section 3.2.8.3. The assessment of the cytotoxicity was first performed on the cysteamine base and hyaluronic acid raw materials. Then, Formulations #3, #9, #10 and #11 were tested at different concentration ranges.

##### 4.2.3.1 MTS assay on Calu-3 cell line

Treatments were added to the 96-well plates according to the procedure described in Section 3.2.8.3. Data were expressed as mean  $\pm$  standard deviation of the percentage of cell viability relative to untreated control. Figure 71 showed the results of the viability test on the raw materials cysteamine base and hyaluronic acid.

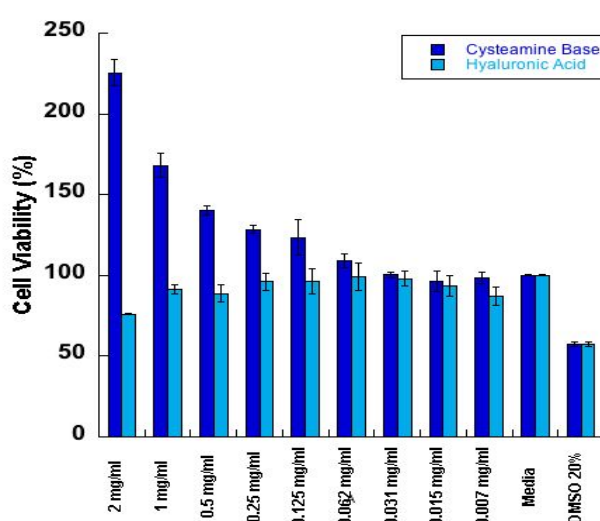


Figure 71. Viability of Calu-3 cell line evaluated after 48 h of exposure to different treatment concentrations. Results are expressed as mean value  $\pm$  standard deviation ( $n=3$ ).

What is more, it can be underlined the fact that cysteamine base raw material showed a proliferative effect at high concentrations that was reduced for lower concentration range values. In fact, from Figure 71 it was clear that in the concentration range between 2 mg/ml and 125  $\mu$ m/ml, the percentage of cell viability after 4 h of exposure reached 200%. This aspect will be deeply investigated in the future.

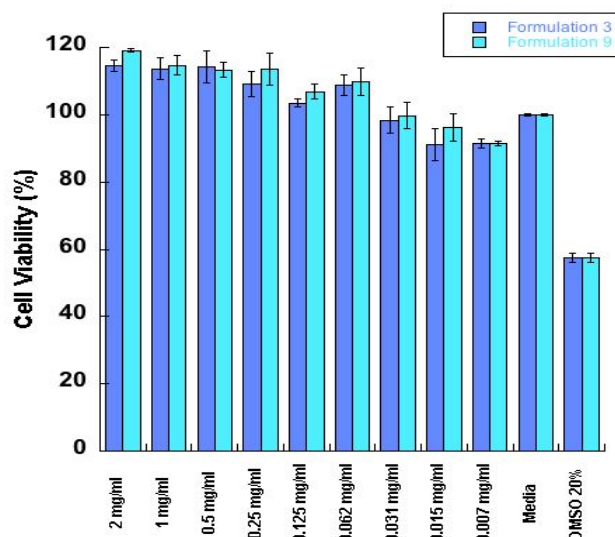


Figure 72. Viability of Calu-3 cell line evaluated after 48 h of exposure to different treatment concentrations of Formulations #3 and #9. Results are expressed as mean value  $\pm$  standard deviation (n=3).

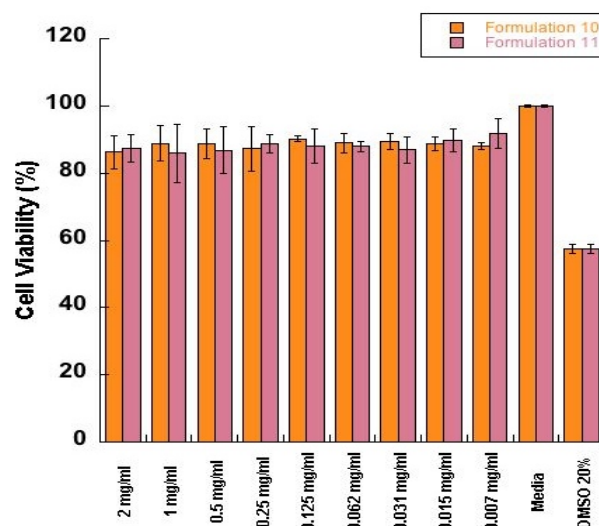


Figure 73. Viability of Calu-3 cell line evaluated after 48 h of exposure to different treatment concentrations of Formulations #10 and #11. Results are expressed as mean value  $\pm$  standard deviation (n=3).

In Figures 72 and 73, the results concerning the spray-dried formulations were presented. As it can be observed, all the formulations, at the selected concentration range, showed to be non-toxic on the Calu-3 cell lines.

#### 4.2.3.2 MTS assay on CuFi-1 cell line

A similar behavior was obtained from the MTS cytotoxicity assay on CuFi-1 cells. Figure 74 reported the results of the cell viability after exposure to various concentrations of cysteamine base and hyaluronic acid whereas in Figures 75 and 76 the assessment of the cell toxicity after treatment with the spray-dried formulations was presented. As it can be observed, CuFi-1 cells resulted to be viable after the exposure to different concentrations of treatments.

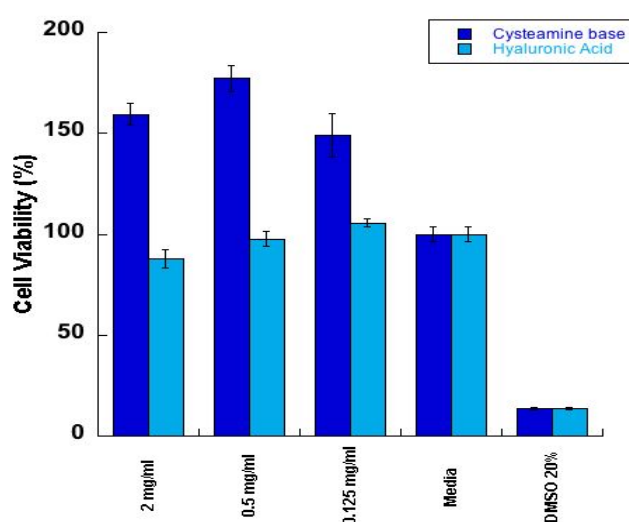


Figure 74. Viability of CuFi-1 cell line evaluated after 48 h of exposure to different treatment concentrations. Results are expressed as mean value  $\pm$  standard deviation (n=3).

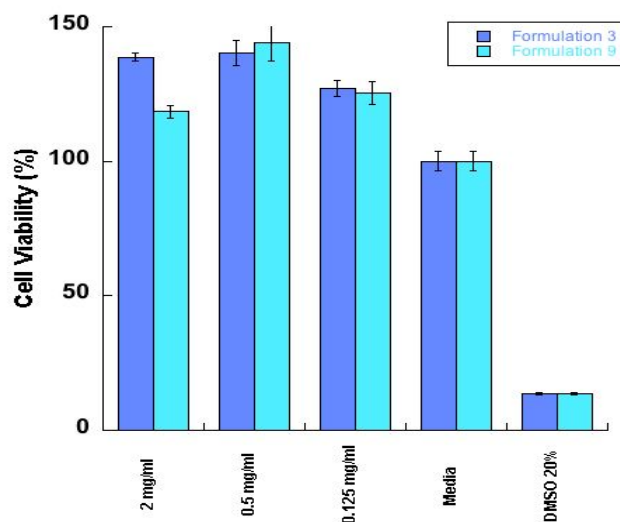


Figure 75. Viability of CuFi-1 cell line evaluated after 48 h of exposure to different treatment concentrations of Formulations #3 and #9. Results are expressed as mean value  $\pm$  standard deviation (n=3).

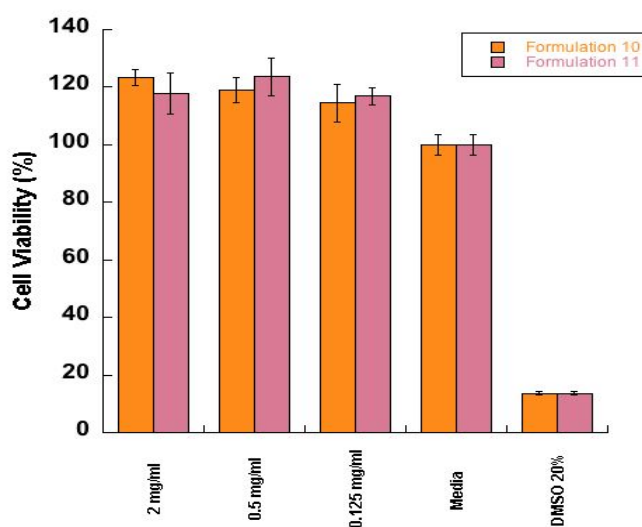


Figure 76. Viability of CuFi-1 cell line evaluated after 48 h of exposure to different treatment concentrations of Formulations #10 and #11. Results are expressed as mean value  $\pm$  standard deviation (n=3).

## 4.2.3.3 MTS assay on NuLi-1 cell line

Even in the case of NuLi-1 cell lines, the results obtained from the viability assays confirmed that the treatments were found to be non-toxic for the cells since the viability after 48 h of exposure was superior to 80%, as reported in Figures 77-79.

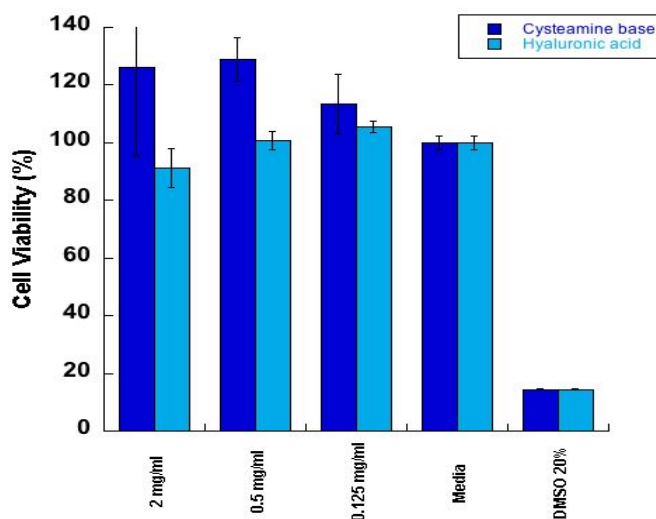


Figure 77. Viability of NuLi-1 cell line evaluated after 48 h of exposure to different treatment concentrations. Results are expressed as mean value  $\pm$  standard deviation (n=3).

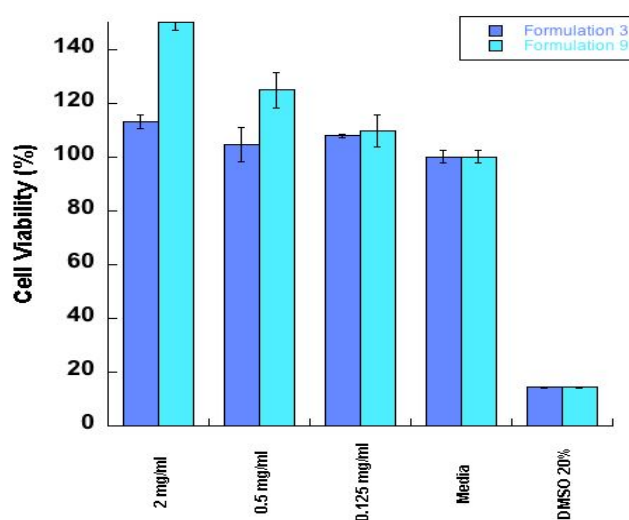


Figure 78. Viability of NuLi-1 cell line evaluated after 48 h of exposure to different treatment concentrations of Formulations #3 and #9. Results are expressed as mean value  $\pm$  standard deviation (n=3).

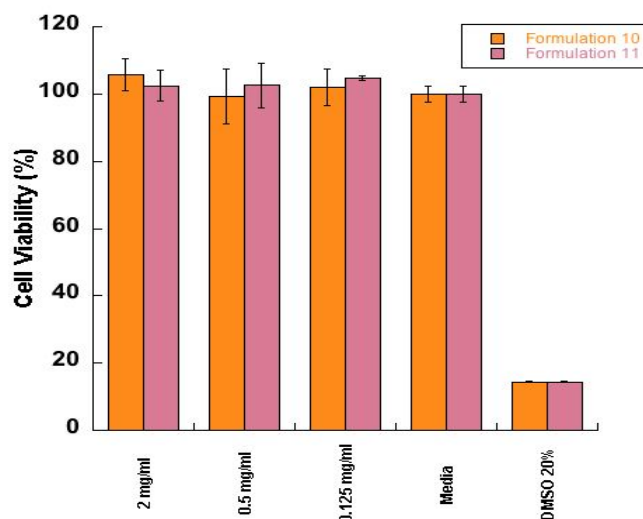


Figure 79. Viability of NuLi-1 cell line evaluated after 48 h of exposure to different treatment concentrations of Formulations #10 and #11. Results are expressed as mean value  $\pm$  standard deviation (n=3).

#### 4.2.4 Airways mucus mimetic models

Since cysteamine base was proved in literature to have a mucolytic activity exercising in this way a therapeutic effect toward the viscous mucus of cystic fibrosis patients, rheological experiments were conducted to assess whether this effect was evident on the spray-dried cysteamine hyaluronate microparticles.<sup>66</sup>

The mucolytic activity of cysteamine base was investigated performing rheological experiments on airways mucus mimetic samples. Treatments were added to various mucus samples following the method described in Section 3.2.9. In detail, the experiments aimed to assess the reduction of both  $G'$  and  $G''$  moduli, after the application of the treatments. Three mucus samples, containing 4, 5.3 and 6.5% of glutaraldehyde (GA) were tested. Saline solution alone was used as control. Cysteamine base was tested alone and in combination with the hyaluronic acid in the spray-dried formulations. In Figures 80-82, the results of the rheological experiments are reported.

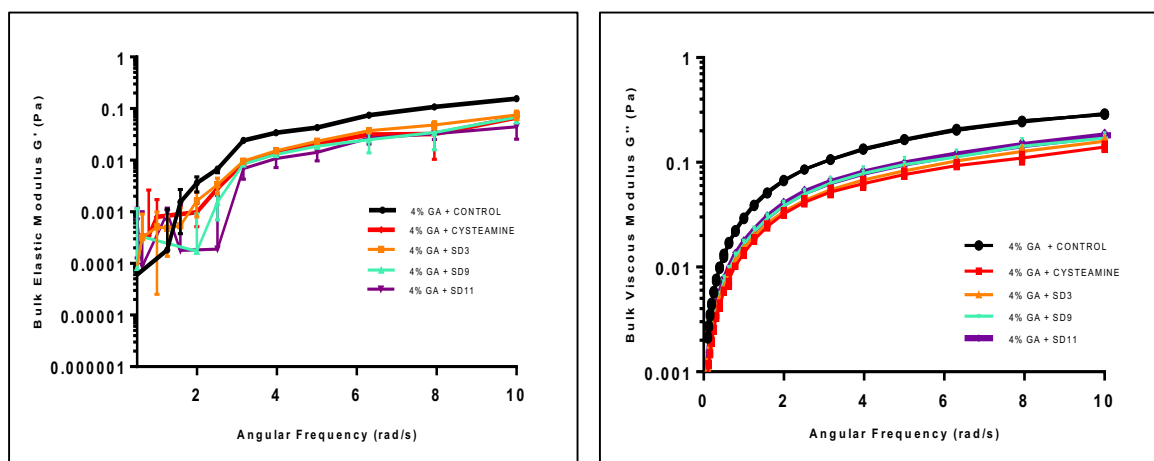


Figure 80. Frequency-dependence of  $G'$  (left) and bulk viscous modulus  $G''$  (right) for crosslinked mucus mimetic sample at 4% of GA. Results are expressed as mean value  $\pm$  standard deviation ( $n=3$ ).  $P<0.0001$ .

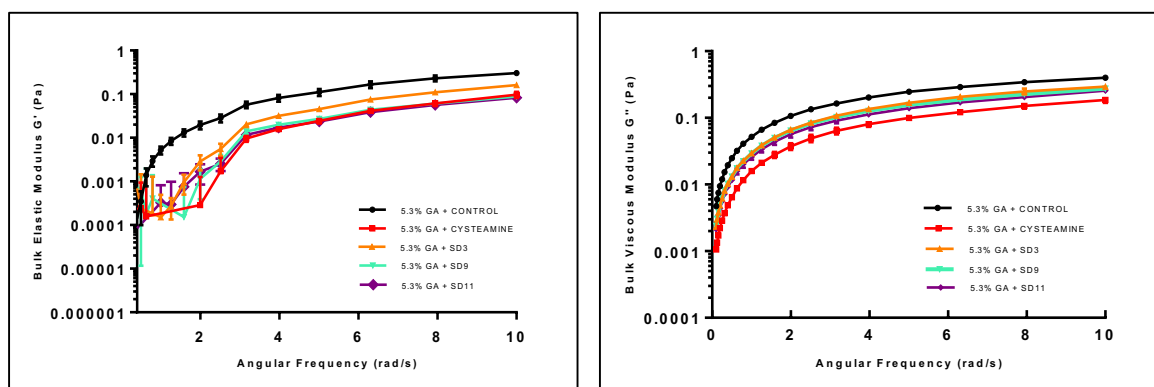


Figure 81. Frequency-dependence of  $G'$  (left) and bulk viscous modulus  $G''$  (right) for crosslinked mucus mimetic sample at 5.3% of GA. Results are expressed as mean value  $\pm$  standard deviation ( $n=3$ ).  $P<0.0001$ .

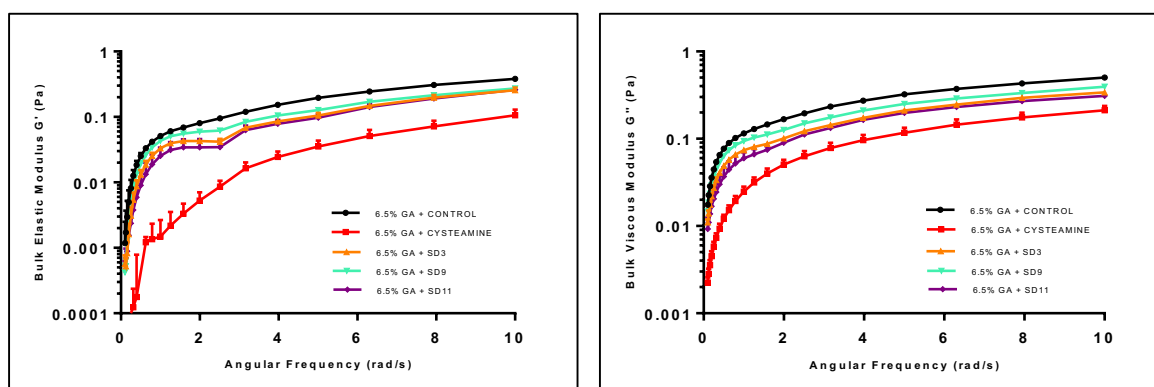


Figure 82. Frequency-dependence of  $G'$  (left) and bulk viscous modulus  $G''$  (right) for crosslinked mucus mimetic sample at 6.5% of GA. Results are expressed as mean value  $\pm$  standard deviation ( $n=3$ ).  $P<0.0001$ .

The graphs on the left referred to  $G'$  modulus, related to the elasticity of the mucus whereas the graphs on the right to  $G''$  modulus, related to the viscosity. As it can be observed, there was a significant reduction (one-way ANOVA/Dunnet:  $p < 0.01$ ) on both the elasticity and the viscosity of the mucus after the application of the treatments. In particular, cysteamine base (red line) showed a higher capacity, compared to the spray-dried formulations, to decrease the elasticity and the viscosity of the mucus. However, due to the high sensitivity of the drug in environmental conditions, it can not be formulated alone.

To conclude, Formulations #3, #9, #10 and #11, characterized by a cysteamine content of between 13 and 14%, were selected as the most promising ones. In fact, for all the formulations, the drug content resulted to be higher than 80%. Considering the particle size distribution and the *in vitro* aerodynamic performances, Formulations #9, #10 and #11, containing L-leucine as excipient, showed FPF values between 55 and 65%. In addition, the assessment of *in vitro* toxicity on specific cell cultures models proved that spray-dried cysteamine hyaluronate microparticles were non-toxic.

### 4.3 Preformulation study of cysteamine bitartrate spray-dried microparticles

For a more classical and maybe less inventive process, the preliminary preformulation study of cysteamine spray-dried powders was also done starting from cysteamine bitartrate. The formulations were manufactured by spray drying technique according to the process parameters reported below in Table XXX.

Table XXX. Spray dryer process parameters employed during the preformulation study of cysteamine bitartrate spray-dried microparticles.

Formulations	Spray-dryer	Inlet Temperature (°C)	Feed Rate (ml/min)	Atomizing Air Rate (L/h)	Nozzle Type
#1	B290	150	3 ml/min	500	Three fluid (coaxial) nozzle
#2	B290	150	3 ml/min	500	Three fluid (coaxial) nozzle
#3	B290	150	3.5 ml/min	500	Three fluid (coaxial) nozzle
#4	B290	120	3 ml/min	600	Three fluid (coaxial) nozzle
#5	B290	120	2.5 ml/min	600	Three fluid (coaxial) nozzle
#6	B290	120	3 ml/min	600	Three fluid (coaxial) nozzle

The spray-dried powders of cysteamine bitartrate obtained are summarized in Table XXXI.

Table XXXI. Composition and yield of the spray-dried powders of cysteamine bitartrate.

Formulations	Composition	Yield (%)
#1	70 % cysteamine bitartrate/20 % L-Leucine/5% Kollidon 12PF/5% trehalose	44.0
#2	70 % cysteamine bitartrate/20 % L-Leucine/5% Kollidon 12PF/5% trehalose (20% EtOH)	27.1
#3	70 % cysteamine bitartrate/20 % L-Leucine/4% Kollidon 12PF/5% trehalose/1% HP $\beta$ CD (20% EtOH)	30.1
#4	70 % cysteamine bitartrate/20 % L-Leucine/5% Kollidon 12PF/5% trehalose/0.8 ml acetic acid (20% EtOH)	34.2
#5	70 % cysteamine bitartrate/20 % L-Leucine/4% Kollidon 12PF/5% trehalose (20% EtOH) (under N <sub>2</sub> atmosphere)	41.7
#6	70 % cysteamine bitartrate/19.9 % L-Leucine/5% Kollidon 12PF/5% trehalose/0.1 % ascorbic acid	43.7

In Formulation #1 and #6 the drug and the excipient were dissolved in MilliQ grade water, while for Formulations #2-5 a hydroalcoholic solution (20% of ethanol) were used. As it can be observed from Table XIII, the yield of the spray drying process was not greater than 44%. This was mainly due to cysteamine bitartrate that was stucked to the cyclone and to the final collector of the spray dryer. Initially, the spray drying of the cysteamine bitartrate aqueous solution was attempted, but without success. Then, it was decided to add L-leucine and other excipients, compatible with the inhalation administration route.

#### 4.3.1 Drug content determination

Following the HPLC method described in Section 3.2.3., the results of the drug content analysis are reported in Table XXXII. Samples were prepared according to the procedure described in Section 3.2.4.

Table XXXII. Drug content of the spray-dried formulations of cysteamine bitartrate microparticles.

Formulations	Theoretical drug content (%)	Experimental drug content (%)
#1	69.7 ± 1.3	49.5 ± 1.2
#2	68.1 ± 1.1	51.6 ± 1.3
#3	69.8 ± 1.0	49.0 ± 1.9
#4	68.0 ± 1.6	55.1 ± 1.0
#5	69.2 ± 1.9	49.8 ± 1.1
#6	68.1 ± 1.4	61.1 ± 1.3

As it can be observed, Formulation #6 was the one that showed the highest value of drug content, equal to 89%. On the contrary, all the other formulations presented drug content values of between 70 and 80%.

#### 4.3.2 Thermogravimetric analysis (TGA)

The content of water in all the spray-dried formulations was performed using the procedure described in Section 3.2.5.3. In Table XXIII the results are summarized. As it be appreciated, the residual water content was not greater than 5%.

Table XXXIII. Water content determination of the spray-dried formulations of cysteamine hyaluronate microparticles.

Formulations	Residual water content (%)
#1	3.4
#2	2.5
#3	4.8
#4	1.1
#5	3.4
#6	3.3

#### 4.3.3 Scanning Electron Microscopy (SEM)

The SEM images of Formulations #1, #2 and #6 are represented in Figures 83-85.

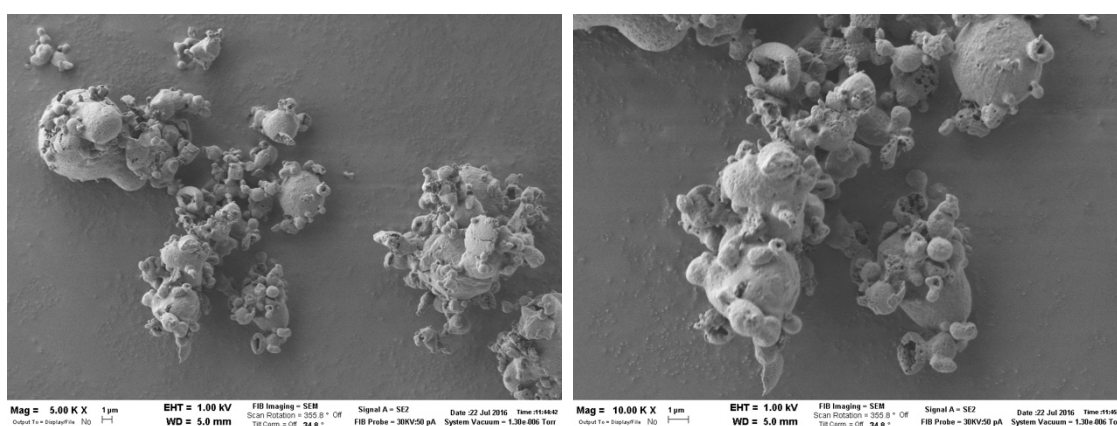


Figure 83. SEM Images of Formulation #1 (70 % cysteamine bitartrate/ 20% L-leucine/ 5% Kollidon 12 PF/ 5% trehalose).

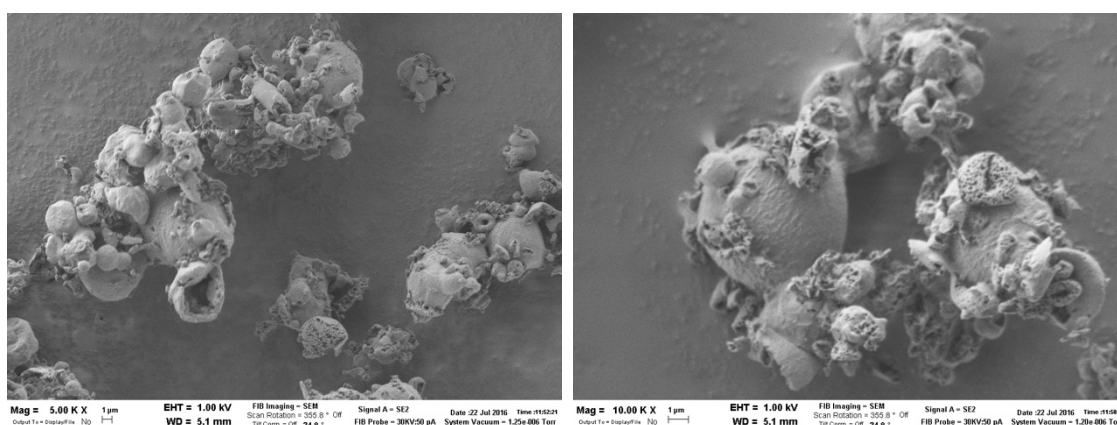


Figure 84. SEM Images of Formulation #2 (70 % cysteamine bitartrate/ 20% L-leucine/ 5% Kollidon 12 PF/ 5% trehalose +20% ethanol).

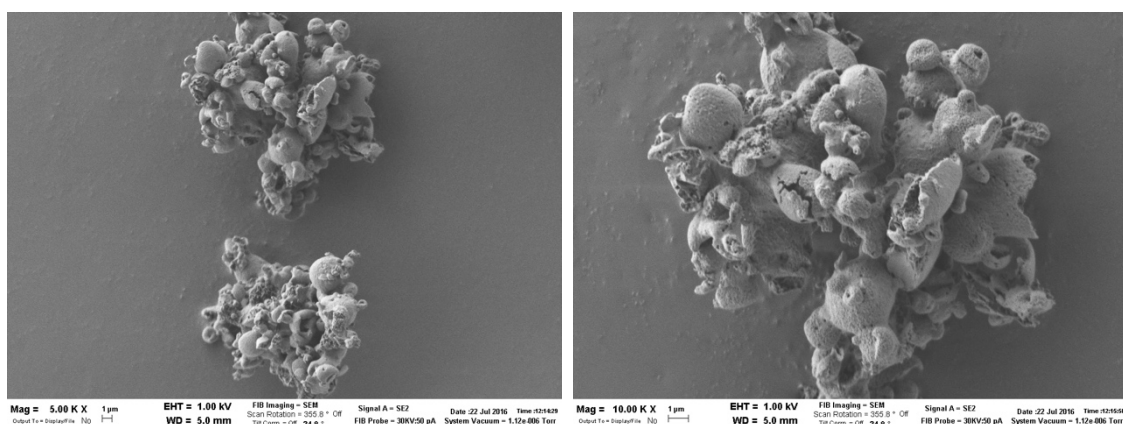


Figure 85. SEM Images of Formulation #6 (70 % cysteamine bitartrate/ 19.9% L-leucine/ 5% Kollidon 12F/ 5% trehalose/ 0.1% ascorbic acid).

#### 4.3.4 *In vitro* aerodynamic characterization

The investigation of the *in vitro* aerodynamic performance was made by means of the Fast Screening Impactor, according to the procedure previously described in Section 3.2.6.1. The FPF (%) values are shown in Figure 86.

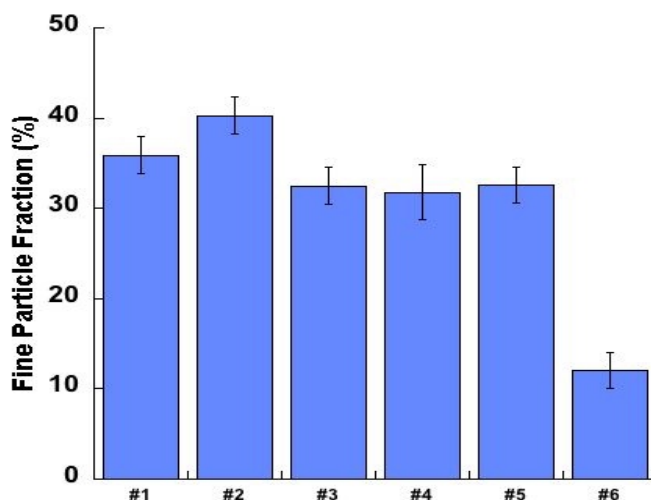


Figure 86. Fine Particle Fraction (FPF) values of the spray-dried cysteamine bitartrate microparticles.

As it can be easily observed, in case of the spray-dried microparticles of cysteamine bitartrate, the fine particle fraction was not greater than 40%.

## 5. CONCLUSIONS

Cysteamine, approved for the treatment of nephropathic cystinosis, has recently been shown to have *in vitro* potential antimicrobial, anti-biofilm and mucoactive properties in the treatment of Cystic Fibrosis patient infections. A dry powder inhaler was identified to be the most appropriate inhalation product of cysteamine for this therapeutic objective since the deposition of drug particles could better perform the antimicrobial, anti-biofilm and mucolytic activities, due to the high drug concentration attainable at the deposition site.

The design of formulation was to face the hygroscopicity and the poor stability of cysteamine by adding appropriate adjuvants that can enhance the stabilization of the drug as well as the respirability, in view of the inhalation administration.

In the preformulation study, cysteamine base hyaluronate salt was obtained by means of spray drying technique. The use of hyaluronic acid as acidic polymer was selected to obtain a stable inhalation spray-dried powder, constituted by the novel cysteamine hyaluronate salt formed during the spray drying process. The formation of a novel salt was confirmed by FT-IR spectroscopy and <sup>13</sup>C NMR analyses. In both the experiments performed, a difference between the spectra of the raw materials and the ones of the spray-dried microparticles were evidenced, proving that an interaction between hyaluronic acid and cysteamine base, thus leading to the obtainment of a novel cysteamine hyaluronate salt, was occurred.

The employment of the coaxial nozzle resulted to be useful in improving the chemical and physical stability of the API. In particular, the presence of L-leucine in the concentration range of 5-20% (w/w) was effective in improving the aerodynamic characteristics of the spray-dried powders. This aspect was confirmed by the morphological analysis of the spray-dried formulations; in fact, the addition of L-leucine led to the formation of porous and spongy microparticles, resulting in good flowability properties suitable for inhalation administration.

From the results of the preformulation study, four formulations of cysteamine hyaluronate microparticles were identified as the most promising in relation to drug content, particle size distribution and fine particle fraction values. These formulations were further investigated in terms of *in vitro* cytotoxicity assays on different cell lines of the respiratory epithelium where they proved to be non-toxic. In fact, cells resulted to be viable after 4 h of exposure at different treatment concentration ranges. Furthermore, rheological experiments were

conducted to assess the mucolytic activity of cysteamine. The results showed that the drug was able to provide a reduction of both the viscous and the elastic properties of different mucus mimetic samples.

Apart from cysteamine base, also cysteamine bitartrate was investigated for the manufacturing of spray-dried microparticles. Excipients like trehalose and cyclodextrins were selected in order to improve the morphology, and then the aerosolization characteristic, of the cysteamine bitartrate microparticles. Despite this, the fine particle fraction values were not greater than 40%. Apart from this, *in vitro* cytotoxicity assays were conducted and the spray-dried cysteamine bitartrate microparticles resulted to be non-toxic toward the cell lines employed.

## REFERENCES

1. Nokhodchi A. et al., "Pulmonary drug delivery, advances and challenges", Wiley Book Series, 2015.
2. Patil J. et al., "Pulmonary drug delivery strategies: a concise, systematic review", Indian Chest Society, 2012, 29(1), p. 44-49.
3. Colombo P. et al., "Inhalation drug delivery", Wiley-Blackwell, 2013.
4. Lau M. et al., "Co-milled API-lactose systems for inhalation therapy: impact of magnesium stearate on physico-chemical stability and aerosolization performance", Drug Development and Industrial Pharmacy, 2017, Vol. 43, No. 6, p. 980-988.
5. Lau M. et al., "A review of co-milling techniques for the production of high dose dry powder inhaler formulation", Drug Development and Industrial Pharmacy, 2017, Vol. 43, No. 8, p. 1229-1238.
6. Kumar S. et al., "The inhalation of active pharmaceutical ingredients and its pharmaceutical studies", Journal of Chemical and Pharmaceutical Research, 2016, 8 (11), p. 102-105.
7. Chow A. et al., "Particle engineering for pulmonary drug delivery", Pharmaceutical Research, Vol. 24, No. 3, March 2007.
8. Lippmann M et al., "Deposition, retention and clearance of inhaled particles", British Journal of Industrial Medicine, 1980, 37, p. 337-362.
9. Borgström L. et al., "Lung deposition of budesonide inhaled via Turbuhaler®: a comparison with terbutaline sulphate in normal subjects", Eur Respir J, 1994, 7, p. 69-73.
10. Cheng Y., "Mechanism of pharmaceutical aerosol deposition in the respiratory tract", AAPS PharmSciTech, 2014, Vol. 15, No. 3.
11. Yeh H. et al., "Factors influencing the deposition of inhaled particles", Environmental Health Perspectives, 1976, Vol. 15, p. 147-156.
12. Cunha L. et al., "Inhalable chitosan microparticles for simultaneous delivery of isoniazid and rifabutin in lung tuberculosis treatment", Drug Development and Industrial Pharmacy, 2019, Vol. 45, No. 8, p. 1313-1320.
13. Sankhala S. et al., "Factors that affect the lung deposition", International Journal of Modern Physics, 2013, Vol. 22, p. 729-732.
14. Labiris N. et al., "Pulmonary drug delivery. Part II: the role of inhalant delivery devices and drug formulations in therapeutic effectiveness of aerosolized medications", Clin Pharmacol, 56, p. 600-612.

15. Martinelli F. et al., "Pierce and inhale design in capsule based dry powder inhalers: effect of capsule piercing and motion on aerodynamic performance of drugs", *International Journal of Pharmaceutics* 2015, 487, p. 197-204.
16. Sanchis J. et al., "Inhaler devices – from theory to practice", *Respiratory Medicines* 2013, 107, p. 495-502.
17. Ibrahim M. et al., "Inhalation drug delivery devices: technology update", *Medical Devices: Evidence and Research*, 2015, 8, p. 131-139.
18. Buttini F. et al., "Accessorized DPI: a shortcut towards flexibility and patient adaptability in dry powder inhalation", *Pharm Res*, 2016, 33, p. 3012-3020.
19. Vehring R., "Pharmaceutical particle engineering via spray drying", *Pharmaceutical Research*, May 2008, Vol. 25, No. 5.
20. Belotti S. et al., "Spray-dried amikacin sulphate powder for inhalation in cystic fibrosis patients: the role of ethanol in particle formation", *European Journal of Pharmaceutics and Biopharmaceutics* 2015, 93, p. 165-172.
21. Kim S. et al., "Development and characterization of sodium hyaluronate microparticle-based sustained release formulation of Recombinant Human Growth Hormone prepared by spray-drying", *Journal of Pharmaceutical Sciences* 2016, 105, p. 613-622.
22. Sosnik A. et al., "Advantages and challenges of the spray-drying technology for the production of pure drug particles and drug-loaded polymeric carriers", *Advances in Colloid and Interface Science* 2015, 223, p. 40-54.
23. Weers J. et al., "Spray-dried Pulmosphere™ formulations for inhalation comprising crystalline drug particles", *AAPS PharmSciTech*, 2019, 20,103.
24. Sou T. et al., "The effect of amino acid excipients on morphology and solid-state properties of multi-component spray-dried formulations for pulmonary delivery of bio macromolecules", *European Journal of Pharmaceutics and Biopharmaceutics* 2013, 83, p. 234-243.
25. Kreft M. et al., "The characterization of the human cell line Calu-3 under different culture conditions and its use as an optimized *in vitro* model to investigate bronchial epithelial function", *European Journal of Pharmaceutical Sciences* 2015, 69, p.1-9.
26. Forbes B. et al., "Human respiratory epithelial cell culture for drug delivery applications", *European Journal of Pharmaceutics and Biopharmaceutics* 2005, 60, p. 193-205.

27. Shen B. et al., "Calu-3: a human airway epithelial cell line that shows cAMP-dependent Cl<sup>-</sup> secretion", American Physiological Society.
28. Haghi M. et al., "Time and passage-dependent characteristics of a Calu-3 respiratory epithelial cell model", Drug Development and Industrial Pharmacy, 2010, 36 (10), p.1207-1214.
29. Zabner J. et al., "Development of cystic fibrosis and non-cystic fibrosis airway cell lines", AJP Lung Cell Mol Physiol, May 2003, Vol. 284.
30. Masters J. et al., "Changing medium and passaging cell lines", Nature Protocols, 2007, Vol. 2, No. 9.
31. Grainger C. et al., "Culture of Calu-3 cells at the air interface provides a representative model of the airway epithelial barrier", Pharmaceutical Research, July 2006, Vol. 23, No. 7.
32. Ong. H. et al., "Pharmaceutical applications of the Calu-3 lung epithelia cell line", Expert Opinion on Drug Delivery, 2013, 10(9).
33. Cooksley C. et al., "TLR response pathways in NuLi-1 cells and primary human nasal epithelial cells", Molecular Immunology 2015, 68, p. 476-483.
34. Haghi M. et al., "Across the pulmonary epithelial barrier: integration of physicochemical properties and human cell models to study pulmonary drug formulations", Pharmacology & Therapeutics 2014, 144, p. 235-252.
35. Cuthbert AW, "New horizons in the treatment of cystic fibrosis", British Journal of Pharmacology 2010, 163, p. 173-183.
36. Fanen P. et al., "Genetics of cystic fibrosis: CFTR mutation classifications towards genotype-based CF therapies", International Journal of Biochemistry & Cell Biology 2014, 52, p. 94-102.
37. Trandafir L. et al., "Current practices and potential nanotechnology perspectives for pain related to cystic fibrosis", Journal of Clinical Medicine, 2019, 8(7), p.1023.
38. Garcia-Contreras L. et al., "Pharmaceutical and biotechnological aerosol for cystic fibrosis therapy", Advanced Drug Delivery Reviews 2002, 54, p. 1491-1504.
39. Bell S. et al., "The future of cystic fibrosis care: a global perspective", Lancet Respiratory Medicine, 2019.
40. Sosnay P. et al., "Molecular genetics of cystic fibrosis transmembrane conductance regulator: genotype and phenotype", CrossMark.

41. Meyer P. et al., "Analysis of the two common alpha-1-antitrypsin deficiency alleles PiMS and PiMZ as modifiers of *Pseudomonas Aeruginosa* susceptibility in cystic fibrosis", Clin Genet, 2002, 62, p. 325-327.
42. Poolman E. et al., "Evaluating candidate agents of selective pressure for cystic fibrosis", J.R. Soc. Interface 2007, 4, p. 91-98.
43. Cystic Fibrosis Foundation Patient Registry, Annual Data Report (Bethesda, Maryland), 2011.
44. Bowen S., et al., "The basic science of cystic fibrosis", Pediatric and Child Health 2015, 25:4.
45. Maguiness K. et al., "Pancreatic enzyme replacement in people with cystic fibrosis", Cystic Fibrosis Foundation.
46. Cayli Y. et al., "Dry powders for the inhalation of ciprofloxacin or levofloxacin combined with a mucolytic agent for cystic fibrosis patients", Drug Development and Industrial Pharmacy, 2017, Vol. 43, No.8, p. 1378-1389.
47. Epps Q. et al., "State of the art in cystic fibrosis pharmacology – Optimization of antimicrobials in the treatment of cystic fibrosis pulmonary exacerbations: I. Anti-methicillin-resistant *Staphylococcus Aureus* (MRSA) antibiotics", Pediatric Pulmonology, 2019, p. 1-25.
48. Russo P. et al., "Gentamicin and leucine inhalable powder: what about antipseudomonal activity and permeation through cystic fibrosis mucus?", International Journal of Pharmaceutics 2013, 440, p. 250-255.
49. Høiby N. et al., "*Pseudomonas Aeruginosa* biofilms in cystic fibrosis", Future Microbiology, 2010, 5(11), p. 1663-1674.
50. Moss R., "Administration of aerosolized antibiotics in cystic fibrosis patients", Chest September 2001, 120, 3.
51. Wilson R. et al., "*Pseudomonas aeruginosa* and other related species", Lung Infections 3, Thorax, 1998, 53, p. 213-219.
52. Antibiotic treatment for cystic fibrosis – 3rd edition, Report of the UK Cystic Fibrosis Trust Antibiotic Working Group, May 2009.
53. Mantero M. et al., "Once daily aerosolized tobramycin in adult patients with cystic fibrosis in the management of *Pseudomonas Aeruginosa* chronic infection", Multidisciplinary Respiratory Medicine, 2017, 12:2.
54. Ramsey B. et al., "Intermittent administration of inhaled tobramycin in patients with cystic fibrosis", The New England Journal of Medicine, 2014, Vol. 340, No. 1.

55. Sexauer W. et al., "Aerosolized antibiotics in cystic fibrosis", *Seminars in Respiratory and Critical Care Medicine*, 2003, Vol. 24, No.6.
56. Bals R. et al., "Antibiotic treatment of CF lung disease: from bench to bedside", *Journal of Cystic Fibrosis*, 2011, Vol. 10, Suppl. 2, p. 146-151.
57. Traini D. et al., "Preparation and evaluation of single and co-engineered combination inhalation carrier formulations for the treatment of asthma", *Journal of Pharmaceutical Sciences*, 2012, Vol. 101, No. 11.
58. Pai V. et al., "Efficacy and safety of aerosolized tobramycin in cystic fibrosis", *Pediatric Pulmonology*, 2001, 32, p. 314-327.
59. Parlati C. et al., "Pulmonary spray dried powders of tobramycin containing sodium stearate to improve aerosolization efficiency", *Pharmaceutical Research*, May 2009, Vol. 26, No. 5.
60. Kozáková J. et al., "Dry powder inhaler of colistimethate sodium for lung infections in cystic fibrosis: optimization of powder construction", *Drug Development and Industrial Pharmacy*, 2019, Vol. 45, No. 10, p. 1664-1673.
61. Ong X. et al., "*In vitro* and *ex vivo* methods predict the enhanced lung residence time of liposomal ciprofloxacin formulations for nebulization", *European Journal of Pharmaceutics and Biopharmaceutics* 2014, 86, p. 83-89.
62. Belotti S. et al., "Spray dried amikacin powder for inhalation in cystic fibrosis patients: a quality by design approach for product construction", *International Journal of Pharmaceutics*, 2014, 471, p. 507-515.
63. Shteinberg M. et al., "Use of inhaled tobramycin in cystic fibrosis", *Adv Ther*, 2015, 32, p. 1-9.
64. Uttley L. et al., "Systematic reviews of the dry powder inhalers colistimethate sodium and tobramycin in cystic fibrosis", *Eur Resp Rev*, 2013, 22, p. 476-486.
65. Devereux G. et al., "Cysteamine as a future intervention in cystic fibrosis against current and emerging pathogens: a patient-based *ex vivo* study confirming its antimicrobial and mucoactive potential in sputum", *EBioMedicine*, 2015, 2, p.1507-1512.
66. Charrier C. et al., "Cysteamine (Lynovex®), a novel mucoactive antimicrobial & antibiofilm agent for the treatment of cystic fibrosis", *Orphanet Journal of Rare Disease*, 2014, 9:189.
67. Zhao T. et al., "N-acetylcysteine inhibit biofilms produced by *Pseudomonas aeruginosa*", *BMC Microbiology*, 2010, 10:140.

68. NoaBiotics pipeline Lynovex<sup>®</sup> (NM001)
69. De Stefano D. et al., "A breathe in cystic fibrosis therapy: a new therapeutic endeavor for cysteamine", *EBioMedicine* 2015, 2, p. 1306-1307.
70. Patent US 2017/0348254, [www.patents.google.com](http://www.patents.google.com)
71. Neo H. et al., "The effect of hyaluronic acid on experimental temporomandibular joint osteoarthritis in the sheep", *Journal of Oral Maxillofac Surg* 1997, 55, p.1114-1119.
72. Brown et al., "Hyaluronic acid: a unique topical vehicle for the localized delivery of drugs to the skin", *JEADV*, 2005, 19, p. 308-318.
73. Petrigni G. et al., "Aerosolized hyaluronic acid prevents exercise-induced bronchoconstriction, suggesting novel hypotheses on the correction of matrix defects in asthma", *Pulmonary Pharmacology & Therapeutics* 2006, 19, p. 166-171.
74. Moreland L., "Intra-articular hyaluronan (hyaluronic acid) and hylans for the treatment of osteoarthritis: mechanism of action", *Arthritis Research & Therapy*, 2003, Vol. 5, No. 2.
75. Fallacara A. et al., "*In vitro* characterization of physico-chemical properties, cytotoxicity, bioactivity of urea-crosslinked hyaluronic acid and sodium ascorbyl phosphate nasal powder formulation", *International Journal of Pharmaceutics* 2019, 558, p. 341-350.
76. Collins S. et al., "Hyaluronan fragments promote inflammation by down-regulating the anti-inflammatory A2a receptor", *American Journal of Respiratory Cell and Molecular Biology*, 2011, Vol. 45.
77. Cantor J., "Potential therapeutic applications of hyaluronan in the lung", *International Journal of Obstructive Pulmonary Disease*, 2007, 2(3), p. 283-288.
78. Stern R., "Hyaluronan fragments: an information-rich system", *European Journal of Cell Biology* 2006, 85, p. 699-715.
79. Buonpensiero P. et al., "Hyaluronic acid improves pleasantness and tolerability of nebulized hypertonic saline in a cohort of patients with cystic fibrosis", *Adv Ther*, 2010, 27(11), p. 870-878.
80. Cho K. et al., "Release of ciprofloxacin from poloxamer-graft-hyaluronic acid hydrogels in vitro", *International Journal of Pharmaceutics* 2003, 260, p. 83-91.
81. Seville P. et al., "Amino acid-modified spray-dried powders with enhanced aerosolisation properties for pulmonary drug delivery", *Powder Technology* 2007, 178, p. 40-50.

82. Kundawala A. et al., "Influence of formulation components on aerosolization properties of isoniazid loaded chitosan microspheres", *International Journal of Pharmaceutical Sciences and Drug Research*, 2011, 3(4), p. 297-302.
83. Raula J. et al., "Structure and dissolution of L-leucine-coated salbutamol sulphate aerosol particles", *AAPS PharmSciTech*, June 2012, Vol. 13, No. 2.
84. Paajanen M. et al., "Direct evidence on reduced adhesion of Salbutamol sulphate particles due to L-leucine coating", *Powder Technology* 2009, 192, p. 6-11.
85. Li L. et al., "L-Leucine as an excipient against moisture on *in vitro* aerosolization performances of highly hygroscopic spray-dried powders", *European Journal of Pharmaceutics and Biopharmaceutics* 2016, 102, p. 132-141.
86. Mehta P., "Imagine the superiority of dry powder inhalers from carrier engineering", *Journal of Drug Delivery*, 2018.
87. Feng A. et al., "Mechanistic models facilitate efficient development of leucine containing microparticles for pulmonary drug delivery", *International Journal of Pharmaceutics* 2011, 409, p.156-163.
88. Traini D. et al., "Polymer coating of carrier excipients modify aerosol performance of adhered drugs used in dry powder inhalation therapy", *International Journal of Pharmaceutics*, 2012, Vol. 438, Issues 1-2, p. 150-159.
89. Application n: EP18425038, Applicant: Recordati Industria Chimica e Farmaceutica S.p.A., Inventors: Barchielli M., Colombo P., Rossi A., Adorni G.
90. Hamed R., "Synthetic tracheal mucus with native rheological and surface tension properties", *Journal of Biomed Mater Res A*, June 2014, 102(6), p. 1788-1798.

## AKNOWLEDGEMENT

Thank you to Prof. Alessandra Rossi and Emeritus Prof. Paolo Colombo for their constant presence and support during the Ph.D. Course.

Thank you to Recordati Industria Chimica e Farmaceutica S.p.A. for the financial support as well as the deposition of two patent applications.

Thank you to Prof. Marco Mor, the Coordinator of the Ph.D. Course, for all the seminars organized and the opportunity to take part to Summer Schools and other enriching events.

Finally, thank you to Prof. Daniela Traini and Prof. Paul Young for hosting me at the Woolcock Institute of Medical Research in Sydney (Australia).